A SYSTEMS-LEVEL APPROACH FOR INTEGRATED SHALE GAS WASTEWATER MANAGEMENT

by

Sakineh Tavakkoli

B.S. Civil and Environmental Engineering, Sharif University of Technology, 2009

M.S. Environmental Engineering, Sharif University of Technology, 2011

Submitted to the Graduate Faculty of

Swanson School of Engineering in partial fulfillment

of the requirements for the degree of

Doctor of Philosophy

University of Pittsburgh

2018

UNIVERSITY OF PITTSBURGH

SWANSON SCHOOL OF ENGINEERING

This dissertation was presented

by

Sakineh Tavakkoli

It was defended on

February 6, 2018

and approved by

Melissa Bilec, Ph.D., Associate Professor

Leanne Gilbertson, Ph.D., Assistant Professor

Natasa Vidic, Ph.D., Assistant Professor

Radisav Vidic, Ph.D., Professor

Dissertation Director: Vikas Khanna, Ph.D., Associate Professor

A SYSTEMS-LEVEL APPROACH FOR INTEGRATED SHALE GAS WASTEWATER MANAGEMENT

Sakineh Tavakkoli, PhD

University of Pittsburgh, 2018

Economic benefits of shale gas production in addition to its potential for enabling energy security are driving the strategic development of unconventional natural gas in the U.S. However, shale gas production poses potential detrimental impacts on the surrounding ecosystems. In particular, sustainable management of high salinity wastewater is one of the critical challenges facing shale gas industry. While recycling shale gas wastewater is a practical short-term solution to minimize total water use in the fracturing process it may not be a viable strategy from a long-term management perspective. Moreover, direct disposal into Salt Water Disposal (SWD) wells which is the most common management strategy in the U.S. is not cost effective in Marcellus shale play due to limited disposal capacity.

This work develops a systems-level optimization framework for guiding economically conscious management of high salinity wastewater in Marcellus shale play in Pennsylvania (PA) with a focus on using membrane distillation (MD) as the treatment technology. Detailed techno-economic assessment (TEA) is performed to assess the economic feasibility of MD for treatment of shale gas wastewater with and without availability of waste heat. Natural gas compressor stations (NG CS) are chosen as potential sources of waste heat and rigorous thermodynamic models are developed to quantify the waste heat recovery opportunities from NG CS. The information from waste heat estimation and TEA are then utilized in the optimization framework

for investigating the optimal management of shale gas wastewater. Wastewater management alternatives ranging from direct disposal into SWD wells to advanced centralized, decentralized, and onsite treatment options using MD are included in the optimization model.

The optimization framework is applied to four case studies in Greene and Washington counties in southwest and Susquehanna and Bradford counties in Northeast PA where major shale gas development activities take place. The results of this analysis reveal that onsite treatment of wastewater at shale gas extraction sites in addition to treating wastewater at NG CS where available waste heat could be utilized to offset the energy requirements of treatment process are the most economically promising management options that result in major economic benefit over direct disposal into SWD.

TABLE OF CONTENTS

LIST OF TABLES

LIST OF FIGURES

ACKNOWLEDGEMENTS

First and foremost, I would like to thank my family for their unconditional love, support, and encouragement throughout my doctoral studies. I would also like to express my special appreciation and thanks to my thesis advisor Vikas Khanna for his guidance, mentorship, patience, and motivation during the development of this work and allowing me to grow as a research scientist.

I would like to thank my dissertation committee members for their guidance and brilliant comments and suggestions; they have been a constant source of inspiration and encouragement throughout my time at University of Pittsburgh. I am deeply grateful to Melissa Bilec, Leanne Gilbertson, Natasa Vidic, and Radisav Vidic for their technical and scientific advice, and insightful discussions.

I would like to acknowledge the Mascaro Center for Sustainable Innovation (MCSI) for graciously providing financial support for this research. Additionally, I want to thank my peers, friends, and staff/faculty in the Civil and Environmental Engineering Department at the University of Pittsburgh, in particular my colleagues in Khanna Lab throughout my time here for all of the fond memories and everlasting friendships. I dedicate this work to my parents, Sobhan Tavakkoli and Parvin Selahshour, my sister, Fatemeh Tavakkoli, my brother-in-law, Valiollah Shakeri, and my nephew, Mohammadsam Shakeri.

1.0 INTRODUCTION

The United States (U.S.) energy landscape is dramatically changing as a result of recent shift toward increased natural gas production [1, 2]. Natural gas production increased from 0.3 trillion cubic feet in 2000 to 9.6 trillion cubic feet in 2012 in the U.S. [2]. Unconventional shale gas represents a promising source of energy that plays a fundamental role in the U.S. energy security as U.S. has become a natural gas exporter in 2017 and it is expected to continue to export more natural gas than it imports throughout 2018 [3, 4]. Besides all these potential benefits of shale gas industry, shale gas production has been controversial as it is accompanied by potential negative impacts on the surrounding ecosystems and raises concerns associated with greenhouse gas (GHG) emissions [5-7], health issues [8, 9], the potential for drinking water [10] and groundwater contamination [11], high water footprint [12], and high salinity wastewater management [13, 14].

In particular, shale gas development poses a critical challenge of managing vast quantities of wastewater with salinity level more than 10 times the salinity of seawater generated in the process of hydraulic fracturing [15]. Wastewater generated during hydraulic fracturing and shale gas production includes flowback and produced water. During hydraulic fracturing, a mixture of water and chemicals (Table 1) known as fracturing fluid [16] is injected in a horizontal well to fracture the formation rock, increase its permeability and facilitate the flow of oil and gas into the well. Flowback returns to the surface after well fracturing and before shale gas production stage, taking up to several weeks while produced water returns to the surface after fracturing is completed and during the shale gas production stage and, therefore, will be generated during the entire gas production stage [17]. The salinity and flowrate of shale gas wastewater changes over time. While the salinity of this wastewater can be less than 1,000 mg/Liter in the first week of hydraulic fracturing it can dramatically increase to about 350,000 mg/Liter by end of gas extraction phase [18]. On the other hand, the volumetric flowrate of this wastewater decreases over time as it can fluctuate between about 500 m^3/day to less than 1 m^3/day [19, 20]. Hence, flowback water is usually associated with lower salinity and higher flow rates compared to produced water which can be saturated with salt but in lower volumetric flow rates [21]. Figure 1 shows how the quantity and quality of flowback water changes over time [20]. The composition of produced water over the lifetime of a well is shown in Figure 2 [22].

However, it is important to note there is no typical fractured well and the quality and quantity of shale gas generated wastewater varies greatly across geographical sites due to differences in the geologic formation, well operator, either the well is drilled vertically or horizontally, and recycling rate of wastewater at wellpads [23, 24]. The high salinity of flowback and produced water calls for proper management of this wastewater [25]. Long-term adoption of shale gas resources requires a comprehensive understanding of the economics and environmental impacts associated with shale gas wastewater management which has been relatively understudied in the existing work on shale gas sustainable development. Currently, a number of shale gas wastewater management strategies are being used including injection in underground wells evaporation, recycling, and advanced treatment. Each of these management strategies is described in the following section.

Table 1. Common chemical additives for hydraulic fracturing [14]

Additive type	Example compounds	Purpose
Acid	Hydrochloric acid	Clean out the wellbore, dissolve minerals, and initiate cracks in rock
Fiction reducer	Polyacrylamide, petroleum distillate	Minimize friction between the fluid and the pipe
Corrosion inhibitor	Isopropanol, acetaldehyde	Prevent corrosion of the pipe by diluted acid
Iron control	Citric acid, thioglycolic acid	Prevent precipitation of metal oxides
Biocide	Glutaraldehyde, 2,2-dibromo-3-nitrilopropionamid (DBNPA)	Bacterial conrol
Gelling agent	Guar/xanthan gum or hydroxyethyl cellulose	Thicken water to suspend the sand
Crosslinker	Borate salts	Maximize fluid viscosity at high temperatures
Breaker	Ammonium persulfate, magnesium peroxide	Promote breakdown of gel polymers
Oxygen scavenger	Ammonium bisulfite	Remove oxygen from fluid to reduce pipe corrosion
pH adjustment	Potassium or sodium hydroxide or carbonate	Maintain effectiveness of other compounds (such as crosslinker)
Proppant	Silica quartz sand	Keep fractures open
Scale inhibitor	Ethylene glycol	Reduce deposition on pipes
surfactant	Ethanol, isopropyl alcohol, 2-butoxyethanol	Decrease surface tension to allow water recovery

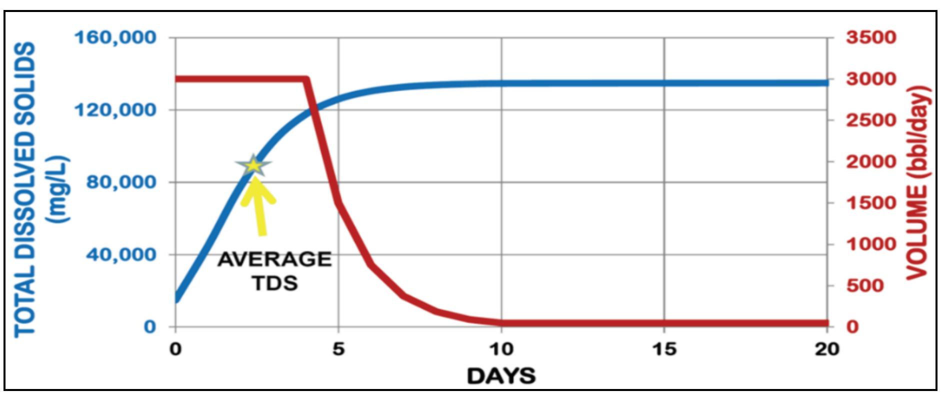

Figure 1. Total dissolved solids (TDS) and flowback volume in the early stage of well completion [20]

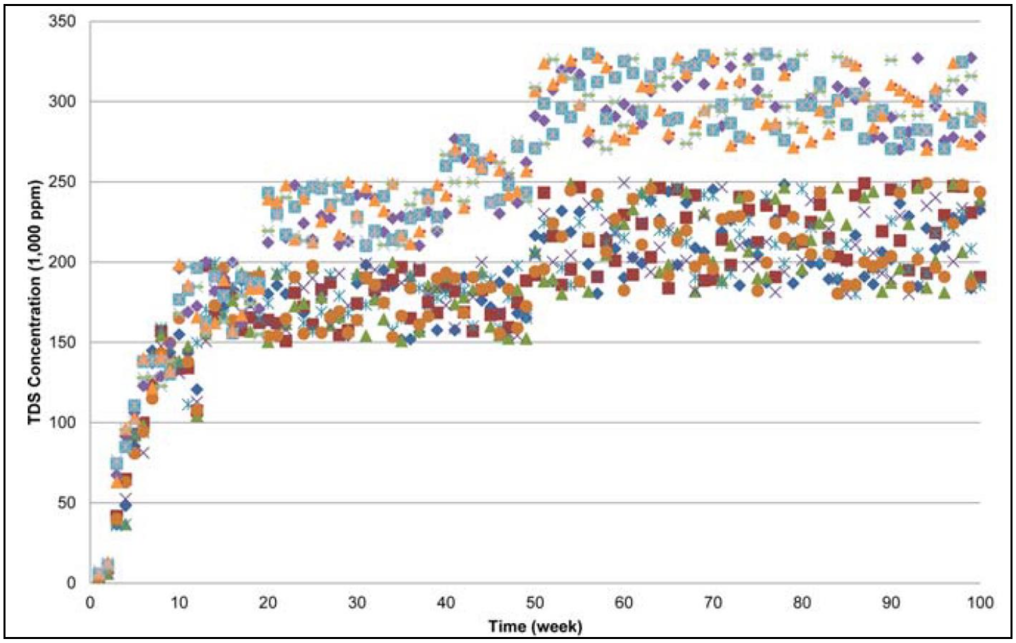

Figure 2. Total dissolved solids in produced water during well production for 14 wellpads represented by different colors over a 100-week time period [26]

1.1 SHALE GAS WASTEWATER MANAGEMENT STRATEGIES

The high salinity of flowback and produced water calls for proper management of this wastewater. Currently, a number of shale gas wastewater management strategies are being used including injecting, evaporation, recycling, and advanced treatment. Each of these management strategies is described in the following section.

1.1.1 Injection

The business-as-usual (BAU) management strategy in the U.S. is to inject high salinity shale gas wastewater at high pressure into disposal wells at depths of several thousand feet [27, 28]. There is a total of about 144,000 class II disposal wells in the U.S. of which 20% is allocated for salt water disposal (SWD) [29]. However, there is not sufficient disposal capacity in states such as Pennsylvania (PA) as there are only 9 SWD wells in this state, with only three of them being commercial wells, as compared to 12,000 and 800 SWD wells in Texas and Oklahoma, respectively [30]. Moreover, this strategy has come under increased scrutiny due to increased seismic activity in the proximity of disposal wells [31].

1.1.2 Evaporation

Shale gas produced wastewater could also be stored in large evaporation ponds where the majority of wastewater evaporates to the atmosphere. However, this strategy may only be used in areas with arid or semi-arid climate because of higher evaporation rate [32]. In addition, this management strategy raises a number of environmental concerns including leakage of wastewater into soil or groundwater sources as well as releasing the volatile compounds present in shale gas wastewater into the atmosphere [32, 33], thus making its utility restricted.

1.1.3 Recycling

In areas of limited disposal capacity (e.g., Pennsylvania) or where water resources are stressed (e.g., Texas and Oklahoma), recycling of shale gas wastewater is an effective alternative to direct underground injection of wastewater. Shale gas wastewater is blended with a portion of freshwater in order to meet the fracturing fluid requirements. This strategy is increasingly being used in PA primarily due to insufficient disposal capacity in the state and long transportation distances to disposal wells in Ohio [32].

1.1.4 Treatment at Centralized Wastewater Treatment (CWT) Facilities

Shale gas wastewater could also be processed at CWT facilities. However, the volumetric flowrate of shale gas wastewater stream is limited to 1% of the plant daily flowrate due to high salinity of shale gas wastewater which may disrupt microbial digestion processes at high concentration [13]. Moreover, while treatment processes at CWT facilities will be effective to remove total suspended solids (TSS) and oil and grease, these processes are not able to provide sufficient treatment for removing total dissolved solids (TDS) in shale gas wastewater [13]. Therefore, Pennsylvania department of environmental protection (PA DEP) requested to cease the discharge of shale gas wastewater into wastewater treatment plants [13].

1.1.5 Advanced Treatment

Although recycling may be an effective short-term solution for shale gas wastewater management, it cannot guarantee the long-term sustainability of shale gas industry especially after all the wells in a given shale play are in the producing stage and no water is needed for future fracturing jobs. This calls for development of innovative desalination technologies designed specifically for shale gas generated wastewater. Desalination technologies such as reverse osmosis (RO) and forward osmosis (FO) have been proposed for shale gas wastewater management [22, 34], however, the applicability of these technologies is limited to wastewater with up to 40,000 and 70,000 mg/L of TDS, respectively, [15, 26, 35] primarily because of the high osmotic pressure requirements [36, 37]. Membrane distillation (MD) is a promising treatment technology for high salinity wastewaters [38]. Recent studies demonstrated the potential of MD to treat very high salinity wastewaters generated from shale gas operations [39, 40]. The performance of six commercially available hydrophobic microfiltration membranes was compared in a direct contact membrane distillation (DCMD) system for treating wastewater with up to 300,000 mg/L total dissolved solids (TDS) [39]. All membranes showed excellent rejection of dissolved ions, including naturally occurring radioactive material (NORM), which is a significant environmental concern with this high salinity wastewater [39].

1.2 MEMBRANE DISTILLATION FOR DESALINATION OF HIGH SALINITY WASTEWATERS

Desalination has emerged as a promising solution to address the world's water scarcity problem by removing dissolved salts from saline or brackish water, thus making it applicable for a number of water sources and uses [41, 42]. Membrane-based processes such as reverse osmosis (RO) and electrodialysis (ED) and thermal processes such as multi effect distillation (MED), multi stage flash (MSF), and vapor compression distillation (VCD) are the two main categories of commercial desalination technologies with RO and MSF accounting for 78% of the desalination capacity worldwide [43]. However, RO is limited to about 40,000 mg/l of total dissolved solids (TDS) in the feed as the hydraulic pressure required for RO systems can be up to 380 bar at the solubility limit of sodium chloride [44]. Among thermal based desalination technologies, membrane distillation (MD) shows the most promising performance for desalination of high salinity wastewaters [45]. Over the past two decades, there have been noticeable improvements in the design of membranes and technical performance of this technology [46]. Prior studies have shown that MD has the potential to achieve up to 99.9% of salt rejection [47-50] and 99.5% rejection of organic materials [51, 52]. These characteristics make MD one of the most promising technologies for treatment of high salinity wastewaters. Membrane distillation operates at near ambient pressure and requires significantly lower capital investment [41]. Desalination of saline waters using different configurations of membrane distillation has been studied extensively [53-57]. With low operating temperatures, relatively low fouling propensity and lower energy requirements for pumping compared to pressure driven membrane processes, membrane distillation may be an attractive alternative for treatment of high salinity wastewaters. MD has been shown to be effective in removing heavy metals from wastewater [58] and concentrating radioactive waste [59] so that the concentrate could be disposed safely. Direct Contact Membrane Distillation (DCMD), where both the hot feed and the recirculating cold permeate are in direct contact with the membrane, has been evaluated for desalination of sea water [47, 54, 60] as well as fruit juice concentration [61-63] and acid recovery [64]. A previous study has demonstrated the potential of membrane distillation to treat very high salinity wastewaters generated from shale gas operations [39]. The performance of six commercially available hydrophobic microfiltration membranes was compared in a direct contact membrane distillation (DCMD) system for treating wastewater with up to 300,000 mg/L total dissolved solids (TDS). All membranes showed excellent rejection of dissolved ions, including naturally occurring radioactive material (NORM), which is a significant environmental concern with this high salinity wastewater [39].

1.3 MARCELLUS SHALE PLAY

Marcellus Shale (Figure 3) is a major natural gas (NG) reservoir with steadily increasing production since 2008 that currently accounts for about 40% of the total U.S. shale gas production [65]. Natural gas extraction from the Marcellus shale in Pennsylvania, West Virginia and Ohio is accompanied by large amounts of produced water that contains high total dissolved solids (TDS). Figure 4 shows shale gas production in different shale plays in the U.S. from 200-2016 [66]. Figure 5 and Figure 6 show shale gas production and flowback and produced water generation in Pennsylvania [30].

Future extraction of shale gas requires economical management of wastewater while also minimizing potential environmental impacts. Produced water injection into Class II Underground Injection Control (UIC) wells is the dominant management alternative in many shale plays with sufficient disposal capacity [15, 67, 68]. There are a total of about 144,000 Class II disposal wells in the U.S. with the majority of wells located in Texas (50,000 wells), California, Kansas, and Oklahoma [69]. Salt water disposal (SWD) wells account for 20% of total disposal wells of which 12,000 are located in Texas, 800 in Oklahoma, and only 8 in Pennsylvania [69]. In the Marcellus shale region, the average cost of produced water transportation from the well site in Pennsylvania to injection wells in Ohio or West Virginia ranges from 10 to 20 $/barrel (bbl) [70, 71]. In addition, the costs associated with deep well injection is estimated at $1/bbl [70]. Lack of sufficient disposal capacity in Pennsylvania requires the development of alternative approaches for management of high TDS produced water [72]. In areas of limited disposal capacity (e.g., Pennsylvania) or where water resources are stressed (e.g., Texas and Oklahoma), reuse and recycling of produced water is an attractive alternative to direct underground injection of produced water. Recent studies have also documented concerns over induced seismic activities due to deep well injection [73-76], further emphasizing the need for the development of innovative management strategies for produced water to avoid unintended environmental consequences. Management strategies such as injecting wastewater into disposal wells, residual waste processing and reuse, roadspreading, and landfilling that are currently used in Pennsylvania may not guarantee the long-term sustainability of shale gas development [30].

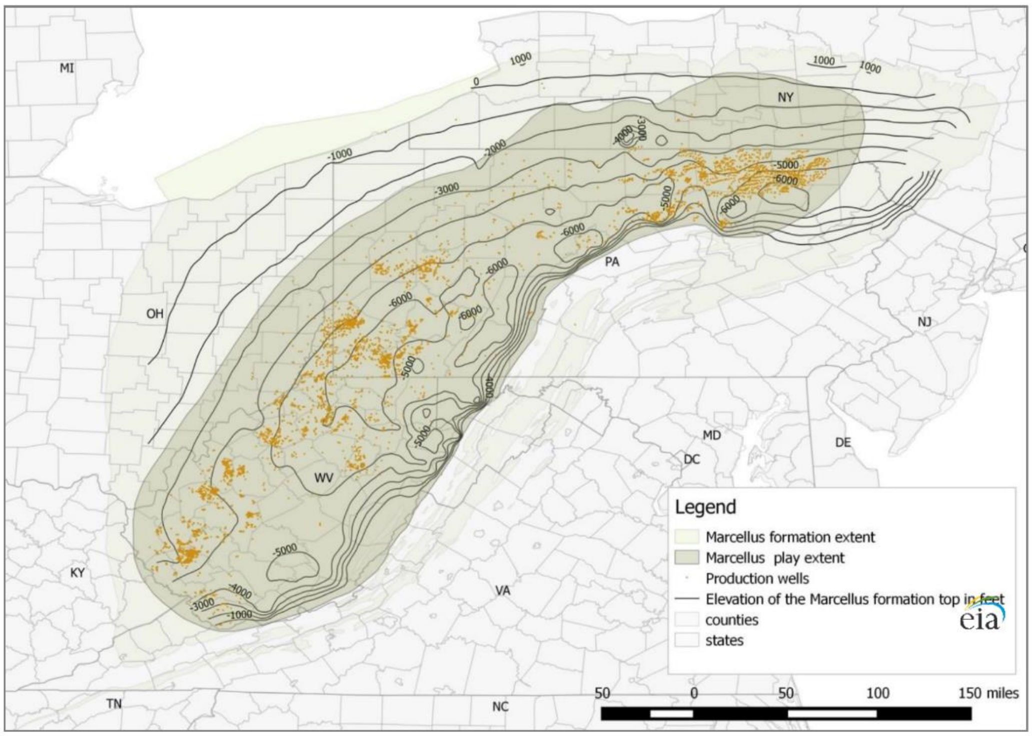

Figure 3. Structure map of Marcellus formation [77]

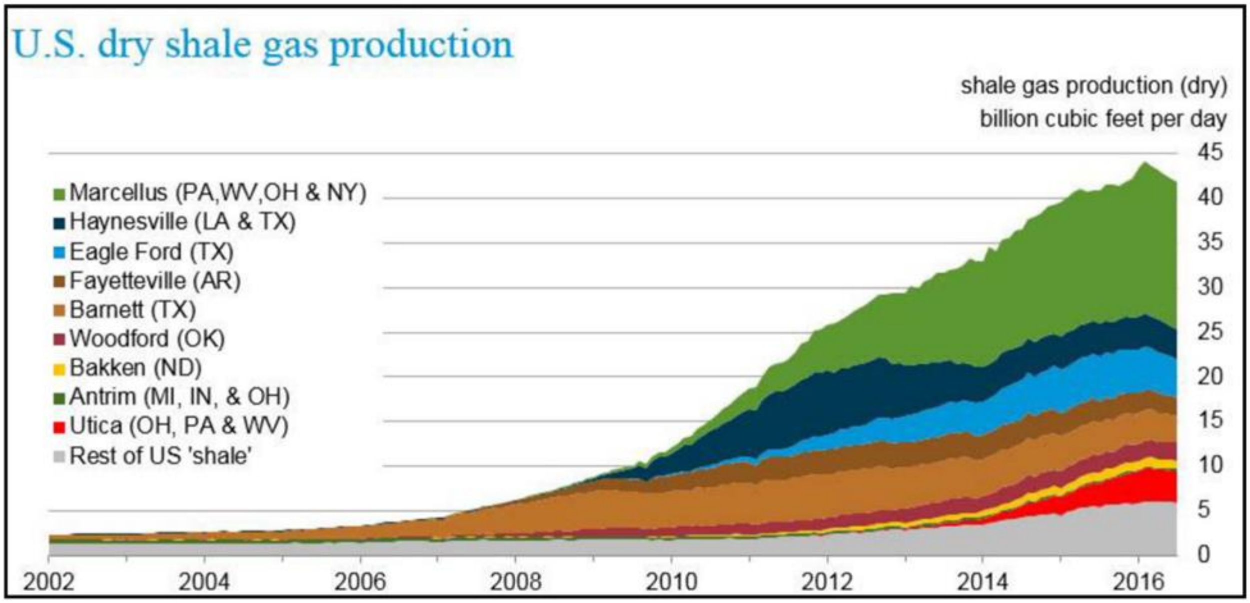

Figure 4. U.S. Energy Information Administration (EIA) official shale gas production data through July 2016 [78]

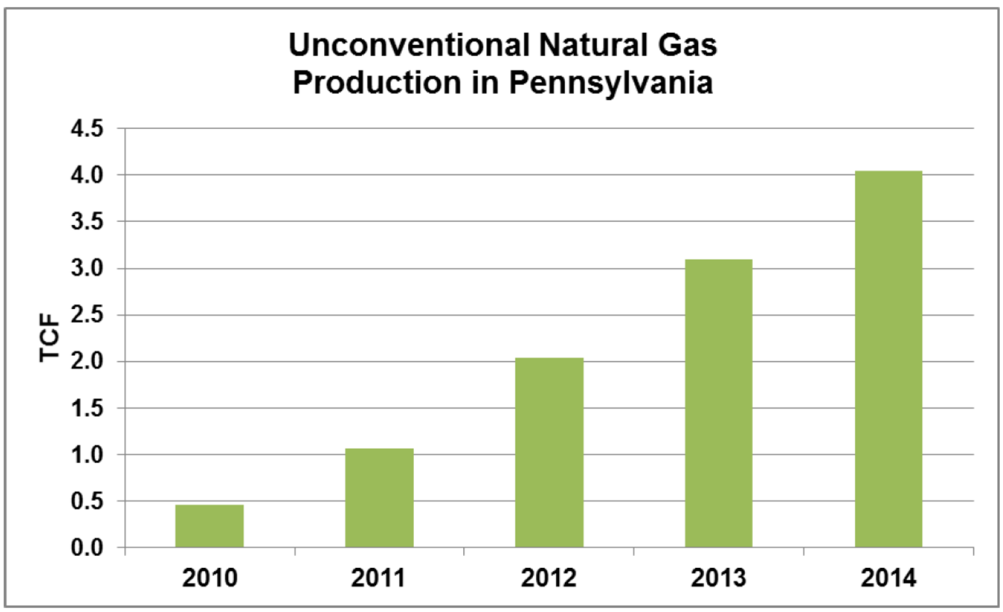

Figure 5. Shale gas production in PA from 2010-2014 stated as trillion cubic feet (TCF) [30]

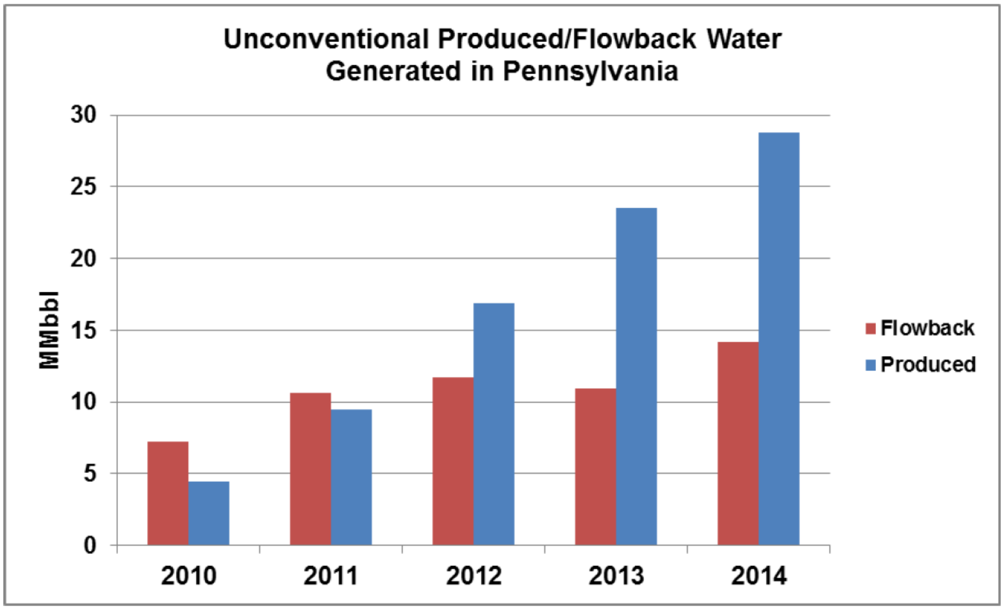

Figure 6. Flowback/produced water generation in PA from 2010-2014 stated as million barrels (MMbbl) [30]

1.4 SYSTEMS LEVEL OPTIMIZATION

Understanding the potential economic impacts of shale gas produced water treatment prior to its widespread commercialization and use is pivotal for avoiding unintended consequences and for guiding the sustainable development of the shale gas industry. As such, techno-economic assessment (TEA) is performed to evaluate the economics of produced water treatment using MD under two scenarios: 1) base case in which thermal energy requirements of the treatment process are met by adding external steam to the process and 2) waste heat integration scenario in which thermal energy requirements for the MD process are met by integrating the treatment process with available waste heat sources at NG CS.

Moreover, holistic assessment of the economic impacts of shale gas wastewater treatment in comparison to other management strategies is imperative. Systems-level optimization has emerged as the prevalent methodological framework for optimal design of shale gas supply chain. Accordingly, a systems-level optimization model is developed in this study that takes into account associated costs of treatment, transportation, and injection of different strategies for shale gas wastewater management, thus aiding to identify the optimum management strategy for a given shale play.

1.5 OBJECTIVES OF THIS STUDY

Several studies evaluated the use of MD to treat high salinity produced water from steam assisted gravity drainage process [79-81], oilfield produced water [82], coal seam gas produced water [83, 84] and produced water generated from natural gas exploration [85]. The feed water used in these studies had total dissolved solids (TDS) ranging from 4,000 to 70,000 mg/l and was concentrated up to 230,000 mg/l [85]. However, none of the studies with oil and gas produced waters included a comparison of different hydrophobic membranes or discussed the potential for membrane fouling by inorganic deposits that are likely to form at high water recoveries and after a prolonged period of operation.

DCMD was evaluated for treatment of high salinity wastewaters from unconventional gas extraction. Initial screening of hydrophobic membranes to select the most promising ones in terms of mechanical stability and permeate flux also evaluated the key membrane parameters that affect its permeability. The morphology and composition of the inorganic deposit formed on the membrane surface when actual produced waters are concentrated up to halite saturation were assessed together with their impact on permeate flux and quality.

Due to low operating temperatures, MD could be employed using solar energy or waste heat to increase the temperature of the feed solution [86]. While many studies reported that integrating MD with waste heat sources can lower its operating cost [41, 87, 88], the focus of those studies was often on a qualitative understanding without identifying specific sources of waste heat or conducting a systems analysis to evaluate the feasibility of integrating full scale MD technology with actual waste heat sources. Furthermore, there are no studies in the literature that are focused on the feasibility of MD technology utilizing waste heat for treatment of high salinity produced water from shale gas extraction.

Relatively abundant and unutilized source of waste heat is available at existing natural gas compressor stations (NG CS) in the U.S. [89]. This study evaluated the synergies and potential of MD technology for treatment of shale gas produced water utilizing this specific source of waste heat. A mathematical model based on the fundamentals of heat and mass transfer processes was developed and calibrated for a DCMD process using laboratory-scale experiments. The model was then used to optimize the design and operating parameters of a full-scale DCMD system. The energy analysis from this model was combined with the information about available waste heat at NG CS in Pennsylvania (PA) region of Marcellus shale to estimate the amount of produced water that can be treated in distributed DCMD wastewater treatment plants. Results from this study provide important insights in the operation of an integrated system and can be extended to other sources of industrial waste heat combined with other thermally-driven water treatment technologies.

While MD offers several advantages over other desalination techniques, techno-economic assessment is necessary to evaluate the economic feasibility of MD for treatment of shale gas produced water treatment. To date, little emphasis has been placed on evaluating the economic performance of MD technology for treating produced water. As such, TEA is also needed to develop a comprehensive understanding of the cost drivers for MD treatment of high salinity shale gas wastewaters.

1.6 RESEARCH OBJECTIVES

The goals of this research are to investigate the water-energy nexus opportunities in shale gas wastewater management. This work will utilize metrics and methodologies derived from multiple disciplines including thermodynamics, applied statistics, economics, industrial ecology, and systems engineering. This interdisciplinary approach allows for a broader understanding of an emerging produced water management technology and potential environmental implications and tradeoffs of commercial scale adoption of this technique as compared to business-as-usual management strategies. *Specific objectives include:*

1. Investigate the waste heat recovery opportunities from NG CS on a state level in the U.S. via thermodynamic modeling of the waste heat generation process while accounting for the uncertainty in operating hours of NG CS and the type of compressor engines.
2. Perform techno-economic assessment (TEA) of MD for shale gas produced water management under two scenarios: a) base case scenario with process heating requirements met by external steam b) integration of MD with waste heat available at NG CS.

3. Estimate the theoretical treatment capacity at individual NG CS using the amount of available waste heat at each station and specific heat requirements for treatment of produced water using MD.
4. Propose and develop an optimization framework to determine the most economical shale gas produced water management strategy while including regional opportunities for integration of MD technology with available waste heat at NG CS in Marcellus shale play.

1.7 ORGANIZATION OF DISSERTATION

The dissertation is organized as follows:

Chapter 2 presents the energy and exergy content of available waste heat at Natural Gas Compressor Stations (NG CS), avoidable life cycle greenhouse gas (GHG) emissions by using available waste heat at NG CS, and electricity generation potential of available waste heat at NG CS for 1,380 nonzero capacity compressor stations in the lower 48 states in the U.S. For each compressor station, comprehensive thermodynamic modeling is performed to estimate the quantity and quality of available waste heat in the exhaust stream of Gas Turbine (GT) and Internal Combustion (IC) compressor engines. Monte Carlo simulation is conducted to capture the uncertainty in the operating hours of compressor stations as the operation of NG CS may not be continuous due to daily or seasonal variability in gas demand.

Chapter 3 develops a Techno-economic Assessment (TEA) model to evaluate the economic feasibility of membrane distillation (MD) for shale gas produced water treatment under two scenarios: (1) base case with external purchase of steam and (2) integrating MD with waste heat from flue gas at NG CS. TEA model accounts for capital as well as operating and maintenance costs for a hypothetical MD plant. This work also compares total cost of treatment with the most common produced water management strategy at shale gas plays in the nation to provide a broader understating of the economics of produced water treatment.

Chapter 4 develops an optimization framework for integrated shale gas produced water treatment. Management alternatives ranging from direct disposal in Class II injection wells to advanced centralized MD plant, treatment plants at NG CS, and onsite MD treatment units are evaluated. The model accounts for associated cost of transportation, treatment, and injection of produced water with each management strategy in order to find the optimum management strategy for four counties in Pennsylvania (PA).

Chapter 5 summarizes the main conclusions of this dissertation and provides direct for future work.

Additional information including detailed calculations and tabulated datasets are provided in the Appendices. Supporting information (S.I.) for Chapter 2 is provided in Appendix A, and S.I. for Chapter 3 is provided in Appendix B.

1.8 INTELLECTUAL MERITS AND BROADER IMPACTS

The results of this dissertation aid in identifying which management strategies are best suited for Marcellus shale play in Pennsylvania; and provide a broader understanding of regional water-energy nexus opportunities in shale gas development. Further, the findings of this research identify potential opportunities for advanced treatment of shale gas wastewater using waste heat sources and provide insights regarding the economics of produced water treatment with and without integrating waste heat sources to the treatment process. This broad-based approach allows for a comprehensive examination of the economics of BAU management strategies as compared to more novel sustainable strategies—information that is pivotal for guiding the sustainable development of shale gas industry. Additionally, this research advances the concepts and framework of shale gas sustainable development via the development, utilization, and coupling of rigorous thermodynamic modeling, statistical models, detailed techno-economic modeling, and systems-level optimization. The body of this work takes the form of several peer-review articles that are at various stages of publication during the final writing herein:

Refereed Journal Articles

1. Lokare, O. R.; Tavakkoli, S.; Khanna V.; Vidic, R. D., Importance of Feed Recirculation for the Overall Energy Consumption in Membrane Distillation Systems. *Desalination* **2018**, 428, pp 250-254

2. Tavakkoli, S.; Lokare, O. R.; Vidic, R. D.; Khanna, V., A Techno-economic Assessment of Membrane Distillation for Shale Gas Produced Water. *Desalination* **2017**, 416, pp 24-34. (Chapter 3 in Thesis)

3. Lokare, O. R.; Tavakkoli, S.; Khanna V.; Vidic, R. D., Fouling in Direct Contact Membrane Distillation of Produced Water from Unconventional Gas Extraction. *Journal of Membrane Science* **2017**, 524, pp 493–501.

4. Lokare, O. R.; Tavakkoli, S.; Rodriguez, G.; Khanna, V.; Vidic, R. D., Integrating Membrane Distillation with Waste Heat from Natural Gas Compressor Stations for Produced Water Treatment in Pennsylvania. *Desalination* **2017**, 413, pp 144-153

5. Tavakkoli, S.; Lokare, O. R.; Vidic, R. D.; Khanna, V., Systems-Level Analysis of Waste Heat Recovery Opportunities from Natural Gas Compressor Stations in the US. *ACS Sustainable Chemistry & Engineering* **2016**, 4 (7), pp 3618–3626. (Chapter 2 in Thesis)

Manuscripts in preparation

1. Tavakkoli, S.; Lokare, O. R.; Vidic, R. D.; Khanna, V., Shale Gas Wastewater Management Using Membrane Distillation: An Optimization Based Approach. Expected Submission February **2018**

2. Tavakkoli, S.; Chopra, S. S.; Khanna, V., Unraveling the Structure and Resilience of the United States Aviation Network. *RSC Open Science*, **under review**

Specific Research Questions (RQ) and the corresponding chapter in which they are addressed are provided in Table 2 below:

Table 2. Research Question (RQ) and corresponding thesis chapter in which they are addressed

#	Research Question (RQ)	Paper	Chapter
1	How much waste heat is available at natural gas compressor stations (NG CS) in the U.S.? What is the quality of available waste heat? What is the geographical distribution of available waste heat across the contiguous United States? What are the environmental sustainability implications of recovering available waste heat?	Tavakkoli, S.; Lokare, O. R.; Vidic, R. D.; Khanna, V., Systems-Level Analysis of Waste Heat Recovery Opportunities from Natural Gas Compressor Stations in the US. *ACS Sustainable Chemistry &*	CH2

Table 2 (continued).

		Engineering 2016, 4 (7), pp 3618–3626.	
2	What is total cost of produced water treatment using membrane distillation (MD) with and without integrating available waste heat from natural gas compressor stations (NG CS)?	Tavakkoli, S.; Lokare, O. R.; Vidic, R. D.; Khanna, V., A Techno-economic Assessment of Membrane Distillation for Shale Gas Produced Water. *Desalination* 2017, 416, pp 24-34.	CH3
3	What is the optimum strategy for produced water management in Pennsylvania? How does cost of produced water treatment using onsite membrane distillation (MD) units and centralized MD plants compare with other strategies such as business-as-usual (BAU) management strategy which is direct disposal into salt water disposal (SWD) wells and installing treatment units at natural gas compressor stations (NG CS) where available waste heat could be utilized to offset the energy requirements of MD process?	Tavakkoli, S.; Lokare, O. R.; Vidic, R. D.; Khanna, V., Shale Gas Wastewater Management Using Membrane Distillation: An Optimization Based Approach. Expected Submission February 2018	CH4

Chapter 2 is the peer reviewed version of the following article:

Tavakkoli, S.; Lokare, O. R.; Vidic, R. D.; Khanna, V., Systems-Level Analysis of Waste Heat Recovery Opportunities from Natural Gas Compressor Stations in the US. *ACS Sustainable Chemistry & Engineering* **2016**, 4 (7), pp 3618–3626. DOI: 10.1021/acssuschemeng.5b01685

which has been published in final form at http://pubs.acs.org/doi/abs/10.1021/acssuschemeng.5b01685. This article may be used for non-commercial purposes in accordance with ACS Publications Terms and Conditions for Self-Archiving.

2.0 A SYSTEMS-LEVEL ANALYSIS OF WASTE HEAT RECOVERY OPPORTUNITIES FROM NATURAL GAS COMPRESSOR STATIONS IN THE U.S.

2.1 INTRODUCTION

Depleting fossil fuels and heightened awareness of climate change have accelerated efforts for alternative energy sources and energy efficiency improvements [90, 91]. At the national level, approximately 62% of the primary energy consumed in the United States is dissipated as waste heat [92]. As such, recovery and productive use of waste heat offers a promising means for mitigating reliance on greenhouse gas (GHG) intensive fossil fuels. The industrial sector is responsible for about one third of total energy use and fossil fuel related GHG emissions in the Unites States. Simultaneously, about 20-50% of the energy consumed in industrial manufacturing processes is ultimately lost as unrecovered waste heat [93]. While developing alternative energy sources is critical for reducing dependence on fossil fuels and a secure energy future, recovery and reuse of waste heat is particularly attractive for improving the overall energy efficiency and environmental impacts of existing industrial processes [94].

The majority of waste heat in industrial processes escapes via combustion exhaust gases, cooling water systems, and sidewall losses. Although industrial waste heat is a relatively abundant source of energy, it often has a low quality (at temperatures below 450^0 F) [93] making it uneconomical and impractical to recover for most heat transfer applications [93]. One approach is to capture and reuse this low quality waste heat to meet the thermal energy demands of low temperature processes, thus minimizing the high exergy loss in converting high grade fossil fuels to low grade energy uses such as space heating and water heating [91]. However, the economic and technical viability of such waste heat recovery technologies still remains uncertain, which in turn, limits their effectiveness and application.

Previous research has focused on minimizing waste heat losses and improving energy efficiency in the industrial sector by employing heat recovery technologies. Existing studies have quantified the potential for waste heat recovery in different processing steps of distinct industrial sectors such as glass manufacturing [95, 96], cement manufacturing [95, 97, 98], iron and steel manufacturing [99, 100], textile industry [101], aluminum production [95, 102], metal casting [103, 104], industrial boilers [105], and ethylene furnaces [105]. Goswami and Kreith provided a comprehensive overview of waste heat recovery potential and associated economic benefits resulting from about 70 waste heat recovery analyses in North America including paper, petroleum, food, minerals, and metals industries [106]. They concluded that annual economic savings of $150 million could be realized if waste heat recovery is employed in the manufacturing sector [106]. A recent study by the U.S. Department of Energy (U.S. DOE) quantified the amount of available waste heat in industrial manufacturing processes and concluded that a total of about 1.6 million TJ (Tera Joules)/yr remains unrecovered in exhaust gases [93].

Waste heat available at thermoelectric power plants has garnered particular attention primarily because of the significant portions of primary energy dissipated as low grade heat. Butcher and Reddy [107] evaluated the efficiency of waste heat recovery based power generation systems using the second law of thermodynamics. They investigated the effect of different operating conditions on heat recovery efficiency and concluded that gas inlet temperature and composition significantly influence the efficiency of power generation using waste heat in thermoelectric power plants [107]. Morrow et al. developed a theoretical model to quantify the available waste heat in three different energy streams in a typical thermoelectric power plant: (1) boiler blowdown, (2) steam diverted from bleed streams, and (3) the cooling water system. They further evaluated the potential for using waste heat streams to run a membrane distillation system.[108, 109] More recently, Gingerich and Mauter evaluated the quantity, quality, and spatial availability of waste heat from thermoelectric power plants.[110] Using the plant level data from Energy Information Agency (EIA), they estimated a total of 18.9 billion GJ_{th} (thermal Giga Joules) of residual heat to be available at power plants, 4% of which is discharged at temperature of 90°C or more.

A relatively poorly understood source of high-grade waste heat are the existing natural gas (NG) compressor stations (CS) in the U.S. The U.S. NG pipeline network is a highly integrated transmission and distribution grid comprised of more than 300,000 [111-113] miles of interstate and intrastate transmission pipelines. To boost and maintain the pressure for forward movement of NG flowing through the pipeline network, 1,799 [111, 113, 114] CS with over 17

[111] million installed horsepower (see Figure 7) are located within this network. The pipeline network moves approximately 25 [115] trillion cubic feet (Tcf) of NG annually to residential, commercial and industrial consumers in the lower 48 States [111]. In each CS, a portion of the NG flowing through the network is combusted to provide energy for compressor engine to pressurize and move the gas through the system. While the size and layout of NG CS vary widely, all CS are comprised of two basic components: a compressor for enhancing the pressure of NG and a mechanical drive [116] used to provide power for the compressor. Internal Combustion (IC) and gas turbine (GT) engines are the two main types of mechanical drive at existing NG CS. Electric motors are not used widely in the U.S. as most NG CS are in remote locations where providing a reliable source of electricity is an operating challenge. Concurrently, about two-thirds of the fuel energy consumed by IC engines and GT is lost as waste heat mainly in the form of high temperature (>800^{0}F) [117] exhaust combustion gases that are ideally suited for heat recovery [118]. However, to date, there has been little emphasis on identifying waste heat recovery potential at existing NG CS.

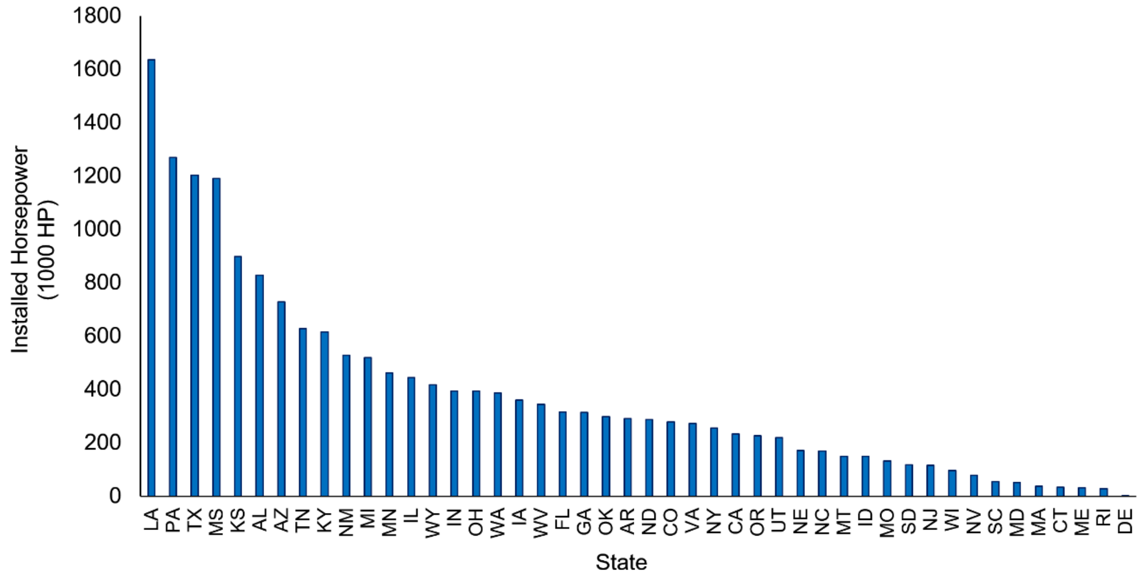

Figure 7. Installed horsepower (HP) at NG CS by state in 2008. Data was obtained from United States Energy Information Administration (EIA)

Previous studies on waste heat has mainly focused on optimizing operation and planning of NG CS [119-123] or minimizing the fuel consumption [124, 125]. Wu et al. proposed a mathematical model to optimize the fuel cost in a network of CS by considering pressure drops at each CS and mass flow rate at each pipeline leg [126]. Ohanian and Kurz analyzed series and parallel arrangements of compressor units in a CS to determine the optimum outlet pressure mode [127]. A 2008 study by the International Natural Gas Association of America (INGAA) evaluated the energy recovery potential of the U.S. NG pipeline network [128]. The study identified the technical and economic factors affecting the energy recovery potential for three options including waste heat recovery for (1) power systems in pipeline compressor drivers, (2) turbo-expanders for pressure letdown recovery, and (3) turbine inlet air-cooling. However, the INGAA study only considered CS with an installed capacity of at least 15,000 HP and an annual load factor at or above 60% for economic viability considerations.

Given the increasing role of NG as a source of primary energy in the U.S. energy mix and the critical need for less-costly energy resources, as well as a desire to mitigate energy related carbon emissions and associated environmental impacts, this work develops a systems-level approach to quantify the available waste heat at existing NG CS in the United States. Using actual data on installed capacity and spatial location of NG CS, we utilize rigorous thermodynamic and Monte Carlo uncertainty analysis for a comprehensive assessment of quantity, quality, and spatial availability of waste heat at existing NG CS. This work serves to add to the existing thin body of literature on waste heat recovery opportunities in the U.S. with a specific focus on NG CS, a highly underappreciated source of high temperature waste heat. The results from this investigation provide several important insights including (1) quantifying the magnitude and spatial availability of waste heat at the state level in the U.S., (2) quantifying the potential of NG CS waste heat in reducing life cycle greenhouse gas emissions, (3) discussing the potential beneficiary end uses for the NG CS available waste heat. These insights can be synthesized with prior studies to inform policy decisions into synergistic energy recovery and environmental improvement opportunities.

2.2 MATERIALS AND METHODS

2.2.1 Compressor stations capacity and uncertainty quantification

There are several steps and challenges in estimating the available waste heat at NG CS. The first step involves acquisition of installed capacity of NG CS. We acquired actual installed horsepower (HP) and spatial location of all NG CS in the U.S. via personal communications with contacts at the U.S. Energy Information Administration (EIA) [129]. Based on EIA report, a total of 1,380 non-zero capacity CS were operating in lower 48 states in 2008 which is in close agreement with a recent study that estimated a total of 1,375 CS on the national level [114]. While other data sources such as the Environmental Protection Agency's Greenhouse Gas Inventory (EPA GHGI) publish more updated information on NG CS [130], location and capacity information for individual CS are not included in these data sources. The installed horsepower of CS aggregated at the state level is shown in Figure 7. The operation of NG CS may not be continuous and is dependent on several factors including daily or seasonal variability in gas demand as well as the capacity of stations. In order to obtain realistic estimates of available waste heat, real data on cyclic operation including annual volume of NG processed at CS is required. However, such operating data is not publicly available and is almost impossible to obtain for individual CS. We address this challenge by considering the installed capacity of each CS and the concept of load factor. Load factor refers to the fraction of time per year the NG CS are actually operating compared to the maximum possible operating time. Based on personal communications with oil and gas companies [131, 132] and Interstate Natural Gas Association of America (INGAA), we account for underlying uncertainty in load factor by representing it using a triangular [133] probability distribution function (PDF) with a minimum value of 20% [133], maximum of 90% [131-133], and mode of 50% [133] instead of considering a single point estimate. Next, we employ Monte Carlo uncertainty analysis with 10,000 trials to randomly sample from the triangular PDF to capture the uncertainty in load factor. A broader understanding of the expected range of available waste heat at NG CS is achieved by addressing uncertainty in a stochastic manner.

2.2.2 Compressor stations mechanical drive type and uncertainty quantification

The type of compressor engine information for all 1,380 NG CS is not publicly available and is critical for quantifying available waste heat from NG CS. In order to obtain realistic estimates of available waste heat, we need to classify each compressor station by type of compressor engine (i.e., GT, IC engine, or electric motor). This information is virtually impossible to obtain for every single operating NG CS. We address this challenge by using a sample of 382 compressor stations with the capacity and type of compressor engine information provided in a recent study by Zimmerle and co-workers [114]. Utilizing the information provided by Zimmerle et al. for 382 NG CS, we develop a statistical pattern recognition approach to assign the type of compressor engine to all compressor stations. We use the concept of k-nearest neighbors algorithm to find the probability of having a specific type of compressor drive within a specific range of capacities [134]. To identify the engine type of a CS, this algorithm chooses the type to which the majority of the CS neighbors (i.e., CS with similar capacities) belong to, with the CS being assigned to the type of compressor engine most common among its k nearest neighbors. Using 90% of the data points in the 382 CS data set available from Zimmerle et al. as the training set, we develop a probability distribution of having a specific type of engine within various predefined capacity ranges. The remaining 10% of the data points in the 382 data set serve as the validation set and are utilized to test the validity of the model. The capacity range size is updated in each trial of the model to get an accuracy of greater than 85% in predicting the type of engine in the validation set. The resulting probability distribution pattern is provided in the Appendix A (Table 5).

It is important to note that all compressor engines in the available data set from Zimmerle et al. are either GT or IC engine and no electric motor compressor engine is reported in the data. Accordingly, we classify each NG CS as either GT or IC engine. However, a recent study [114] suggests that up to 9% of NG transmission compression capacity is accomplished by electric motor based compressor engines. While waste heat estimate for electric motor CS is likely different than the results of this work and merits further investigation, their relative compression capacity is marginal compared to GT or IC CS and thus does not alter the broad-based conclusions of this study.

2.2.3 Operation of NG CS and thermodynamics-based waste heat estimation

2.2.3.1 Gas turbine CS

Figure 27 in the Appendix A shows a process schematic of a typical NG CS. At each CS, a portion of the NG flowing through the pipeline system (typically about 2-5%) [122, 126] is burned in a combustion unit to provide the energy required for the operation of the compressor engine (gas turbine). Gas turbine supplies the energy required to drive the NG through the gas network by compressing NG in the compressor unit. This process releases waste heat in the form of exhaust gas from the gas turbine [135]. We analyze the quantity and quality of available waste heat by a combination of thermodynamic analysis and best available engineering knowledge as follows. It is important to note that the waste heat in this study considers the thermal energy in the exhaust gas of compressor engine, and does not account for losses via conduction, convection, or radiation from hot surfaces and heated equipment.

We assume that the output power of gas turbine ($\dot{W}_{turb}$) is equal to the installed capacity of CS ($\dot{W}_{comp}$) (equation 1). In equation 1, we assume a mechanical efficiency of 100% for gas turbine which is a conservative assumption for estimating the amount of waste heat and is consistent with the existing literature [136]. As such, the resulting estimates of available waste heat at NG CS are conservative lower bounds. The generated power by a gas turbine is a function of the difference between input enthalpy (h_{in}) and output enthalpy (h_{out}) and the mass flow rate ($\dot{m}$) of combustion gases as shown in equation 2 [137]. In addition, enthalpy of combustion gases is a function of temperature as shown in equations 3 and 4.

$$\dot{W}_{comp} = \dot{W}_{turb} \tag{1}$$

$$\dot{W}_{turb} = \dot{m}(h_{in} - h_{out}) \tag{2}$$

$$h_{in} = f(T_{in}) \tag{3}$$

$$h_{out} = f(T_{out}) \tag{4}$$

The inlet stream to the gas turbine comes from the combustion process. In order to find the inlet temperature T_{in} of combustion gases to the turbine, we model the combustion process in the combustion chamber as an adiabatic process by assuming complete combustion of NG with 10% excess air which results in an adiabatic flame temperature of 2140°K (Kelvin). However, gas turbines typically operate with a higher percentage of excess air [138, 139]. As such, we model the combustion process with 100% excess air which results in an adiabatic flame temperature of 1478°K and compares favorably with gas turbine inlet temperature reported in the literature [140]. However, in order to be conservative, we assume a typical inlet temperature of 1400°K for subsequent calculations [141]. Detailed information on natural gas composition and the procedure for determining adiabatic flame temperature is available in Appendix A. The outlet and inlet stream temperatures of gas turbine are related as shown in eq 5 [142] where we assume an isentropic efficiency (η) of 80% [136, 143] for gas turbine. The ratio of specific heat (k) for NG is assumed to be 1.3 and is consistent with the literature values [144, 145]. It is assumed that a typical gas turbine expands the outlet stream pressure (P_{out}) to one fourth of the inlet pressure (P_{in}) [146]. By using equation 5, the temperature of exhaust gas is estimated to be 921°K.

$$\frac{T_{out}}{T_{in}} = [1 + \frac{1}{\eta}((\frac{P_{out}}{P_{in}})^{\frac{k-1}{k}})] \tag{5}$$

We next calculate the mass flow rate of the exhaust flue gas stream. To do so, we first need to calculate the mole fraction and enthalpy content of all species in the flue gas [137].

Assuming the thermal efficiency of gas turbine to be 80%, the mass flow rate of exhaust gases ($\dot{m}$ in equation 2) is calculated and subsequently the total waste heat (WH) is estimated for each CS using eq 6 where h_{in} is the enthalpy of exhaust stream at 921˚K and h_{out} corresponds to the enthalpy of this stream when it is cooled down to 333˚K (60˚C) [93, 147]. Detailed procedure for determining the flue gas composition and enthalpy of each species in the exhaust stream is available in Appendix A.

$$WH = \dot{m}(h_{in} - h_{out}) \tag{6}$$

2.2.3.2 Reciprocating IC engine CS

This section describes the procedure for estimating the temperature, flow rate, and subsequently the amount of available waste heat contained in the exhaust of reciprocating IC engine compressor stations. IC engines include 2-stroke cycle lean-burn, 4-stroke lean-burn, and 4-stroke rich-burn designs [128, 148] differing in characteristic exhaust temperatures ranging from 533 to 922˚K [128] Most IC engines are lean-burn 2-stroke cycle which have lower exhaust temperature [128], as such, we assume an average temperature of 645˚K as the representative flue gas exhaust temperature for IC engines in our analysis based on the existing literature [128]. In an IC engine, four internally reversible processes occur in series representing four principal states of a cycle (see Figure 28 in Appendix A) shown by u_1 to u_4 in equation 7. We calculate the exhaust mass flow rate for each compressor station using equation 7 where W_{cycle} is the net work per cycle m is the mass of air.

$$\frac{W_{cycle}}{m} = (u_3 - u_4) - (u_2 - u_1) \quad (7)$$

We use typical values for minimum, maximum and intermediate temperatures and find the corresponding specific internal energy for each principal state of cycle for IC engines [137]. Then, we assume that total required power by compressor is being provided by the IC engine (W_{cycle}), and calculate the air mass flow rate using equation 7. The mass flow rate of flue gas exhaust is calculated using stoichiometric ratios in the combustion equation (see equation 65 in Appendix A). Next, we calculate the heat content of exhaust gases using the same procedure described for GT compressor drives and assuming that the waste heat is cooled down to 333°K (60°C) [93, 147]. We also quantify the exergy content of available waste heat from NG CS. The detailed procedure and results of exergy calculation are provided in Appendix A.

2.2.3.3 Estimation of available GHG emissions and electricity generation potential of waste heat

We also quantify the life cycle GHG emissions reduction potential associated with the available waste heat at NG CS. We assume that if recovered, the waste heat at NG CS will displace the heat that would otherwise have to be derived by combustion of NG. The life cycle GHG emissions of NG is obtained from the Ecoinvent database [149]. This information is then utilized to quantify the aggregate life cycle GHG reduction potential of NG CS waste heat at the state level. We also quantify the electricity generation potential of available waste heat at NG CS by assuming an overall efficiency of 30% for the power generation process [91, 150, 151]. This efficiency includes real losses for a typical organic Rankine cycle, however, the detailed electricity generation modeling from NG CS waste heat recovery systems is beyond the scope and goal of this work.

Finally, we quantify the life cycle GHG emissions reduction potential associated with electricity generation using the available waste heat at NG CS. We assume that the electricity generated via waste heat will displace the existing generation mix for individual states reported by the EIA [152]. The average life cycle GHG emissions intensity of state-level electricity generation mixes is estimated using the latest state specific electricity mix reported by EIA for the year 2013 [152] and US life cycle inventory (USLCI) database [153].

2.3 RESULTS

Figure 8 shows the estimated quantity of available waste heat from NG CS in the U.S. These results indicate that available waste heat from NG CS range from 0.005 TJ/day in Delaware to 64.7 TJ/day in Louisiana. As shown in Figure 8, the top four states with the maximum amount of waste heat are Louisiana, Pennsylvania, Mississippi, and Texas, which also have the greatest share of total installed horsepower (Figure 7). Collectively, these four states account for 30% of total average available waste heat at NG CS in the U.S. The error bars in Figure 8 represent the 10^{th} and 90^{th} percentile for available waste heat obtained via Monte Carlo simulations to account for uncertainty in load factor.

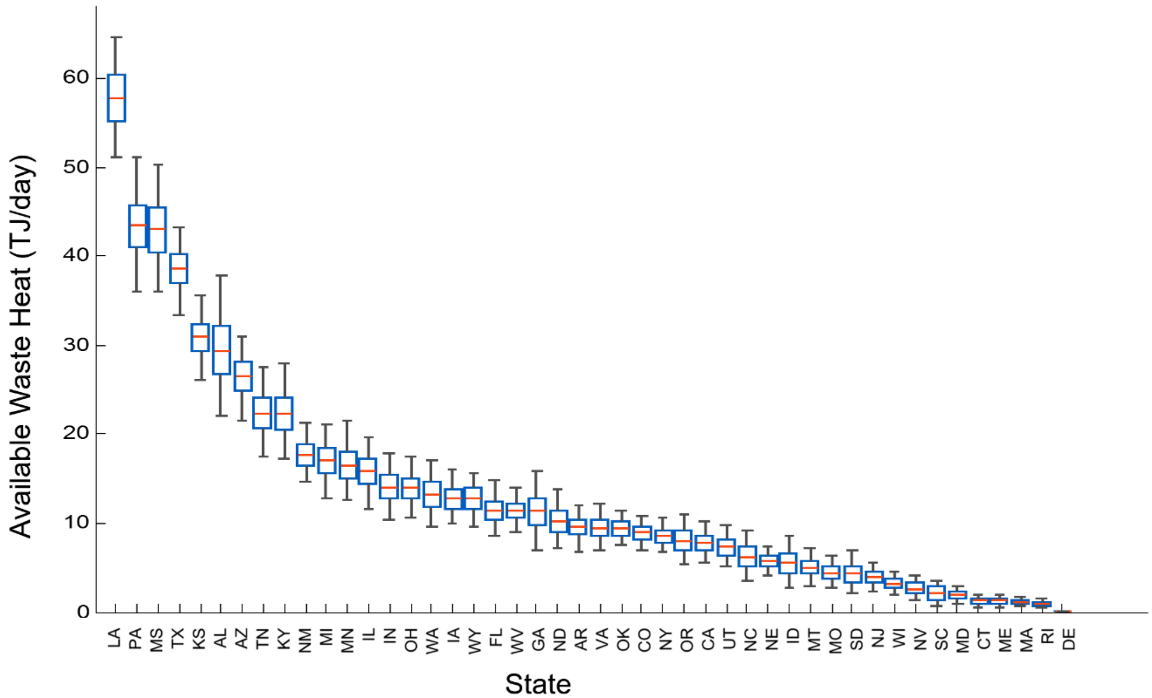

Figure 8. Estimates of available waste heat from NG CS in the U.S. stated as Tera Joules (TJ) per day. The box represents the middle 80% of the data; average value of available waste heat in each state is shown in the middle of each box. Upper and lower whiskers represent the upper and lower 10% of the distribution and extend from the maximum to the minimum value of available waste heat.

The results in Figure 9 show the spatial distribution of available waste heat from NG CS aggregated by states. Average point estimates are reported in Figure 9 and all subsequent analyses involving waste heat including associated GHG emissions reduction and electricity generation potential. The black triangles show the location of CS in each state. No CS are reported to be located in Hawaii, New Hampshire, and Vermont in 2008 and, as a result, these states have zero estimated available waste heat and are not considered in subsequent analyses.

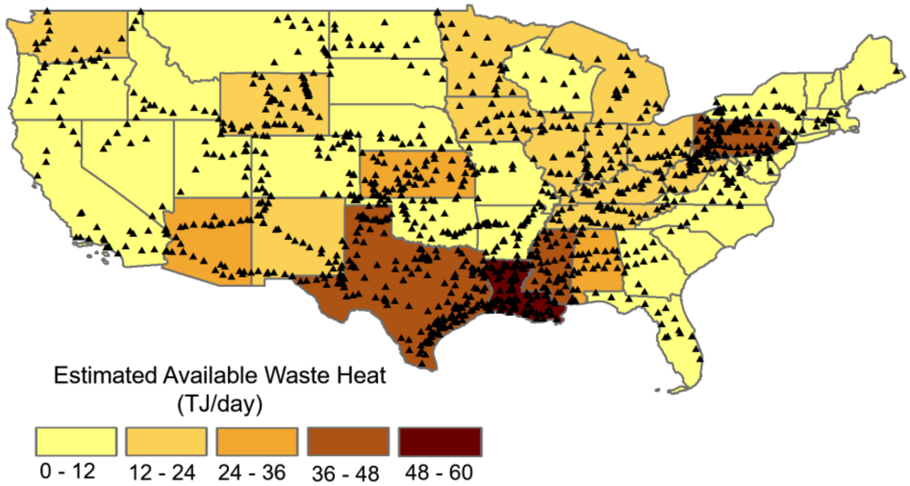

Figure 9. Spatial distribution of estimated available waste heat at NG CS in the U.S. stated as Tera Joules (TJ) per day; Average values obtained via Monte Carlo analysis are shown. Black triangles represent the actual location of CS obtained from the U.S. Energy information Agency.

To provide a broader understanding of the environmental significance of utilizing waste heat, Figure 10 shows the avoidable life cycle GHG emissions potential of waste heat available at NG CS. The avoidable GHG emissions potential ranges from 1 to 4430 metric tonnes of CO_2 equivalent per day. The general trend in Figure 10 mirrors those in Figure 9 with the waste heat available in Louisiana, Pennsylvania, Mississippi, and Texas having the maximum life cycle GHG reduction potential. It is important to note that the results in Figure 10 do not consider the GHG emissions associated with building the infrastructure that would be needed to capture waste heat.

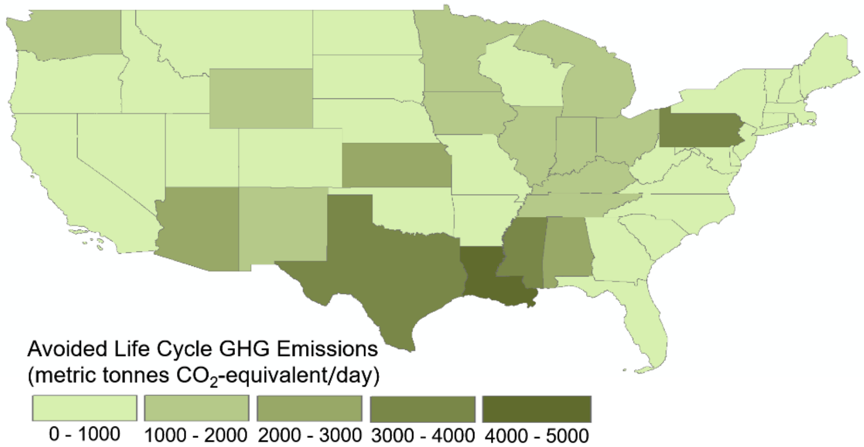

Figure 10. Average avoidable life cycle GHG emissions of available waste heat at NG CS. It is assumed that the available waste heat could substitute the heat generated using NG. Average values of available waste heat obtained via Monte Carlo simulation are used to calculate the avoidable life cycle GHG emissions.

Figure 11 plots the theoretical electricity generation potential of available waste heat at NG CS in the U.S. It also shows the avoidable life cycle GHG emissions if the waste heat were to be utilized for generating electricity. The findings in Figure 11 on the theoretical amount of electricity production potential of waste heat from NG CS compare favorably with prior estimates. For example, our estimates show an electricity generation potential of 21.6 MW from NG CS in North Carolina (NC) state with total installed horsepower of 170,000 HP. This is in close agreement with a prior study that reported an actual electricity production of 26.6 MW from existing power recovery systems at five compressor stations with total installed horsepower of about 176,000 HP [128]. It is important to note that states such as Kentucky (KY), Indiana (IN), and Wyoming (WY) have relatively low electricity generation potential using available waste heat at NG CS but a high carbon footprint of existing electricity generation as the majority of the electricity in these states is currently generated using carbon intensive fossil fuels (details are shown in Table 9 in Appendix A). Additionally, the total amount of avoidable life cycle

GHG emissions by using available waste heat as a substitute for NG is about 47,000 metric tonnes CO_2-equiv./day while the total avoidable life cycle GHG emissions by utilizing waste heat for electricity generation is about 34,400 metric tonnes CO_2-equiv./day. This finding highlights the greater potential of avoidable environmental burdens of utilizing waste heat for direct heat applications.

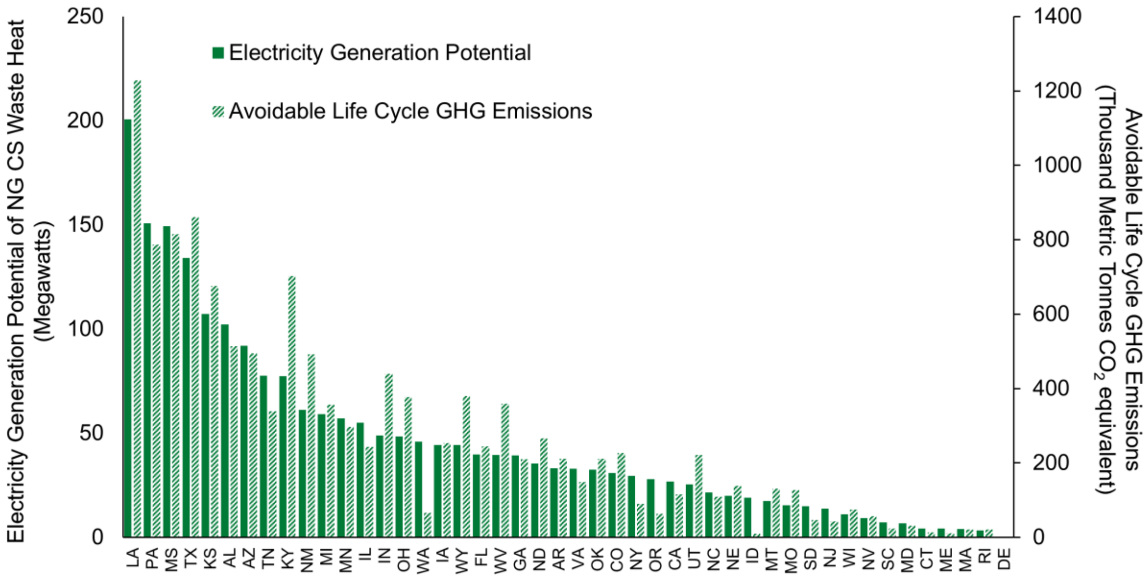

Figure 11. Electricity generation potential of available waste heat from NG CS and accompanying avoidable life cycle greenhouse gas emissions.

2.4 DISCUSSION

This work estimates the quantity and spatial availability of waste heat at NG CS in the United States. An estimated total maximum of 757 TJ/day of waste heat was produced at NG CS in the United States in 2008 with the amount of waste heat varying across states primarily due to differences in installed capacity and load factor. Analysis also indicates that recovering available waste heat at NG CS has the potential to reduce environmental impacts in the U.S. by offsetting consumption of carbon intensive fossil fuels. It is important to note that states such as Pennsylvania, West Virginia, and Ohio have major NG development primarily due to unconventional gas production from Marcellus and Utica shale plays. Unconventional NG production from Marcellus and Utica shale plays accounted for 85% of the increase in total NG production in the U.S. between 2012-2015 and is projected to further increase steadily [154]. This is expected to lead to increases in available waste heat from NG CS as the demand for NG compression capacity is projected to rise to meet the growing NG production in these states. It is important to note that the waste heat recovery potential from existing NG CS is based on the compression capacity as opposed to NG production/consumption data. Although NG production has increased since 2008, it is more likely that the existing CS operate longer hours as these stations are already overdesigned. Furthermore, most of the existing CS roughly have a 50% load factor based on personal communications with oil and gas industry professionals further suggesting that increases in NG flowing through the pipeline network and hence the increased compression requirements are likely to be met via increases in load factor. This uncertainty in load factor is already captured using Monte Carlo analysis and the resulting error bars shown in Figure 8.

Currently more than 60% of energy input to CS is ultimately lost as waste heat in the form of high temperature exhaust flue gases making NG CS a particularly attractive avenue for waste heat recovery. Recovering the waste heat has gained traction and is appealing for its ability to increase the energy efficiency of industrial processes while simultaneously reducing the external fuel input, GHG emissions, and other environmental impacts [155, 156]. However, there has been little emphasis on quantifying and recovering the large quantity of waste heat from existing NG CS, with only one practical example of waste heat recovery at CS [128]. Several technical and economic challenges must be addressed to make waste heat recovery from existing NG CS feasible on a commercial scale. NG CS are very sophisticated systems consisting of several compressor units with different configurations and characteristics, which makes the waste heat recovery a complicated task. Additionally, most existing NG CS do not run continuously and the resulting temporal availability of waste heat raises practical constraints on waste heat recovery. Additionally, the economic feasibility of waste heat recovery is likely to be strongly influenced by the capacity and temporal availability of NG CS and must be evaluated in future studies.

Besides identifying potential sources of waste heat and heat recovery technologies, a comprehensive understanding of waste heat end uses must be established [93]. Typical existing uses of waste heat include preheating combustion air and other feed streams [157] to improve the overall thermal efficiency of heating systems [158, 159]. A large range of waste heat from low to high quality could also be utilized for space heating. Collectively, space heating and water heating are responsible for 38% of low temperature energy consumption in the U.S. [91]. The use of waste heat for space heating offers the advantage of eliminating the need for fuel as well as the space heating equipment [160]. However, temporal and spatial availability of waste heat limits its viable applications. While some NG CS are located adjacent to industrial or commercial users offering the potential for space heating, most NG CS are in isolated locations rendering the waste heat of limited value for space heating unless it is transported. Heat transport has its own set of challenges including significant loss of heat to the environment and varying economic feasibility under fluctuating NG prices [110].

The use of high temperature waste heat available at cement kilns, refineries, and thermoelectric power plants to generate power is another attractive option that is discussed in the literature [161-165]. More recently, selectricity generation using the available waste heat at NG CS has gained attention. However, more research and development is needed to ensure that electricity generation using waste heat at NG CS stations is technically feasible and economically viable. Additionally, it has been argued that power generation using NG CS waste heat is economically feasible for CS with a minimum operating capacity of 15,000 HP thus making electricity generation using NG CS waste heat of limited value as only 30% of compressor stations in the U.S. have installed capacity greater than 15,000 HP. The results presented in our work indicate that a total of 2,100 MW of electricity can be produced from the waste heat available at NG CS. This translates into 0.5% of total electricity generation capacity in the U.S. for the year 2013. Moreover, converting waste heat to electricity is accompanied by high unavoidable exergy losses compared to direct thermal use of waste heat [91].

Many end-uses do not necessarily require the high grade energy inherent to fossil fuels. On-site water/wastewater treatment is a promising application for available waste heat at NG CS. Water treatment technologies such as Forward Osmosis (FO) [166], Reverse Osmosis [167, 168], Multi Effect Distillation (MEF) process [169], and Membrane Distillation (MD) [170, 171], have low thermal energy requirements and offer the potential to be integrated with waste heat sources. It is worth noting that NG pipeline capacity is increasing primarily due to increases in domestic

NG production, demand of NG imported from Canada, and expansion of NG fired electricity generation, which results in expansion of current compression capacity by adding new compressor stations or upgrading existing stations with additional compressor units [172]. Between 1996 and 2006, total installed horsepower of NG pipeline network increased by 653,000 HP. During the same period, 290 NG pipeline expansion projects were completed of which 195 involved expanding the capacity of existing CS or adding new CS. An increase of 1,000-1,500 miles of new transmission pipeline is anticipated to occur each year between 2013 and 2030 in order to meet the U.S. and Canadian NG consumption needs [117]. Subsequently, the compression capacity is expected to follow an increasing pattern with an anticipated increase of 250,000 HP/year [117]. This is expected to translate into a 10 TJ/day increase in available NG CS waste heat between 2013 and 2030, thus further highlighting the importance of potential waste heat recovery opportunities at NG CS in the U.S.

The results of this work provide information about the geospatial distribution of waste heat at NG CS across the U.S. Analysis reveals that a large amount of high quality waste heat is available at existing NG compression stations. Additional research is required to fully understand the technological and economic feasibility, and environmental implications of commercial scale implementation of waste heat recovery at NG CS. Furthermore, a comprehensive evaluation of integrating waste heat to end-uses applications is encouraged as the economic performance of reusing waste heat depends on cost of fuel, electricity, and the distance for transferring the waste heat to its end-use applications [173].

Chapter 3 is the peer reviewed version of the following article:

Tavakkoli, S.; Lokare, O. R.; Vidic, R. D.; Khanna, V., A Techno-economic Assessment of Membrane Distillation for Shale Gas Produced Water. *Desalination* **2017**, 416, pp 24-34.

which has been published in final form at https://doi.org/10.1016/j.desal.2017.04.014. This article may be used for non-commercial purposes in accordance with Elsevier Terms and Conditions for Self-Archiving.

3.0 TECNO-ECONOMIC ASSESSMENT OF MEMBRANE DISTILLAION FOR TREATMENT OF MARCELLUS SHALE PRODUCED WATER

3.1 INTRODUCTION

Desalination has emerged as a promising solution to address the world's water scarcity problem by removing dissolved salts from saline or brackish water, thus making it applicable for a number of uses [41, 42]. Membrane separation based processes such as reverse osmosis (RO) and electrodialysis (ED) and thermal processes such as multi effect distillation (MED), multi stage flash (MSF), and vapor compression distillation (VCD) are two main categories of commercial desalination technologies with RO and MSF accounting for 78% of the desalination capacity worldwide [43]. Among thermal based desalination technologies, novel membrane distillation (MD) shows the most promising performance for desalination of high salinity wastewaters [45]. Specially, over the past two decades there has been noticeable improvements in the design of membranes and technical performance of this technique [46]. Prior studies have shown that MD has the potential for achieving up to 99.9% of salt rejection [47-50] and 99.5% of organic materials removal [51, 52] where most pure thermal processes or pressure driven membrane processes have limited applicability [54, 174], thus making MD one of the most promising technologies for treatment of high salinity wastewaters.

One potential application of MD is for management of high salinity wastewater generated by the rapidly developing unconventional shale gas industry. Unconventional shale gas is a promising energy resource with major economic benefits but is accompanied by a host of environmental challenges including increased level of methane emissions at shale gas production sites [6, 7], and the potential for drinking water [10] and groundwater contamination [11]. One of the critical challenges is the management of vast quantities of high salinity wastewater generated in the process of hydraulic fracturing [175]. Shale gas produced wastewater has significantly higher salinity than seawater and also contains various organic and inorganic fractions including dissolved and dispersed oil compounds and dissolved minerals, toxic metals, and radioactive materials [176-179]. Produced water from Marcellus shale play has an average salinity of 100,000 mg/Liter [18] while typical seawater has salt concentration of 35,000 mg/Liter [180, 181]. This type of wastewater is different from those commonly treated by membrane and thermal based desalination techniques. Subsequently, there is an urgent need to develop new techniques for treating oil and gas industry produced water [82, 176, 182, 183]. Although treatment techniques such as RO and forward osmosis (FO) have been suggested for treating oil and gas produced wastewater [22, 34], their application is expected to be economically infeasible for wastewaters containing more than 40,000 and 70,000 mg/Liter total dissolved solids (TDS), respectively, [15, 26, 35] primarily because of the high osmotic pressure requirements [36, 37]. MD can treat wastewaters with up to 350,000 mg/Liter TDS and can operate at lower temperatures (30-90^{0}C) and pressure relative to conventional desalination technologies [184]. The low operating temperature of MD also makes it ideally suited for integration with renewable energy sources such as wind and solar or low grade waste heat sources [185-188] to make it attractive for treatment of high salinity wastewaters from shale gas activities [184]. This may be of economic interest under rising energy prices as mature commercialized desalination technologies such as MSF and RO require high quality energy sources [189, 190].

While MD offers several advantages over other desalination techniques, techno-economic assessment is necessary to evaluate the economic feasibility of MD for treatment of shale gas produced water treatment. To date, little emphasis has been placed on evaluating the economic performance of MD technology for treating produced water. As such, TEA is also needed to develop a comprehensive understanding of the cost drivers for MD treatment of high salinity shale gas wastewaters. It is important to note that cost estimates are site-specific and vary from installation to installation [191] primarily due to differences in system boundaries, site-specific economic indexes, and life expectancy of the project [191]. As such, comparing the results of different studies as well as drawing conclusions based on studies carried out in a different geographic location requires specific consideration as it can significantly change the real cost of treated water [192].

Previous work on TEA of desalination technologies was focused on economic evaluation of seawater purification using MSF, MED, RO, and MD. The unit cost of water production from seawater by conventional desalination technologies is around \$1.4/m^3 of permeate for MSF [193], \$1/m^3 for MED [193, 194], and \$0.5/m^3 for RO [195]. Previous studies also report a wide range of cost estimates for desalination of seawater using MD with estimates varying from 0.5 \$/m^3 to more than 15 \$/m^3 of purified water [41, 196]. The large difference in cost estimates across studies is attributable to several factors including plant capacity, feed water salinity, and energy sources. Al-Obaidani et al. conducted an extensive exergy analysis and cost assessment for a direct contact membrane distillation (DCMD) unit and identified the most sensitive parameters in MD performance and total cost of water treatment. They performed a TEA for a hypothetical DCMD plant with permeate capacity of 24,000 m^3/day and estimated a water cost of \$1.17/m^3 for DCMD which can be reduced to \$0.5/m^3 if a low-grade thermal energy source is available [196]. Kesieme et al. evaluated the performance of a laboratory scale DCMD unit for desalination of seawater with an overall recovery of about 90%. They also presented a cost analysis framework and reported a cost of \$0.66/m^3 for a hypothetical 30,000 m^3/day DCMD desalination plant [41].

Previous studies have also argued that integrating MD with industrial waste heat has the potential for significant improvements in economic viability of this desalination technology. Sirkar et al. operated a small pilot plant for DCMD based desalination using various configurations of membrane modules and membrane surface area in order to study the plant performance. They reported a permeate production rate achieved of 3.38 m^3/day for feed rate of 92.67 m^3/day and total water cost of \$0.7/m^3 under the assumption that industrial waste heat is available to meet the thermal energy requirements of the MD process [197]. Burrieza et al. performed a TEA for a pilot-scale MD unit (100 m^3/day of permeate) with thermal energy requirements met by solar energy and concluded that solar MD is cost competitive with photovoltaic RO for small plant capacities [198].

While MD holds great promise for treatment of high salinity wastewaters [38] , there has been little emphasis on using MD for treating shale gas produced water with only a handful of recent studies focusing on experimental evaluation of MD for treating this water [80, 81, 85, 199] and only one study on TEA of MD for oilfield produced water [82]. Macedonio et al. concluded that MD has an overall salt and carbon rejection of over 99% and 90% respectively, for treatment of oilfield produced water and estimated that the total water cost varies from \$0.72/m^3 to \$1.28/m^3 depending on feed water temperature and MD recovery factor [82].

Previous research has also proposed a combination of membrane based techniques for enhancing the performance and economics of water treatment process [82, 200-203]. For example, Macedonio et al. have evaluated the economics of seven different configurations of integrated membrane systems including microfiltration, NF, RO, MD, and membrane crystallization and concluded that adoption of integrated membrane systems provides an opportunity for increasing plant recovery factor, reducing the brine disposal problem, and environmental impacts [204].

The business-as-usual (BAU) strategy for shale gas produced water management is injecting produced water into Class II underground injection control (UIC) wells. However, this strategy has come under increased scrutiny because of heightened seismic activity [73, 75, 205, 206] in regions in close proximity to injection wells and potential for groundwater contamination [26]. Underground injection of produced water is also not feasible for shale gas production sites far away from the UIC wells. Finally, with increasing shale gas production, there is a critical need for developing economical and environmentally conscious alternative management strategies for shale gas produced water.

This work presents a detailed TEA to understand the cost drivers and assess the total cost of treating high salinity produced water using DCMD. The TEA is conducted for Marcellus shale play with a specific focus on Pennsylvania primarily due to its limited UIC disposal capacity necessitating produced water recycling and other alternative management strategies. The TEA model is developed by a combination of experimentally determined MD performance, an ASPEN process model, cost data for equipment available in the literature and provided by manufacturers, and best available engineering knowledge. We also performed sensitivity analysis to identify technical and economic parameters that have the major influence on the TEA results. We also assess the impact of integrating waste heat with the MD process on the total cost of produced water treatment. One potential source of waste heat is the heat contained in the exhaust stream of compressor engines at natural gas (NG) compressor stations (CS) with highly understudied waste heat recovery opportunities. Chapter 2 evaluated the quantity and quality of available waste heat at NG CS and concluded that an average of 43 TJ (terajoules) per day is available in Pennsylvania at temperatures above 645 K [207]. This work serves to add to the sparse literature on the economics of shale gas produced water management in the U.S. by providing a comprehensive economic assessment of MD treatment of produced water in Marcellus shale play as an alternative management strategy to the current practice of reuse for hydraulic fracturing or disposal in Class II UIC wells. It is important to note that although treated produced water could also be used for hydraulic fracturing operations, the quality of permeate generated by MD is well suited for other beneficial purposes such as agricultural or industrial uses. The results from our work provides several important insights including (1) quantifying the total treatment cost of produced water using MD under base case and waste heat integration scenarios, (2) identifying technical and economic parameters with the highest impact on cost of produced water treatment using MD, and (3) comparison of our findings with the BAU produced water management strategy to highlight the potential and limitations of the MD technology for produced water treatment in Marcellus shale play. These insights can be informative to guide decision-making into best strategies for shale gas produced water management.

3.2 METHODOLOGY

3.2.1 MD experimentation and process description

Produced water samples used for experiments were collected from Marcellus shale region in Pennsylvania. The samples obtained from Tioga and Washington counties have a TDS of 308,300 and 92,800 mg/Liter, respectively. The experimental setup used for evaluating DCMD performance consists of a custom made acrylic module with a channel width of 2 cm and length of 20 cm. The membrane used for the study is polytetrafluoroethylene membrane with polypropylene support and a membrane distillation coefficient of 5.6 $kg/m^2/hr/kPa$. Previous work by Lokare et al. has established mathematical models for predicting permeate flux for DCMD module while explicitly accounting for temperature and concentration polarization effects. The model was also validated with experimental findings [39]. Details regarding produced water compositions and the experimental setup can be found in [39]. The experimental results were then used to develop an ASPEN model to simulate the plant-level setup for DCMD.

Figure 12 shows the plant-level process flow sheet adapted from a case study of DCMD based desalination [197] for produced water treatment using MD technology. The original flow sheet is modified with a series of internal heat recovery steps in order to minimize the external thermal energy requirements for the MD treatment plant. The stream numbers along with the temperature and mass flow rate are shown in Figure 12 with brine and permeate streams shown in red and blue colors, respectively. It is assumed that produced water (stream 1) enters the MD plant at an ambient temperature of 20 ^{o}C and TDS of 10%, expressed as weight-to-volume fraction (w/v). A series of heat exchangers (HX-3 and HX-4) is used to increase the feed stream

(stream 9) temperature to 90 ^oC before it enters the MD array. The temperature of feed stream decreases to 40 ^oC as it moves through the MD array primarily due to the latent heat of vaporization corresponding to permeate flux as well as conduction heat losses through the membrane. On the other hand, the permeate stream (stream 13) enters the MD array at 30 ^oC and leaves at 67 ^oC. Heat exchanger HX-2 is used to recover a portion of heat energy from the permeate stream to increase the inlet feed temperature (stream 6). In addition, heat exchanger HX-1 is used to cool down the permeate stream further to 30 ^oC while simultaneously raising the temperature of the fresh feed. In order to reach the desired concentration level, the feed side solution has to be recycled through the MD system multiple times; however, to avoid salt accumulation in the system, a purge stream (stream 11) is necessary. The concentration of dissolved salts in the purge stream leaving the MD system is fixed at 30% salinity (w/v). Theoretically, MD could concentrate the feed solution to the saturation limit (~ 35% for sodium chloride for water). However, we assumed a final TDS of 30% for the purge stream in order to ensure a safety factor to prevent the salts from crystallizing in the MD system. While the internal heat recovery can increase the feed temperature to 57 ^oC (stream 8), it still needs to be heated further to the operating temperature of 90 ^oC required by the MD array. This is accomplished via HX-3 using medium pressure steam (360 kPa, 140 ^oC). We consider two scenarios for medium pressure steam: 1) base case with external purchase of steam and 2) integrating MD with waste heat from flue gas at NG CS that is used to produce medium pressure steam using HX-4.

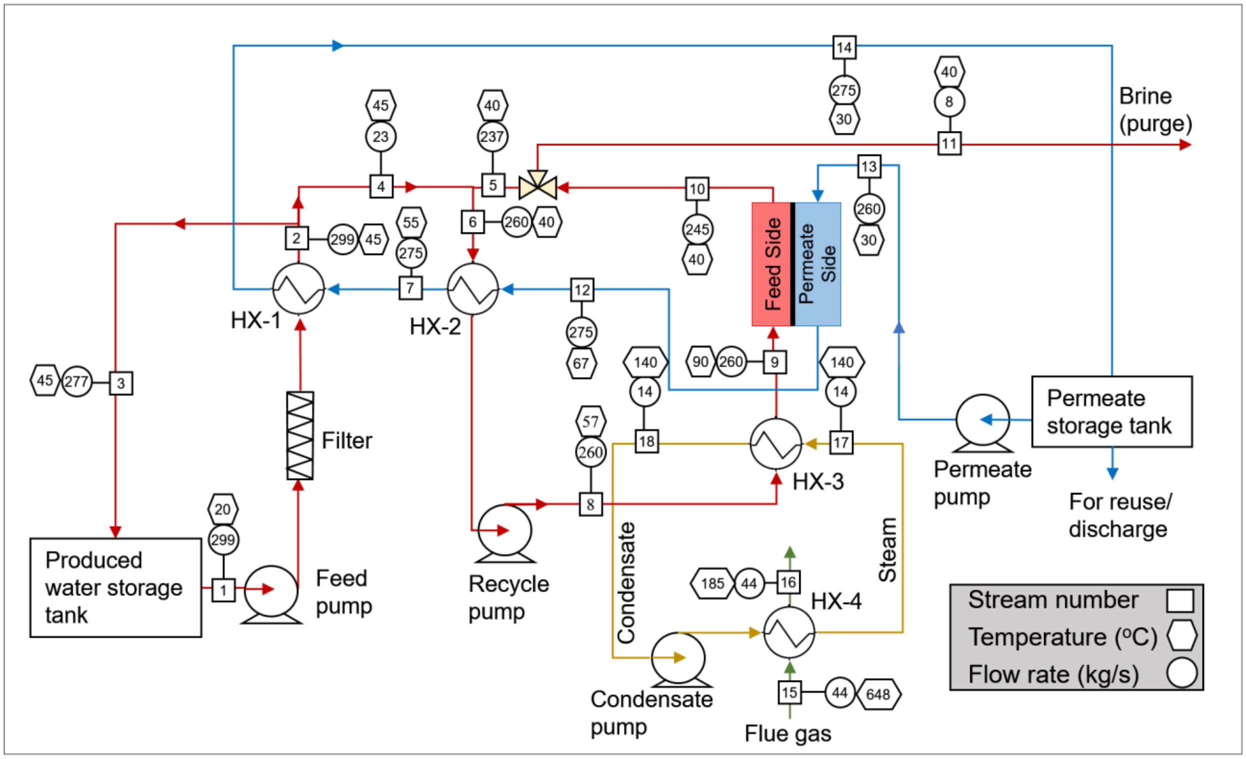

Figure 12. Proposed plant scale MD configuration adapted from *[197]* and modified for concentrating produced water from 10% to 30% salinity. A steam loop is incorporated into the configuration to recover the waste heat from flue gases at natural gas compressor stations.

3.2.2 Techno-economic (TEA) model

The total cost of produced water desalination includes direct and indirect capital costs and annual operating and maintenance costs. The TEA model is developed for a prospective 0.5 million gallons per day (MGD) DCMD plant concentrating produced water from 10% (100,000 mg/Liter) to 30% salinity (i.e. recovery factor of 66.7%) for two different scenarios: 1) base case scenario in which the thermal energy requirements are met by external steam 2) thermal energy requirements are met by integration of MD with waste heat. It is important to note that plant capacity in this study, refers to feed water capacity as opposed to plant distillate capacity used in the majority of the existing literature on TEA of desalination technologies that are focused on seawater desalination. However, the goal of this study is to provide estimates of associated costs of treating produced water using MD technology as a possible strategy for shale gas wastewater management. Additionally, it is important to note that the analysis and results are presented for a feed water salinity of 100,000 mg/Liter. In reality, produced water salinity varies over a wide range of TDS levels in Marcellus shale play. We performed sensitivity analysis to analyze the effect of changing feed TDS and other parameters on the results of the TEA model. The TEA model is developed based on a combination of experimental results, ASPEN Plus process model, and best available engineering knowledge combined with the most recent economic data. For equipment specific to produced water handling and treatment, cost data were obtained via personal communications with equipment manufacturers; otherwise, data available in the peer-reviewed literature were used. Table 11 in Appendix B summarizes all economic assumptions used in this analysis.

Capital cost also known as capital expenditure (CAPEX) includes direct and indirect capital costs. Direct capital costs refer to costs associated with the land purchase, plant construction, purchasing process equipment, and installation charges [208]. Indirect capital cost includes freight and insurance, construction overhead, owner's, and contingency costs [82]. Two approaches are common for calculating indirect capital costs: (1) each element of indirect cost can be estimated as a percentage of total direct cost or total direct material and labor cost. Freight and insurance costs make up 5% of the total direct cost [208]. Construction overhead costs include labor cost, fringe benefits, field supervision, temporary facilities (canteen, common room, recreational facilities, restrooms, etc.), construction equipment, small tools, miscellaneous items, and contractor's profit and is generally estimated as 15% of the direct material and labor cost [209, 210]. The owner's cost includes land acquisition, engineering design, contract administration, administrative expenses, commissioning and/or start-up costs, and legal fees and generally works out at 10% of the direct materials and labor costs [209, 210]. The cost of contingencies account for possible additional services and are typically estimated at 10% of the total direct costs [209, 210]. (2) Total indirect capital cost can also be estimated as a percentage of total direct capital cost. In this analysis, we used the second approach and estimated the total indirect capital cost as 10% of total direct capital cost. Details for direct capital cost estimation are presented below.

Land cost and site development

Land cost is site-specific and varies from location to location, therefore, this cost is not included in this analysis. Site development is a one-time cost including the cost of buildings, roads, fences, and other modifications that are needed for equipment installation. Site development cost is calculated using equation 8 in which the representative site development cost for an MD plant is assumed to be 26.42 $\frac{\$}{\frac{m^3}{day}}$ [211].

$$Site\ Development\ cost\ (\$) = plant\ capacity\ \left(\frac{m^3}{day}\right) * 26.42\ \left(\frac{\$}{\frac{m^3}{day}}\right) \tag{8}$$

Pretreatment

Before introducing feed to the MD unit, the feed water needs to be pretreated to remove suspended matters, free oil and grease (FOG), iron, and microbiological contaminants [68].

Capital cost of pretreatment is calculated using equation 9 where the representative cost of pretreatment is adopted from the literature to be \$79.25/m^3/day [197]. It is important to note that the present study did not consider any additional pretreatment for removing organics as the produced water from Marcellus shale play typically has very low organic content [39].

$$pretreatment\ cost\ (\$) = plant\ capacity\ \left(\frac{m^3}{day}\right) * 79.25\ \left(\frac{\$}{\frac{m^3}{day}}\right) \tag{9}$$

Pumps and heat exchangers

Capital cost for pumps is calculated based on the required pump capacity expressed as corresponding flow rate of streams passing through each pump (please see Figure 12) obtained from ASPEN plus simulations. The corresponding prices are then determined using the pump-cost curves published by National Energy Technology Laboratory (NETL) [212]. Additionally, in the base case scenario, three heat exchangers are considered in the plant configuration in order to recover the heat from hot streams and minimize the total heat requirement of desalination process. The total cost of heat exchangers is calculated based on the required heat exchanger area obtained from ASPEN Plus simulations and corresponding size-specific cost curves published by NETL [212]. Cost curves published by NETL dates back to the base year 1998 and we used the most recent chemical engineering plant cost indices (CEPCI) for heat exchangers and pumps to convert all costs to year 2015 prices [213, 214]. It is important to note that the material used for pumps and heat exchangers needs to be resistant to corrosive nature of the produced water stemming from high TDS content. As such, we selected Monel as the material of construction for pumps and heat exchangers using the detailed corrosion data on construction materials [215].

Membrane and membrane module

Required membrane area is calculated based on the total required permeate mass flow rate of the plant and the trans-membrane flux (see equation 10) obtained from experimental results and ASPEN Plus simulations. Process simulations showed that the optimum flux rate is obtained when 12 membrane modules in series with a total membrane area of 2.4 m^2 are arranged in parallel configuration to meet the total membrane area requirement of the plant. Details regarding membrane configuration optimization are provided in the previous study [216]. Total membrane cost is then calculated using equation 11 where membrane cost per unit area is obtained via personal communications with membrane manufacturers [217]. Membrane cost varies from \$60-115/m^2 with lower range (i.e., \$60/m^2) corresponding to larger purchases (i.e., more than 1850 m^2) due to economies of scale. We assumed \$60/m^2 as the unit cost of polytetrafluoroethylene (PTFE) membrane used in this study corresponding to a total membrane area of 1997 m^2 required for the DCMD plant considered in our analysis.

$$area = \frac{\left(permeate\ mass\ flow\ rate\ (\frac{kg}{hr})\right)}{flux\left(\frac{kg}{m^2.hr}\right)} \tag{10}$$

$$total\ cost\ of\ membrane = membrane\ required\ area * membrane\ cost\ per\ unit\ area$$

(11)

The cost of membrane modules varies significantly depending on the chosen application and membrane type. Spiral wound, hollow fiber, tubular, and plate and frame are four different types of membrane modules [196]. We used the plate and frame modules in the experimental set-up and hence used the corresponding representative cost data available in the literature [197].

Storage tanks and utilities

The size of storage tanks needed for both feed wastewater and permeate is calculated based on the plant capacity and recovery factor assuming that feed water and permeate can be stored at the plant location for up to five days. The price of storage tanks is obtained via personal communications with storage tank suppliers in order to get the most updated prices [218, 219]. Utilities include power supply systems for electricity and high voltage alternating current, and external plumbing required for water supply, heating, and sanitation in the desalination plant. Cost of utilities is calculated using representative value of \$42.27/m^3/day [197, 211].

Other capital costs

Controls, pressure vessels, and electrical subsystems, shipping and installation, and equipment related engineering are other capital cost elements in a DCMD treatment plant. Each of these costs are calculated using the representative costs available in the literature [197].

3.2.2.1 System size correction factor

Economies of scale is an important consideration in total cost estimation of an industrial project as the plant size affects the cost of individual unit operations and hence the overall plant costs. Size correction factor method can be applied to estimate the total direct cost of a plant for which specific cost data are unavailable or for specific categories of direct cost for which data are not available. The cost of a new system is correlated to the cost of a known system using a nonlinear relationship between the capacity and cost as shown in equation 12, where n is the scale factor (also known as the capacity factor) which is derived from actual cost data. Scale factor varies depending on the type of process plant. Many conventional distillation processes follow the "six-tenth" scaling rule wherein the scale factor is 0.6. Membrane based systems have a higher scaling factor in the range of 0.75 to 1. In this study, representative costs for site development, utilities, pretreatment, membrane modules, controls, pressure vessel, electrical subsystems, shipping and installation, and equipment related engineering are adopted from a plant with a capacity of 1 million gallons per day [197, 211]. Equation 13 is used to estimate these costs for our proposed system given the known cost for a plant of 1 MGD capacity.

$$size - corrected\ system\ direct\ capital\ cost = base\ system\ direct\ capital\ cost * \left(\frac{actual\ system\ size}{base\ system\ size}\right)^{n} \tag{12}$$

$$size - corrected\ system\ direct\ capital\ cost \left(\frac{\$}{\frac{m^3}{day}}\right) = base\ system\ direct\ capital\ cost \left(\frac{\$}{\frac{m^3}{day}}\right) * \left(\frac{actual\ system\ size}{base\ system\ size}\right)^{n-1} \tag{13}$$

3.2.2.2 Annual capital cost

The annual capital cost is calculated using the net present value (NPV) method shown in equation 14 and 15. In equation 15, *n* is the lifetime of the plant and is assumed to be 30 years [41] in this study, and r is the interest rate which is assumed to be 5% [41, 208, 220]. The effect of variation in interest rate on the total cost is captured via sensitivity analysis.

$$Annual\ capital\ cost = total\ capital\ cost * Amortization\ factor \tag{14}$$

$$Amortization\ factor = \left(\frac{i(1+i)^n}{(1+i)^n - 1}\right) \tag{15}$$

3.2.2.3 Normalized annual capital cost

Plant availability factor refers to the fraction of time per year the plant is operating compared to the maximum possible operating time. We assumed the plant availability to be 0.9 [41, 194, 196, 221] and calculated the annual production capacity using equation 16. The normalized annual capital cost (annual cost per unit amount of treated water) is then calculated using total annual capital cost and annual production capacity.

$$annual\ production\ capacity = plant\ capacity * plant\ availability\ factor * 365 \tag{16}$$

3.2.2.4 Operating and maintenance cost

Annual O&M costs represent the costs incurred after plant commissioning and during plant operation including the costs for energy (heating and electricity), equipment replacement, chemicals, labor, and regular maintenance inspections.

Thermal energy cost

In a DCMD plant, the main energy requirement is the thermal energy required to heat the feed stream to the operating temperature of the MD unit. Thermal energy requirement is calculated in ASPEN Plus utilizing experimental flux rates. Thermal energy cost is then estimated based on the most recent thermal energy cost available in the literature as shown in equation 17.

$$thermal\ energy\ cost\ \left(\frac{\$}{year}\right) = steam\ consumption\ \left(\frac{kg}{year}\right) * cost\ of\ steam\ \left(\frac{\$}{kg}\right) \tag{17}$$

It is important to note that unlike capital expenses, utility prices do not correlate simply with conventional inflationary indexes as both inflation and energy cost influence utility prices [222]. Basic energy costs, such as fuel cost in an electricity generation plant, vary erratically and are not dependent on capital and labor as compared to manufacturing expenses that rely on labor and capital and follow inflationary indexes [222]. A two-factor cost equation is suggested in the literature to account for this dual dependence [222]. We utilized the most recent thermal energy prices available in the literature [41] for the year 2013 and conducted sensitivity analysis to account for variability in the energy prices.

Electricity cost

In addition to thermal energy, DCMD plant requires electricity for pumping. Four centrifugal pumps are included in the proposed DCMD plant configuration: (1) produced water feed pump, (2) produced water circulation pump, (3) permeate circulation pump, and (4) steam condensate pump. The electricity requirement for each pump was calculated using equation 18 where q_v is the mass flow rate through the pump, ΔP is the pressure difference, and η is the pump efficiency. Electricity cost is then calculated as shown in equation 19 using specific electricity cost obtained from the U.S. Energy Information Administration (US EIA) for the base year 2015 [223].

$$E_P = \frac{q_v \, \Delta P}{\eta} \tag{18}$$

$$energy\ cost \left(\frac{\$}{m^3}\right) = cost\ of\ electricity \left(\frac{\$}{kWh}\right) * specific\ energy\ consumption\ \left(\frac{kWh}{m^3}\right) \tag{19}$$

Intake

Feed water intake cost is one of the significant factors in the capital and operating cost of a desalination plant that varies greatly with intake configuration. Surface open intake, beach well, horizontal well, radial well, and constructed seabed/infiltration gallery are different types of intake configurations mainly for conventional seawater desalination plants [224]. In the case of shale gas produced water, transportation via pipeline or trucking are the two possible intake alternatives to transport the produced water from shale gas production wells to treatment plants. When comparing the results of this study with the BAU management strategy, we assumed that produced water is transported via trucks to a prospective MD plant. Therefore, the capital cost associated with feed water intake is assumed to be zero and the operating cost is calculated as a function of transportation distance. We assumed a 100 miles trucking distance to the prospective MD plant and estimate the operating cost of produced water intake using the unit cost of trucking shale gas produced water in Marcellus shale play which is assumed to be \$0.25/mile/m^3 based on existing documented costs [20, 68] for the year 2014.

Filter

Filters that are used for pretreatment of produced water have varying lifetime depending on the quality of feed water. We assumed that the plant is equipped with standard filters rated at 5-25 µm and used representative cost information available in the literature to estimate the filter cost [197].

Brine disposal cost

Brine disposal cost for desalination plants is typically assumed to be \$0.0015/m^3 [41, 196] which is the representative cost for disposing of the concentrate for RO based desalination plants. However, as this study deals with desalination of shale gas produced water, we accounted for the cost of transportation as well as injecting the concentrate into disposal wells when comparing with the BAU produced water management strategy i.e., disposal in class II injection wells. It is important to note that only 33.3% of the high salinity feed water is sent to disposal wells as the remaining 66.7% is desalted in the MD plant. Shale gas wastewater transportation cost varies in different shale regions depending on the proximity of disposal wells to produced water generation location. Due to limited disposal capacity in Pennsylvania, the majority of produced water is transported to Ohio. As such, an average of 500 miles is considered for two-way transportation distance from shale gas wells to Class II disposal wells for the BAU management strategy [20]. The two-way transportation distance from the hypothetical MD plant to disposal wells is considered to be 400 miles assuming that the centralized plant is located 100 miles from shale gas sites [20]. We also assumed a unit transportation cost of \$0.25/mile/m^3 for the year 2014 [20, 68] and concentrate injection cost of \$6.29/m^3 [69, 225] to calculate brine disposal cost.

Cost of chemicals, spares, and labor

Produced water needs to be pretreated before entering the MD unit, which typically requires chemical addition. We estimated the cost of typical chemicals utilized for pretreatment of produced water (e.g., acids, alkalis, surfactants, oxidants, chelates [226]) using the representative cost of chemicals (\$0.018/m^3) for MD plants available in the literature [197, 202, 211]. Cost of spares refers to the cost of replacing parts needed to maintain the system operating including pumps, valves, and miscellaneous parts. Cost of replacing filters, membrane, and membrane modules as well as consumable chemicals is not included in this category. The representative cost of spares for MD plants is assumed to be \$0.033/m^3 [197, 211]. Cost of labor varies depending on the region where the plant is located as well as the number of operators required to operate a desalination plant. We assumed the labor cost to be \$0.03/m^3 [41, 196, 197].

Membrane replacement cost

Membrane replacement cost varies between 10-20% of total membrane cost per year for membranes treating low-salinity and high salinity wastewaters, respectively. We assumed a 20% rate of membrane replacement because of the high salinity of produced water in Marcellus shale play.

3.2.3 Integrating MD with waste heat

We also investigated the economics of MD for treating produced water under the scenario where waste heat is utilized to meet the thermal energy requirements of the MD process. Specifically, we focused on utilizing waste heat available at natural gas compressor stations in the Marcellus shale play. Our prior analysis of waste heat from existing NG CS in the U.S. revealed that a total of 43 TJ/day of high quality waste heat is available in the form of hot flue gases at NG CS in Pennsylvania [207]. Our recent work highlighted that waste heat available at NG CS in Pennsylvania is sufficient to meet the thermal energy requirements for MD treatment of all produced water generated in the state from shale gas activities [227]. For the scenario where the MD plant is integrated with waste heat, we assumed that medium pressure steam is generated by recovering heat from the flue gas generated at NG CS (HX-4). The resulting medium pressure steam is then utilized to heat the high salinity wastewater to the inlet operating temperature of the MD unit. While the focus of our analysis is on utilizing waste heat from NG CS, MD process could be integrated with other available sources of waste heat.

3.3 RESULTS

Table 12 in Appendix B provides a detailed split of the capital and O&M expenses for a 0.5 MGD DCMD plant. As shown in Table 12, the total cost of treating produced water using MD is $\$5.70/m^3_{feed}$ of desalted water for the base case scenario which decreases significantly to $\$0.74/m^3_{feed}$ when MD is integrated with a source of waste heat. These findings are compelling as they suggest that integrating MD with a source of waste heat could result in significant reduction in produced water treatment using MD technology. It is important to note that integrating MD with waste heat available at NG CS could contribute to a total savings of $3.11 million/year in O&M costs corresponding to 0.43 million metric tonnes of steam consumption. However, the total capital cost is $436,000 higher for the DCMD plant with waste heat integration due to additional cost of heat exchangers for heat recovery. Nonetheless, savings in O&M costs will compensate the additional capital cost in the first two months of plant operation. In addition, utilizing available waste heat will potentially increase the environmental sustainability of shale gas produced water treatment as it results in avoided environmental impacts associated with combustion of primary fuels to generate thermal energy for the MD process as compared to capturing the waste heat that would be otherwise lost to the environment.

Figure 13 shows the percentage contribution of different cost elements to the capital and O&M expenses for the proposed MD plant under base case and waste heat integration scenarios. The results in Figure 13 show that heat exchangers and storage tanks are the two major cost drivers of the capital cost while thermal energy cost constitutes the largest share of O&M costs for the base case scenario. This finding compares favorably with prior work on cost estimation of seawater desalination that concluded thermal heat requirement to be the major cost driver for MD technology [196]. While thermal energy constitutes the largest share of O&M for base case, electricity and membrane replacement are the major contributors to O&M for the waste heat integration scenario.

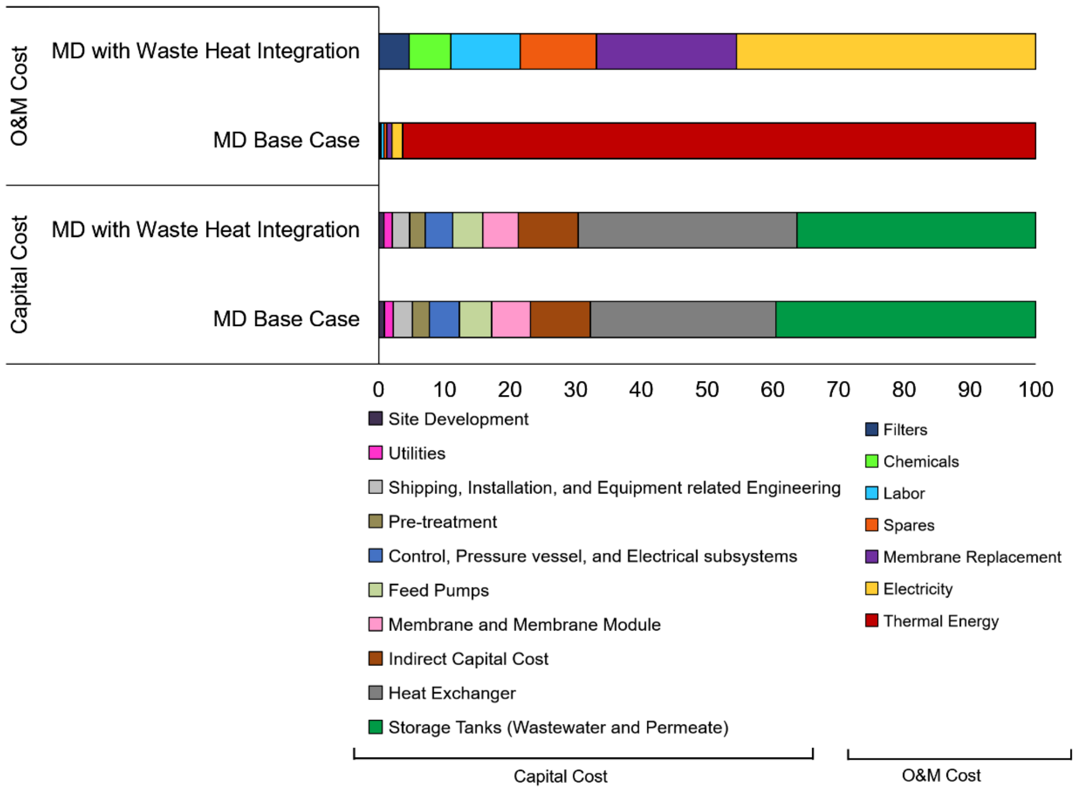

Figure 13. Fractional contribution of capital and O&M costs by various cost elements for base case and MD with waste heat integration scenarios

We performed sensitivity analysis to understand how variations in technical and economic parameters affect the total cost of produced water treatment using MD technology under base case and MD with waste heat integration scenarios (Figure 14). This analysis revealed that the total cost of produced water treatment is most sensitive to changes in feed TDS level and steam price for the base case scenario (Figure 14a). The results in Figure 14a show that a 25% increase in the steam price (i.e., from \$0.008/kg to \$0.01/kg) resulted in 22% increase in total water cost indicating the high sensitivity of MD process to thermal energy price. Moreover, the total water cost increases with an increase in the feed water salinity for base case as well as MD with waste heat integration scenarios. It is interesting to note that changes in parameters such as interest rate, number of days for storing produced water and purified water at the MD plant, membrane price, and plant capacity have a much less effect on the total cost of produced water treatment.

Figure 15 presents the impact of feed water salinity on thermal energy requirements for the base case scenario as well as total cost of produced water treatment using MD. It is important to note that the salinity of final brine leaving the system is assumed to be fixed at 30% (300,000 mg/Liter), which is achieved by recirculating produced water through the MD array. As a direct consequence, lower salinity produced water consumes significantly higher amount of energy as it needs to be recirculated more to reach the desired TDS level, resulting in higher thermal energy requirement and O&M costs. While lower TDS feed has higher O&M costs, it also results in larger volume of permeate compared to higher TDS produced water where a larger portion of the feed water is rejected as the purge stream. As a result, the energy requirement per unit amount of permeate varies slightly across different TDS levels, which compares favorably with prior studies [228, 229].

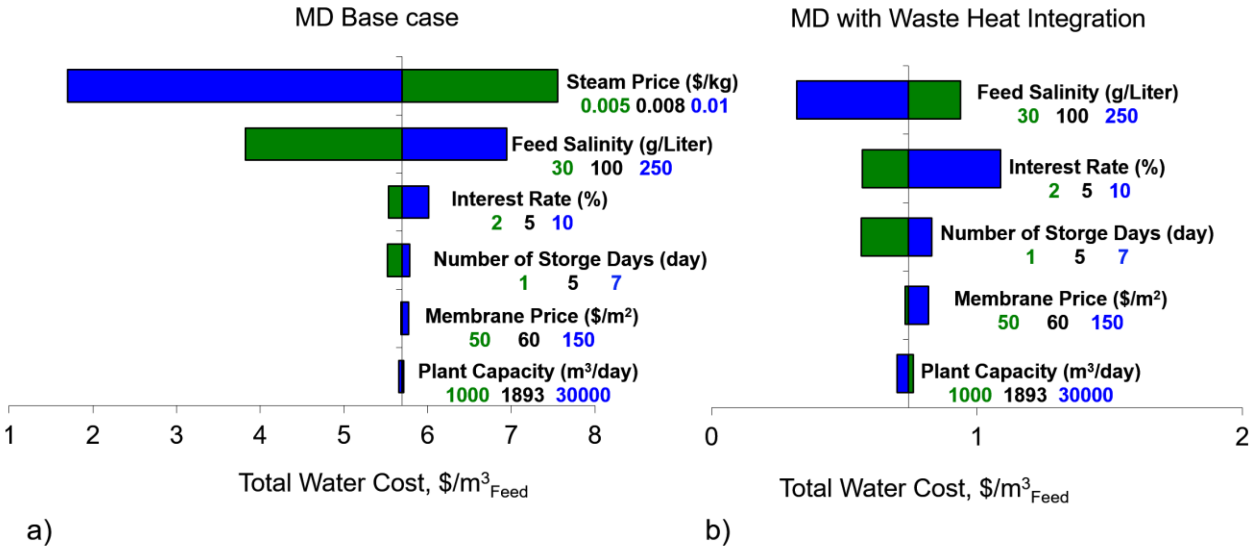

Figure 14. Sensitivity analysis of total water cost for produced water treatment using MD technology for a) base case scenario, and b) MD with waste heat integration scenario

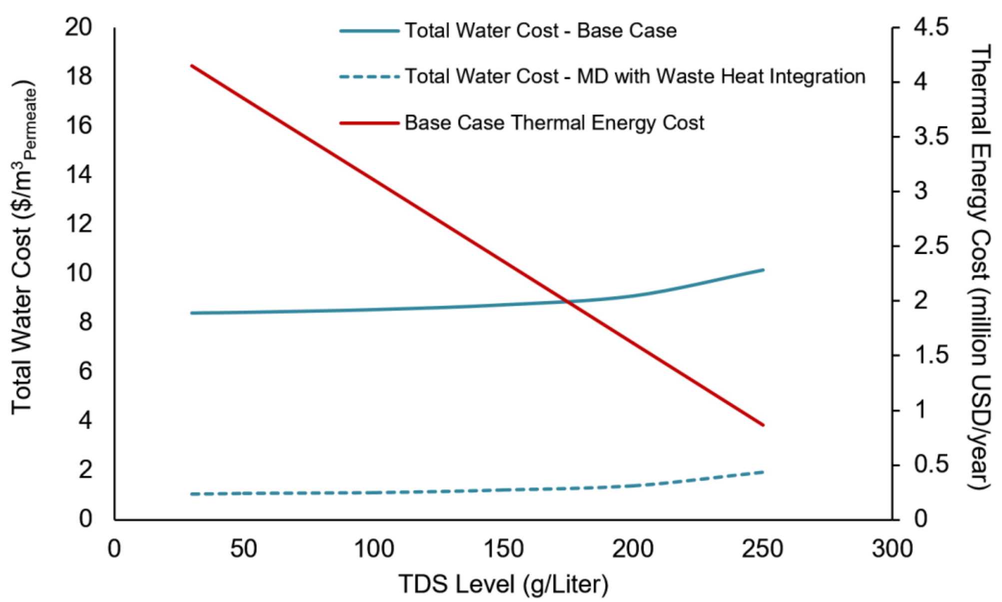

Figure 15. Impact of feed TDS level on the base case scenario thermal energy cost and total cost of produced water treatment using MD technology

MD treatment of produced water provides environmental benefits by generating high quality permeate that can have beneficial use and by avoiding greenhouse gas (GHG) emissions, specifically when waste heat is utilized by the MD facility. To provide a broader understanding of the economic benefits of treating shale gas produced water with MD technology, the results of the present study are compared to associated costs of the most dominant management strategy which is injection in Class II disposal wells. Figure 16a shows that the capital and O&M costs for the base case scenario of $\$0.51/m^3_{feed}$ and $\$5.19/m^3_{feed}$, respectively are reduced to $\$0.55/m^3_{feed}$ and $\$0.19/m^3_{feed}$ when the waste heat is available for the operation. However, even when MD treatment is considered, the cost of produced water transportation from shale gas wells to the DCMD plant (cost of intake) and the cost of transporting and injecting concentrated brine in class II injection wells (brine disposal cost) needs to be accounted for to provide a realistic comparison with the BAU strategy. After accounting for cost of intake and brine disposal, the results in Figure 16b show that the total cost of produced water management using MD technology of $\$66/m^3_{feed}$ for the base case scenario can be reduced $\$61/m^3_{feed}$ if a source of waste heat is available for the MD process. The cost of BAU management strategy is calculated assuming an average transportation distance of 500 miles [20] and unit transportation cost of $\$0.25/mile/m^3$ [20, 68] and $\$6.29/m^3$ [69, 225] for injecting produced water into disposal wells which translates into total cost of $\$132.1/m^3_{feed}$. As shown in Figure 16, the cost of produced water treatment using MD technology shows a steep change when feed intake and brine disposal costs are included. Nonetheless, produced water treatment using MD technology can result in over 50% reduction in total cost of produced water management over the BAU strategy. These results are promising as they suggest that adoption of MD technology for shale gas produced water management could result in lower total cost when compared to current management strategies.

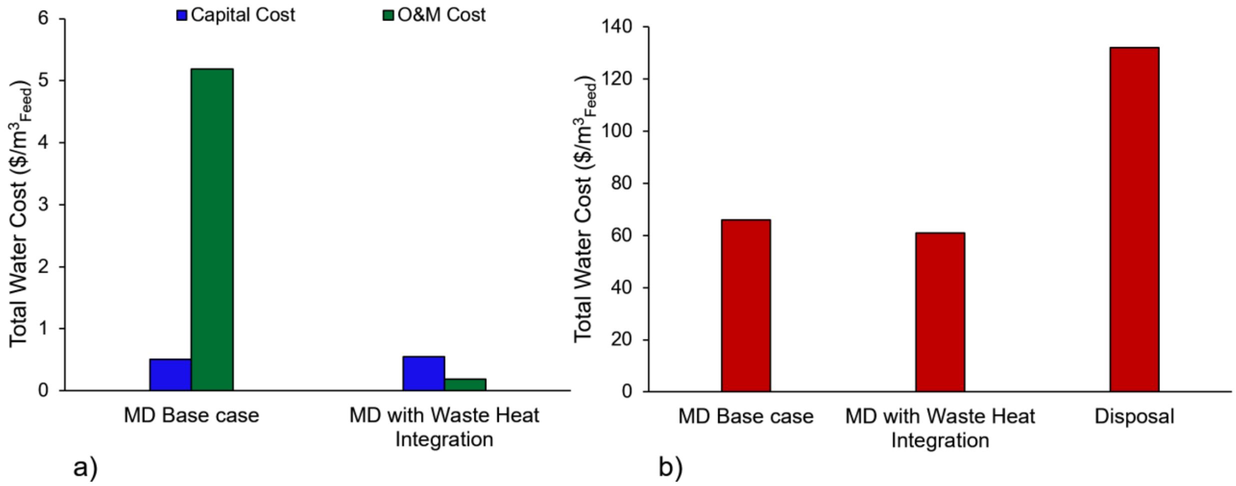

Figure 16. a) Split of capital and O&M costs for base case and MD with waste heat integration scenarios, and b) Comparison of total cost (including intake and brine disposal) of shale gas produced water management using MD technology with the BAU management strategy

3.4 DISCUSSION

This study evaluated the cost of shale gas produced water desalination using DCMD. The results of this work indicate that total cost of produced water desalination is $5.70/m^3$ of feed water with thermal energy comprising around 88% of the total cost. Further analysis revealed that integrating MD with waste heat available from NG CS could significantly reduce the cost of produced water desalination resulting in total water treatment cost of $0.74/m^3_{feed}$. Additionally, the results of sensitivity analysis revealed that variations in thermal energy cost and feed water TDS have the greatest overall impact on the cost of treating produced water. The TEA model and results presented in this study are subject to several sources of uncertainty. Some of these are addressed via sensitivity analysis, while others are discussed as follows.

The TEA model for produced water treatment presented in this study focused on Marcellus shale gas play. Produced water from Marcellus shale play has negligible amount of organic compounds [39, 230]. As a result, no additional pretreatment is considered in the TEA model beyond suspended solids removal. However, the produced water from other shale plays such as Eagle Ford and Barnett is expected to have different characteristics and may require additional pretreatment [230]. The cost of pretreatment and hence the total water treatment cost may increase for produced water containing significant amount of organics, and should be evaluated in future TEA studies. Second, the TEA model presented in this study assumes that the produced water is concentrated to a final concentration of 30% with subsequent disposal of the reject stream in disposal wells. However, innovative techniques aimed at reducing the total amount of rejected brine including the membrane distillation-crystallization (MDC) could offer further cost reduction associated with brine disposal by concentrating the brine beyond halite supersaturation [54, 231] in addition to generating salt as a useful byproduct for deicing applications in Marcellus shale region [232-235]. The TEA model also did not account for the revenue generation associated with sale and beneficial reuse of high quality permeate for industrial or agricultural purposes, thus resulting in higher estimates of produced water treatment.

A comparison of the shale gas produced water treatment using MD with business-as-usual strategy in Marcellus shale gas play revealed interesting and promising results. The current dominant produced water management strategy is disposal in Class II injection wells. There are a total of about 144,000 class II disposal wells in the U.S. with the majority of wells located in Texas (50,000 wells), California, Kansas, and Oklahoma [69]. Salt water disposal (SWD) wells account for 20% of total disposal wells of which 12,000 are located in Texas, 800 in Oklahoma, and only 8 in Pennsylvania [69]. In areas of limited disposal capacity (e.g., Pennsylvania) or where water resources are stressed (e.g., Texas and Oklahoma), reuse and recycling of produced water is an effective alternative to direct underground injection of produced water. When feed water transportation and brine transportation and injection costs are taken into account, the total cost of produced water treatment using MD for the base case scenario is $\$66/m^3_{feed}$ which can be reduced to $\$61/m^3_{feed}$ for MD with waste heat integration. In comparison, the total cost of BAU strategy for produced water treatment is $\$132.1/m^3_{feed}$ when trucking and injection of produced water in disposal wells is taken into account. These results are compelling and highlight that MD technology (*with or without integration with waste heat*) may offer both economic and environmental advantages over the BAU strategy for produced water management from shale gas plays. It is important to note that we assumed a 100 miles transportation distance for feed water intake and 400 miles transportation distance from the MD plant to disposal wells for reject brine disposal [20, 68]. However, future analysis using rigorous optimization techniques for identifying the location of prospective MD treatment facilities can aid in minimizing the total transportation distance and associated costs of wastewater management.

4.0 OPTIMIZATION OF SHALE GAS WASTEWATER MANAGEMENT

4.1 INTRODUCTION

The economics of desalination technologies has been evaluated in the existing literature [193-195], however, to date, there has been only a handful of studies on techno-economic assessment (TEA) of these technologies for shale gas high salinity wastewaters [236]. Chapter 3 describes a detailed TEA of DCMD for produced water treatment in Marcellus shale gas has revealed that the total cost of produced water treatment using DCMD is about \$5.8/m^3_{feed}. However, due to relatively lower operating temperatures, MD can be integrated with available waste heat sources in the industrial processes to offset the energy requirements of desalination process. We specifically investigated the economics of MD under the scenario of integrating this technology with available waste heat sources at natural gas compressor stations (NG CS) [207, 216]. The results of this analysis have shown that total cost of produced water treatment can be reduced to \$0.8/m^3_{feed} when a source of waste heat is available. In addition, thermal energy price as well as produced water TDS level are shown to have a significant impact on total treatment cost.

In addition to choosing a treatment technology that is suitable for the salinity level of shale gas wastewater and accounting for the associated cost of treatment process, it is imperative that a holistic approach is employed for integrated shale gas wastewater management for a given shale gas region. Direct disposal of shale gas wastewater involves wastewater transportation and its injection into SWD. However, it is important to recognize that even when treatment of shale gas wastewater is considered, wastewater needs to be transported to treatment facilities and then the concentered brine needs to be transported and injected into SWD. Therefore, a systematic optimization framework is required that takes into account associated costs of treatment, transportation, and injection of various management strategies as opposed to ad hoc strategies. A handful of recent studies have focused on shale gas water management using optimization techniques. However, the majority of existing work is focused on short-term planning where shale gas wastewater could be recycled for future hydraulic fracturing requirements with little emphasis on long-term planning of wastewater management.

Prior studies have focused on using life cycle assessment (LCA) to quantify the environmental impacts including greenhouse gas emissions, and water consumption of shale gas production [7, 237-240]. However, existing LCA studies ignore the impact of available treatment technologies on the economic sustainability of shale gas water management. Recent work in the field of process systems engineering (PSE) has also focused on the strategic planning and design of shale gas supply chain networks for water management [22, 68, 241-243]. Cafaro and Grossman developed a mixed-integer nonlinear programming (MINLP) model to determine the optimal design of shale gas supply chain including well drilling schedule, hydraulic fracturing strategy, size and location of gas separation plants and compressors as well as pipeline infrastructure in order to maximize the net-present value (NPV) of the project [241]. While this study accounts for freshwater availability and the possibility of recycling flowback water, long-term planning of shale gas wastewater treatment and final disposal are not considered [241]. Previous research has also focused on integration of water management into shale gas supply chain design [244] as well as investigating the optimal shale gas wastewater management under uncertainty [245-247]. Yang et al. have addressed the problem of optimizing freshwater acquisition and wastewater handling in shale gas development through a mixed-integer linear programming (MILP) model using average cost data reported by industry and concluded that using desalination technologies for shale gas wastewater treatment can be cost-effective [26]. Moreover, transportation cost is shown to contribute significantly to total cost of shale gas supply chain management [26]. However, prior studies on shale as supply chain optimization use average transportation distances from shale gas sites to treatment facilities or disposal wells. This simplification could considerably affect the cost of shale gas wastewater management and may lead to sub-optimal economic solutions [248].

Given the critical need for developing strategies that could guarantee the long-term sustainability of shale gas, this work develops an optimization framework to tackle the problem of managing high salinity shale gas wastewater by focusing on advanced treatment of shale gas wastewater using MD technology. Moreover, this study proposes to explore industrial waste heat sources to be integrated with shale gas wastewater treatment process using the concept of industrial ecology defined as the science studying industrial systems to minimize the environmental impacts where waste equals food [249, 250]. To the best of our knowledge, there is no other study in the literature on shale gas supply chain management that takes into account the regional synergistic industrial ecology opportunities to understand the economic suitability of shale gas wastewater management. The optimization model will be applied to Marcellus shale play in PA where 34 out of 67 counties are shale gas producing as is shown in Figure 17. Marcellus shale is a major natural gas (NG) reservoir with steadily increasing production since 2008 that currently accounts for about 40% of the total U.S. shale gas production [65]. This work serves to add to the emerging literature on optimization studies on shale gas wastewater management by (1) incorporating detailed cost estimates obtained from TEA of MD technology for shale gas wastewater treatment utilizing the results of experimental studies on MD performance for shale gas wastewater treatment in Marcellus shale play; (2) accounting for detailed transportation distances using actual location of shale gas wells as well as treatment and disposal facilities; (3) applying the optimization framework to four real world case studies with major shale gas development in PA. Furthermore, the framework and insights provided in this study can be applied to other shale gas plays to provide a holistic understanding of using alternative management strategies as compared to BAU management strategy.

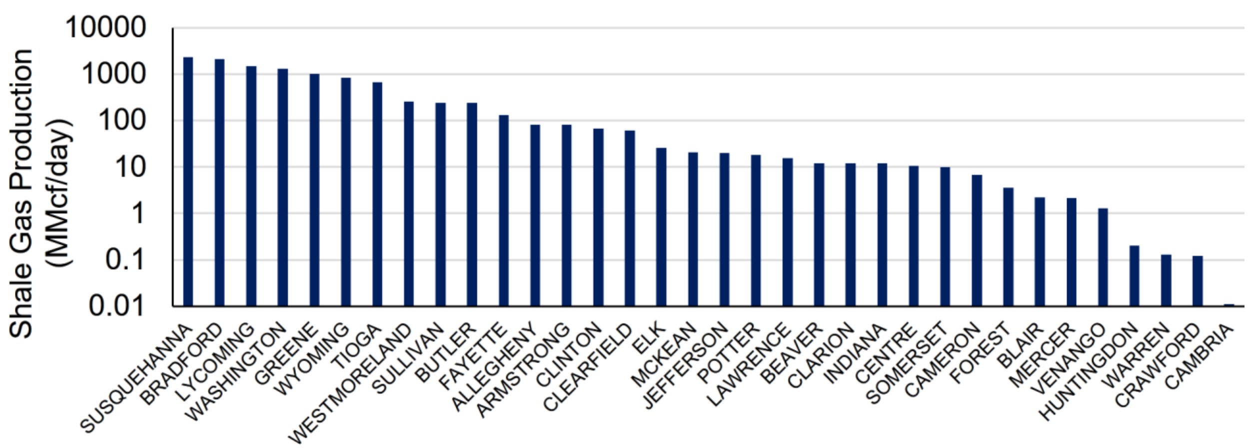

Figure 17. Shale gas production on the county level in PA stated as million cubic feet per day (MMcf/day)

4.2 METHODOLOGY

The quality of shale gas wastewater varies over a wide range after well stimulation and during gas production stage. The results of sampling on Marcellus shale flowback water has shown that

TDS level can reach up to 100,000 mg/L in the first two weeks after hydraulic fracturing and during well completion stage [251]. In addition, the TDS level could further increase to above 250,000 mg/L during the production stage [26]. We performed the analysis for TDS levels of 100,000 mg/L and 250,000 mg/L in order to capture two extremes and the consequential influence the TDS level may impose on optimum management strategy.

Shale gas production data for each well is obtained from PA DEP for the year 2014 which is the most updated available statistics at the time of this analysis [252]. 5,188 active unconventional gas wells were operating in 2014 in PA with a total natural gas production of 5.1×10^{10} m^3 [253]. Produced water generation from shale gas wells is estimated through a deterministic scenario in which the produced water generation is correlated to shale gas production. However, produced water generation per amount of gas production varies across shale gas extraction sites primarily due to differences in the geology of shale formation [254]. The amount of produced water generation is estimated using county specific produced water generation reported in the literature [30]. Four different counties are included in this analysis; Susquehanna and Bradford counties in Northeast PA and Greene and Washington counties in Southwest PA, collectively accounting for about 75% of total shale gas production in PA [252].

4.2.1 Problem statement

In the proposed model, we address the problem of finding the optimal design for shale gas produced water management including transportation, treatment and disposal of produced water over the planning horizon of one year as well as determining the size and location of treatment facilities in order to minimize the total cost of handling produced water. Figure 18 shows the superstructure of shale gas produced water management strategies presented in this study for the specific case of using MD as the treatment technology. Figure 18 includes 1) existing drilling sites where produced water is generated ($i \in I$), 2) potential sites for installation of centralized MD plants to treat the shale gas produced water ($m \in M$) 3) existing compressor stations with available waste heat that can be utilized as the energy source for produced water treatment using MD technology ($j \in J$), 4) potential on-site treatment facilities using MD ($o \in O$), 5) existing SWD wells to inject the produced water ($d \in D$), 6) existing transportation routes to connect nodes *i* to *m* (shale gas production sites to centralized MD plants), *i* to *j* (shale gas production sites to MD units at compressor stations), and *i* to *d* (shale gas production sites to disposal wells) , 7) existing transportation routes to transport the concentrate brine from nodes *m* to *d* (centralized treatment plants to disposal wells), *j* to *d* (compressor stations to disposal wells), and *o* to *d* (onsite treatment units to disposal wells).

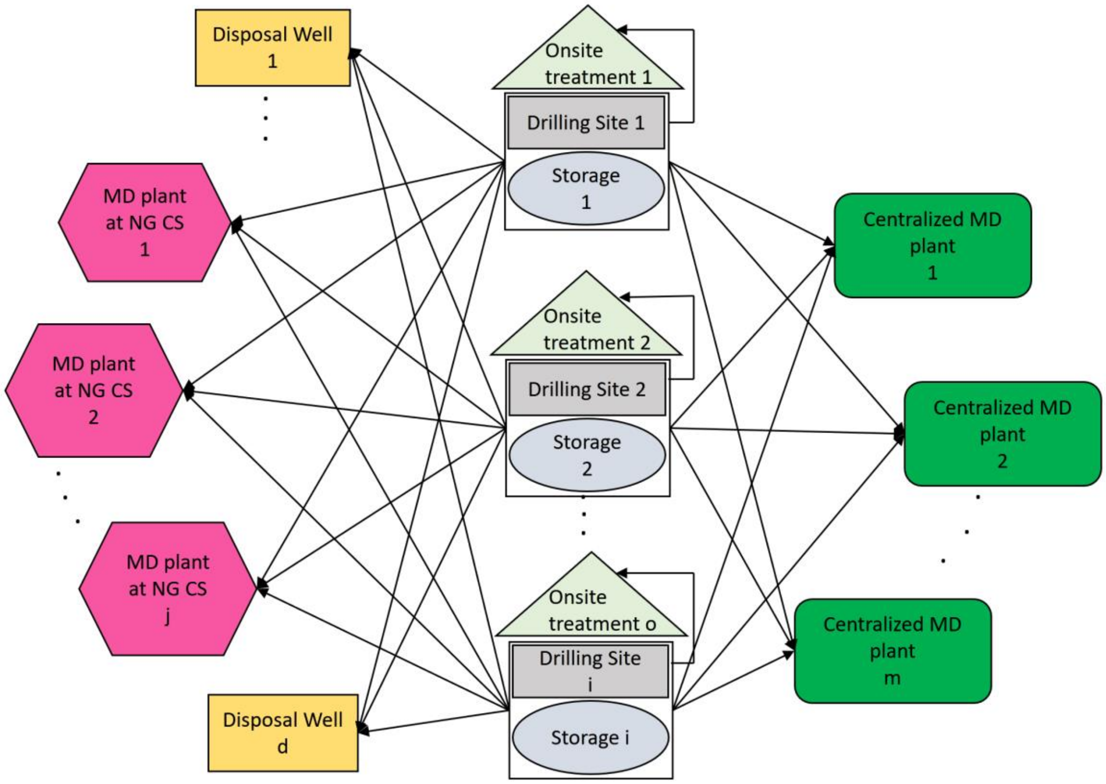

Figure 18. Superstructure of shale gas produced water management options

Given the problem described above, the goal is to optimally determine: a) the size and location of centralized MD treatment plants, MD plants at NG CS, and onsite MD treatment units and b) the amount of shale gas produced water transported to each treatment option and/or disposal wells.

The main assumptions for present optimization problem can be summarized as follows:

1. Produced water volume and composition are known.
2. Produced water trucking cost is volume and distance dependent. The unit costs for produced water and brine transportation is given.
3. A fixed time horizon consisting of days as time intervals is considered.

4. A set of produced water management strategies are available including direct disposal in SWD wells, onsite treatment at wellpads using MD, centralized MD plants, and MD treatment at NG CS.
5. Each treatment option is associated with capital and operating cost. In addition, cost of transporting wastewater to treatment facilities as well as transportation of concentrated brine and its injection into SWD wells are included in total cost of wastewater management.
6. Direct disposal option is associated with transporting shale gas wastewater to disposal wells and its injection into SWD wells.
7. The maximum capacity for MD plants at NG CS is constrained by theoretical treatment capacity at each NG CS.
8. The maximum capacity or size for each treatment option is provided.
9. A set of storage/pits are available to store the produced water at shale gas sites; associated costs for storage are not included in this model as it is assumed that storage facilities are constructed as part of site development operations.
10. MD technique concentrates produced water to maximum of 30% salinity.
11. MD can desalinate the produced water to surface water discharge standard.
12. Cost of desalination is normalized per amount of produced water. Unit cost of treatment calculated from TEA model is used in the optimization model.
13. Only one capacity range of each treatment facility is installed at each location.
14. The transportation distance from drilling sites to onsite treatment units is negligible compared to other transportation distances considered in the model.
15. This study does not consider any constraints on the capacity of disposal wells.

4.2.2 Model inputs

Treatment cost calculation

Associated cost with each treatment strategy ($\$/m^3_{\text{produced water}}$) is estimated using detailed TEA framework developed for shale gas produced water treatment using MD technology as described in Chapter 3 [236]. The TEA model accounts for capital as well as operating and maintenance costs of produced water treatment. It is assumed that thermal energy requirements for the treatment process is met by external purchase of steam for onsite and centralized MD plant treatment options while for treatment at NG CS using available waste heat the cost of thermal energy is set to zero [236].

Transportation cost calculation

It is important to note that trucks transporting produced water will be loaded one way but empty on the return trip, thus making it necessary to account for the round trip of trucks. In addition, TDS level of produced water will impact the fuel economy as higher salinity produced water has higher density. We have addressed this issue by considering round trip trucking charges and assumed a unit transportation cost of $\$0.25/mile/m^3$ obtained from peer-reviewed literature and personal communications [20, 68, 255, 256].

Injection cost calculation

Injection cost varies across different shale plays. An injection cost of $\$6.29/m^3_{\text{produced water}}$ for Marcellus shale play obtained from peer-reviewed literature [69, 225].

The location of centralized plants

The location of centralized MD plant is defined in a separate optimization procedure to minimize the transportation distance associated with the treatment of wastewater at centralized MD plant.

We used the Haversine formula shown in equations 20-22 to calculate the great circle distance between two points which is the shortest distance over the earth's surface between the points [257].

$$\boldsymbol{a = sin^2\left(\frac{\Delta\varphi}{2}\right) + cos\varphi_1 \,.\, cos\varphi_2 \,.\, sin^2(\Delta\lambda/2)} \quad (20)$$

$$\boldsymbol{c = 2arctan2(\sqrt{a}, \sqrt{a-1})} \quad (21)$$

$$\boldsymbol{d = Rc} \quad (22)$$

where φ and λ are latitude and longitude of the points, respectively and R is earth's radius. The model is implemented in Python programming language and particle swarm optimization algorithm is used to find the optimum location of centralized MD plant accounting for the location and amount of production from each shale gas well in addition to location of disposal wells as the concentrated brine from treatment process is transported to disposal wells. It is important to note that we find the optimum location of centralized MD plant for each TDS level as it is assumed that MD technology concentrates produced water to a maximum of 30% salinity, as such, depending on the salinity of feed water, a percentage of input feed water to the centralized MD plant will be sent to disposal wells.

Treatment capacity at NG CS

Chapter 2 describes the thermodynamic modeling of NG CS to evalute the spatial availability of waste heat at NG CS in the U.S. and concludes that a total of 43 TJ (terajoules) per day is available at NG CS in PA at temperatures above 645 K [207]. In order to explore beneficial synergies between produced water treatment and available waste heat at NG CS, an ASPEN model is developed for a hypothetical MD plant assuming that waste heat contained in the flue gas of NG CS is used to produce medium pressure that can be used as the energy source to drive the MD process [207, 216]. The treatment capacity at each NG CS is calculated based on the available waste heat at the station and required thermal energy per unit amount of produced water obtained from ASPEN simulation. Details regarding treatment capacity at NG CS can be found in [216].

Distance matrix calculation

It is assumed that shale gas wastewater and concentrated brine are transported using trucks. Accurate driving distance is then calculated between each origin-destination pair locations using one of google Application Program Interface (APIs) [258] in MATLAB programming language.

4.2.3 Model Formulation

The optimization problem for the long-term planning of shale gas produced water management is formulized in terms of a linear programming (LP) model described in the following section.

4.2.3.1 Constraints

Mass balance constraints

Total amount of produced water at shale gas sites equals the produced water routed to compressor stations, centralized treatment plants, onsite treatment units, and disposal wells as is shown in equation 23.

$$\boldsymbol{PW_{i,t}} = \sum_{j} \boldsymbol{wj_{i,j,t}} + \sum_{m} \boldsymbol{wm_{i,m,t}} + \sum_{d} \boldsymbol{wd_{i,d,t}} + \sum_{o} \boldsymbol{wo_{i,o,t}}, \forall \boldsymbol{i,t} \tag{23}$$

where $pw_{i,t}$ is total produced water at shale gas site i at time period t, $wj_{i,j.t}$ is the amount of produced water from shale gas site i transported to compressor station j at time period t, $wm_{i,m,t}$ is amount of produced water from shale gas site i transported to centralized MD treatment plant m at time period t, $wd_{i,d,t}$ is the amount of produced water from shale gas site i transported to disposal well d at time period t, and $wo_{i,o,t}$ is the amount of produced water from shale gas site i treated at onsite treatment o at time period t.

At each treatment facility, produced water is treated and recovered by a certain recovery factor and the rest is disposed at SWD wells, expressed by equations 24-26.

$$\sum_{d} \boldsymbol{sj_{j,d,t}} = \sum_{i} (\boldsymbol{1} - \boldsymbol{CR}).\boldsymbol{wj_{i,j,t}}, \forall \boldsymbol{j,t} \tag{24}$$

$$\sum_{d} \boldsymbol{sm_{m,d,t}} = \sum_{i} (\boldsymbol{1} - \boldsymbol{CR}).\boldsymbol{wm_{i,m,t}}, \forall \boldsymbol{m,t} \tag{25}$$

$$\sum_{d} \boldsymbol{so_{o,d,t}} = \sum_{i} (\boldsymbol{1 - CR}). \boldsymbol{wo_{i,o,t}}, \forall \boldsymbol{o, t} \qquad (26)$$

where $sj_{j,d,t}$ is the amount of concentrated brine from compressor station j transported to disposal well d at time period t, CR is the recovery factor at a given TDS level, $wj_{i,j,t}$ is the amount of produced water from shale gas site i transported to compressor station j at time period t, $sm_{m,d,t}$ is the amount of concentrated brine from centralized MD plant m transported to disposal well d at time period t, $wm_{i,m,t}$ is the amount of produced water from shale gas site i transported to centralized MD treatment plant m at time period t, $so_{o,d,t}$ is the amount of concentrated brine from onsite treatment unit o transported to disposal well d at time period t, and $wo_{i,o,t}$ is the total amount of produced water from shale gas site i transported to onsite treatment unit o at time period t.

Treatment capacity constraints

Total amount of produced water transported from all shale gas sites to a treatment facility should not exceed the capacity of that facility as in shown in equations 27-29.

$$\sum_{i} \sum_{t} \boldsymbol{wj_{i,j,t}} \leq \boldsymbol{TJ_j}, \forall \boldsymbol{j} \qquad (27)$$

$$\sum_{i} \sum_{t} \boldsymbol{wm_{i,m,t}} \leq \boldsymbol{TM_m}, \forall \boldsymbol{m} \qquad (28)$$

$$\sum_{i} \sum_{t} \boldsymbol{wo_{i,o,t}} \leq \boldsymbol{TO_o}, \forall \boldsymbol{o} \qquad (29)$$

where $wj_{i,j,t}$ is the amount of produced water from shale gas site i transported to compressor station j at time period t, TJ_j is the maximum treatment capacity at compressor station j, $wm_{i,m,t}$ is the amount of produced water from shale gas site i transported to centralized MD plant m at time period t, TM_m is the maximum treatment capacity at centralized MD plant m, where $wo_{i,o,t}$ is the amount of produced water from shale gas site i transported to onsite treatment unit o at time period t, TO_o is the maximum treatment capacity at onsite treatment unit o. Maximum treatment capacity at centralized MD plants is determined to be 20% higher than total wastewater generated in each case study as different counties are considered as case studies and three potential locations are identified for constructing a centralized MD plant in each county. Moreover, maximum treatment capacity at onsite treatment units is determined to be equal to total wastewater generated in each county as it is possible that wastewater from one wellpad is transported to other wellpads for onsite treatment.

4.2.3.2 Objective function

The model objective is to minimize the total cost of shale gas wastewater management, as expressed in equation 30.

$$\mathbf{min}\, \boldsymbol{C} = \boldsymbol{C}_{\boldsymbol{transportation}} + \boldsymbol{C}_{\boldsymbol{treatment}} + \boldsymbol{C}_{\boldsymbol{injection}} \tag{30}$$

where $C_{transportation}$ denotes the total cost of transportation; $C_{treatment}$ denotes the total cost of treatment; and $C_{injection}$ denotes the total cost of injection.

Total cost of transportation is given by equation 31.

$$\boldsymbol{C_{transportation} = C^{cs}_{t-shale} + C^{dw}_{t-CS_S} + C^{cmp}_{t-shale} + C^{dw}_{t-cmp_S} + C^{dw}_{t-shale} + C^{dw}_{t-ons_S}} \qquad (31)$$

where $C^{cs}_{t-shale}$ denotes the total transportation cost from shale gas sites to compressor stations; $C^{dw}_{t-CS_S}$ denotes the total transportation cost from compressor stations to disposal wells; $C^{cmp}_{t-shale}$ denotes the total transportation cost from shale gas sites to centralized MD plants; $C^{dw}_{t-cmp_S}$ denotes the total transportation cost from centralized MD plants to disposal wells; $C^{dw}_{t-shale}$ denotes the total transportation cost from shale gas sites to disposal wells; and $C^{dw}_{t-ons_S}$ denotes the total transportation cost from onsite treatment units to disposal wells.

Total transportation cost from shale gas sites to compressor stations is given by equation 32 where VTC is variable transportation cost of produced water using trucks, $wj_{i,j,t}$ is the amount of produced water from shale gas site i transported to compressor station j at time period t, and $DJ_{i,j}$ is the driving distance from shale gas site i to compressor station j.

$$\boldsymbol{C^{cs}_{t-shale} = \sum_{i\in I}\sum_{j\in J}\sum_{t\in T}(\mathrm{VTC}.\, wj_{i,j,t}.\, DJ_{i,j})} \qquad (32)$$

$C_{t-CS_S}^{dw}$, $C_{t-shale}^{cmp}$, $C_{t-cmp_S}^{dw}$, $C_{t-shale}^{dw}$, $C_{t-ons_S}^{dw}$ are given in equations 33-37 where $SJ_{j,d}$ is the driving distance from compressor station j to disposal well d, $DM_{i,m}$ denotes the driving distance from shale gas site i to centralized MD plant m, $SM_{m,d}$ denotes the driving distance from centralized MD plant m to disposal well d, $DD_{i,d}$ denotes the driving distance from shale site i to disposal well d, and $SO_{o,d}$ denotes the driving distance from onsite treatment unit o to disposal well d.

$$\boldsymbol{C_{t-CS_S}^{dw}} = \sum_{j \in J} \sum_{d \in D} \sum_{t \in T} (\mathbf{VTC}.\, \boldsymbol{sj_{j,d,t}}.\, \boldsymbol{SJ_{j,d}}) \tag{33}$$

$$\boldsymbol{C_{t-shale}^{cmp}} = \sum_{i \in I} \sum_{m \in M} \sum_{t \in T} (\mathbf{VTC}.\, \boldsymbol{wm_{i,m,t}}.\, \boldsymbol{DM_{i,m}}) \tag{34}$$

$$\boldsymbol{C_{t-cmp_S}^{dw}} = \sum_{m \in M} \sum_{d \in D} \sum_{t \in T} (\boldsymbol{VTC}.\, \boldsymbol{sm_{m,d,t}}.\, \boldsymbol{SM_{m,d}}) \tag{35}$$

$$\boldsymbol{C_{t-shale}^{dw}} = \sum_{i \in I} \sum_{d \in D} \sum_{t \in T} (\mathbf{VTC}.\, \boldsymbol{wd_{i,d,t}}.\, \boldsymbol{DD_{i,d}}) \tag{36}$$

$$\boldsymbol{C_{t-ons_S}^{dw}} = \sum_{o \in O} \sum_{d \in D} \sum_{t \in T} (\mathbf{VTC}.\, \boldsymbol{so_{o,d,t}}.\, \boldsymbol{SO_{o,d}}) \tag{37}$$

Total cost of treatment is given by equation 38. The unit cost of treatment for each treatment option is obtained from detailed techno-economic assessment and varies for feed TDS levels [236].

$$C_{treatment} = C_{treat}^{cs} + C_{treat}^{cmp} + C_{treat}^{ons} \tag{38}$$

C_{treat}^{cs} denotes the total cost of treatment at NG CS; C_{treat}^{cmp} denotes the total cost of treatment at centralized MD plants; and C_{treat}^{ons} denotes the total cost of treatment at onsite treatment units.

Treatment cost at NG CS is given by equation 39.

$$C_{treat}^{cs} = \sum_{i}\sum_{j}\sum_{t} wj_{i,j,t} . CJ \tag{39}$$

where $wj_{i,j,t}$ is the amount of produced water from shale gas site i transported to compressor station j at time period t, and CJ is the unit cost of treating produced water with a specific TDS level at compressor station j.

Similarly, C_{treat}^{cmp} and C_{treat}^{ons} are given by equations 40 and 41. CM is the unit cost of treating produced water with a specific TDS level at centralized MD plant m. CO is the unit cost of treating produced water with a specific TDS level at onsite treatment unit o.

$$C_{treat}^{cmp} = \sum_{i}\sum_{m}\sum_{t} wm_{i,m,t} . CM \tag{40}$$

$$\boldsymbol{C_{treat}^{ons}} = \sum_{i}\sum_{o}\sum_{t} \boldsymbol{wo_{i,o,t}.CO} \tag{41}$$

Total cost of injection is given by equation 42

$$\boldsymbol{C_{injection}} = \boldsymbol{C_{in-shale}^{dw}} + \boldsymbol{C_{in-cs_S}^{dw}} + \boldsymbol{C_{in-cmp_S}^{dw}} + \boldsymbol{C_{in-ons_S}^{dw}} \tag{42}$$

where $C_{in-shale}^{dw}$ denotes the cost of injecting produced water routed from shale gas sites to disposal wells which is expressed as equation 43 in which $wd_{i,d,t}$ is the amount of produced water routed from shale gas site i to disposal well d at time period t, and CD is the unit cost of injecting produced water into SWD wells.

$$\boldsymbol{C_{in-shale}^{dw}} = \sum_{i}\sum_{d}\sum_{t} \boldsymbol{wd_{i,d,t}.CD} \tag{43}$$

$C_{in-cs_S}^{dw}$ denotes the cost of injecting concentrated brine routed from compressor station j to disposal wells d expressed as equation 44.

$$\boldsymbol{C_{in-cs_S}^{dw}} = \sum_{j}\sum_{d}\sum_{t} \boldsymbol{sj_{j,d,t}.CD} \tag{44}$$

$C_{in-cmp_S}^{dw}$ denotes the cost of injecting produced water routed from shale gas sites to disposal wells, expressed as equation 45.

$$\boldsymbol{C_{in-cmp_S}^{dw}} = \sum_{\boldsymbol{m}} \sum_{\boldsymbol{d}} \sum_{\boldsymbol{t}} \boldsymbol{sm_{m,d,t}} . \boldsymbol{CD} \quad (45)$$

$C_{in-ons_S}^{dw}$ denotes the cost of injecting produced water routed from shale gas sites to disposal wells, expressed as equation 46.

$$\boldsymbol{C_{in-ons_S}^{dw}} = \sum_{\boldsymbol{o}} \sum_{\boldsymbol{d}} \sum_{\boldsymbol{t}} \boldsymbol{so_{o,d,t}} . \boldsymbol{CD} \quad (46)$$

4.2.3.3 Modeling the problem as mixed-integer nonlinear program (MINLP) model

It is important to note the problem of finding the optimum management strategies for shale gas produced water could also be modeled through a mixed-integer nonlinear programming (MINLP) model where staircase function is used for treatment cost calculation [259]. Different capacity ranges are considered for each treatment option and depending on the amount of produced water allocated to each treatment facility, the size of a treatment option is defined. Associated cost of treatment is then calculated using a staircase total cost function. In the original model explained above, we have simplified the MINLP model to an LP model since the results of TEA have shown that plant capacity plays an insignificant role in total cost of treatment [236].

However, the model formulation as an MINLP model is described in the following section. As an example, if three levels of sizing denoted as a_1, a_2, and a_3 are considered for treatment facilities at NG CS as is explained in equations 47-49, Equations 50-52 will be used as additional constraints to decide the optimum installed capacity, and then Equation 33 will replace Equation 19 in the objective function to account for the cost of treatment at NG CS.

If $\mathbf{0} \leq \boldsymbol{max} \sum_i \sum_c \boldsymbol{wj}_{i,j,c,t} \leq \boldsymbol{a_1}, \forall \boldsymbol{j}, \boldsymbol{t}$ then capacity range a_1 is selected (47)

If $\boldsymbol{a_1} < \boldsymbol{max} \sum_i \sum_c \boldsymbol{wj}_{i,j,c,t} \leq \boldsymbol{a_2}, \forall \boldsymbol{j}, \boldsymbol{t}$ then capacity range a_2 is selected (48)

If $\boldsymbol{a_2} < \boldsymbol{max} \sum_i \sum_c \boldsymbol{wj}_{i,j,c,t} \leq \boldsymbol{a_3}, \forall \boldsymbol{j}, \boldsymbol{t}$ then capacity range a_3 is selected (49)

Capacity range constraints

In Equations 30-32, $wj_{i,j,t}$ denotes the amount of produced water transported from wellpad i to compressor station j at time period t, ε is a very small number and U_1 and U_2 are binary variables.

$$\boldsymbol{a_1 U_1} \leq \left(\boldsymbol{max} \sum_i \boldsymbol{wj}_{i,j,t} \right) - \boldsymbol{\varepsilon}, \forall \boldsymbol{j}, \boldsymbol{t} \tag{50}$$

$$\left(\boldsymbol{max} \sum_{i} \boldsymbol{wj}_{i,j,t} \right) \leq \boldsymbol{a}_1 + (\boldsymbol{a}_2 - \boldsymbol{a}_1)\boldsymbol{U}_1 + (\boldsymbol{a}_3 - \boldsymbol{a}_2)\boldsymbol{U}_2, \forall \boldsymbol{j}, \boldsymbol{t} \tag{51}$$

$$\boldsymbol{a}_2\boldsymbol{U}_2 \leq \left(\boldsymbol{max} \sum_{i} \boldsymbol{wj}_{i,j,t} \right) - \boldsymbol{\varepsilon}, \forall \boldsymbol{j}, \boldsymbol{t} \tag{52}$$

In equation 53, $CJ_{j,c,a1}$ denotes the treatment cost at compressor station with capacity a_1; $CJ_{j,c,a2}$ denotes the treatment cost at compressor station with capacity a_2; and $CJ_{j,c,a3}$ denotes the treatment cost at compressor station with capacity a_3.

$$C_{treat}^{cs} = \sum_{i}\sum_{j}\sum_{c}\sum_{t} \boldsymbol{wj}_{i,j,c,t} . ((\boldsymbol{1} - \boldsymbol{U}_1)\boldsymbol{CJ}_{j,c,a1} + (\boldsymbol{U}_1 - \boldsymbol{U}_2)\boldsymbol{CJ}_{j,c,a2} + (\boldsymbol{U}_1 . \boldsymbol{U}_2)\boldsymbol{CJ}_{j,c,a3}) \tag{53}$$

Similarly, if three levels of sizing k_1, k_2, and k_3 are considered for treatment facilities at centralized MD plants, Equations 54-56 will be used to decide the optimum installed capacity, and then equation 57 will replace equation 40 in the objective function to account for the cost of treatment at centralized MD plants. $wm_{i,m,t}$ denotes the amount of produced water transported from wellpad i to centralized MD plant m at time period t

$$\boldsymbol{k}_1\boldsymbol{U}_1 \leq \left(\boldsymbol{max} \sum_{i} \boldsymbol{wm}_{i,m,t} \right) - \boldsymbol{\varepsilon}, \forall \boldsymbol{j}, \boldsymbol{t} \tag{54}$$

$$\left(\boldsymbol{max} \sum_{\boldsymbol{i}} \boldsymbol{wm}_{\boldsymbol{i,m,t}} \right) \leq \boldsymbol{k_1} + (\boldsymbol{k_2} - \boldsymbol{k_1})\boldsymbol{U_1} + (\boldsymbol{k_3} - \boldsymbol{k_2})\boldsymbol{U_2}, \forall \boldsymbol{j}, \boldsymbol{t} \tag{55}$$

$$\boldsymbol{k_2 U_2} \leq \left(\boldsymbol{max} \sum_{\boldsymbol{i}} \boldsymbol{wm}_{\boldsymbol{i,m,t}} \right) - \boldsymbol{\varepsilon}, \forall \boldsymbol{j}, \boldsymbol{t} \tag{56}$$

In equation 57, $\mathrm{CM}_{m,c,k1}$ denotes the treatment cost at compressor station with capacity k_1; $\mathrm{CM}_{m,c,k2}$ denotes the treatment cost at compressor station with capacity k_2; and $\mathrm{CM}_{m,c,k3}$ denotes the treatment cost at compressor station with capacity k_3.

$$\boldsymbol{C^{cs}_{treat}} = \sum_{\boldsymbol{i}} \sum_{\boldsymbol{m}} \sum_{\boldsymbol{c}} \sum_{\boldsymbol{t}} \boldsymbol{wm}_{\boldsymbol{i,m,c,t}} . ((\boldsymbol{1} - \boldsymbol{U_3})\boldsymbol{CM}_{\boldsymbol{m,c,k1}} + (\boldsymbol{U_3} - \boldsymbol{U_4})\boldsymbol{CM}_{\boldsymbol{m,c,k2}} + (\boldsymbol{U_3} . \boldsymbol{U_4})\boldsymbol{CM}_{\boldsymbol{m,c,k3}}) \tag{57}$$

If we consider three levels of sizing l_1, l_2, and l_3 for onsite treatment facilities, equations 58-60 will be used to decide the optimum installed capacity, and then Equation 61 will replace equation 40 in the objective function to account for the cost of treatment at onsite treatment units. In equations 58-61, $wo_{i,o,t}$ denotes the amount of produced water transported from wellpad i to onsite treatment unit o at time period t.

$$\boldsymbol{l_1 U_1} \leq \left(\boldsymbol{max} \sum_{\boldsymbol{i}} \boldsymbol{wo}_{\boldsymbol{i,o,t}} \right) - \boldsymbol{\varepsilon}, \forall \boldsymbol{j}, \boldsymbol{t} \tag{58}$$

$$\left(\boldsymbol{max} \sum_{i} \boldsymbol{wo}_{i,o,t} \right) \leq \boldsymbol{l}_1 + (\boldsymbol{l}_2 - \boldsymbol{l}_1)\boldsymbol{U}_1 + (\boldsymbol{l}_3 - \boldsymbol{l}_2)\boldsymbol{U}_2, \forall \boldsymbol{j}, \boldsymbol{t} \tag{59}$$

$$\boldsymbol{l}_2\boldsymbol{U}_2 \leq \left(\boldsymbol{max} \sum_{i} \boldsymbol{wo}_{i,o,t} \right) - \boldsymbol{\varepsilon}, \forall \boldsymbol{j}, \boldsymbol{t} \tag{60}$$

In equation 61, $\mathrm{CO}_{o,c,l1}$ denotes the treatment cost at onsite treatment unit with capacity l_1; $\mathrm{CO}_{o,c,l2}$ denotes the treatment cost at onsite treatment unit with capacity l_2; and $\mathrm{CO}_{o,c,l3}$ denotes the treatment cost at onsite treatment unit with capacity l_3.

$$\boldsymbol{C}_{treat}^{ons} = \sum_{i}\sum_{o}\sum_{c}\sum_{t} \boldsymbol{wo}_{i,o,c,t}.((\mathbf{1} - \boldsymbol{U}_5)\boldsymbol{CO}_{o,c,l1} + (\boldsymbol{U}_5 - \boldsymbol{U}_6)\boldsymbol{CO}_{o,c,l2} + (\boldsymbol{U}_5.\boldsymbol{U}_6)\boldsymbol{CO}_{o,c,l3}) \tag{61}$$

4.3 RESULTS

The optimization model is applied to four real-world case studies with major shale gas development activities in Marcellus shale play in PA. Each case study includes one county, and in total four counties of Susquehanna and Bradford in the Northeast PA and Washington and Greene in the Southwest PA are examined (see Figure 19). These case studies differ in terms of their proximity to disposal wells in Ohio as well as the distribution of available waste heat sources at NG CS in each county.

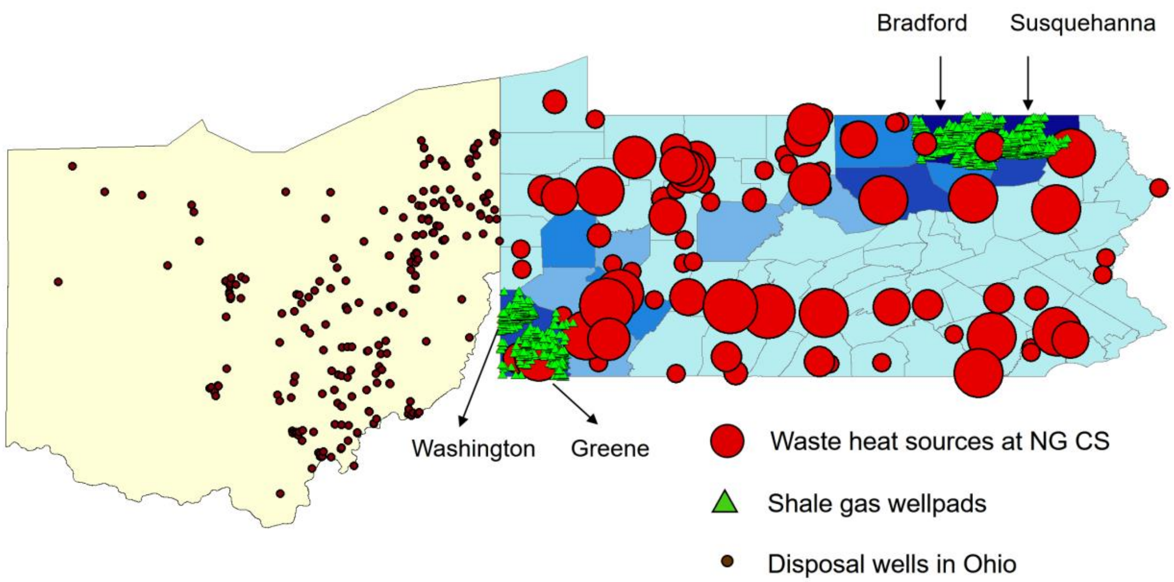

Figure 19. Case studies examined in this work. Spatial location of waste heat sources at NG CS, shale gas wellpads, and SWD wells in Ohio are shown.

Table 3 presents the number of active shale gas wells, number of wellpads, shale gas production, and produced water generation per unit of shale gas production for each county. Shale gas wells with same longitude-latitude are integrated into wellpads based on the location data published by PA DEP [252]. It is important to note that shale gas production is not linearly correlated with the amount of produced water generation across the counties primarily due to differences in the geology of shale gas extraction regions. Figure 20 shows the county level produced water generation as well as the theoretical treatment capacity at NG CS in each county. Details regarding treatment capacity estimation can be found in [216]. As shown from Table 3, Susquehanna county is the top shale gas producing county according to the statistics published by PA DEP [252], however, it is ranked number three in terms of produced water generation (see Figure 20) [30].

Table 3. Number of wells and wellpads, shale gas production, and produced water generation in four case studies

County	Number of Wells	Number of Wellpads	shale gas production (MMcf-6months period)	produced water per amount of shale gas (bbl/MMcf)
Susquehanna	614	217	389,595	3
Bradford	801	399	349,857	3
Washington	758	189	197,505	13
Greene	528	162	172,099	9

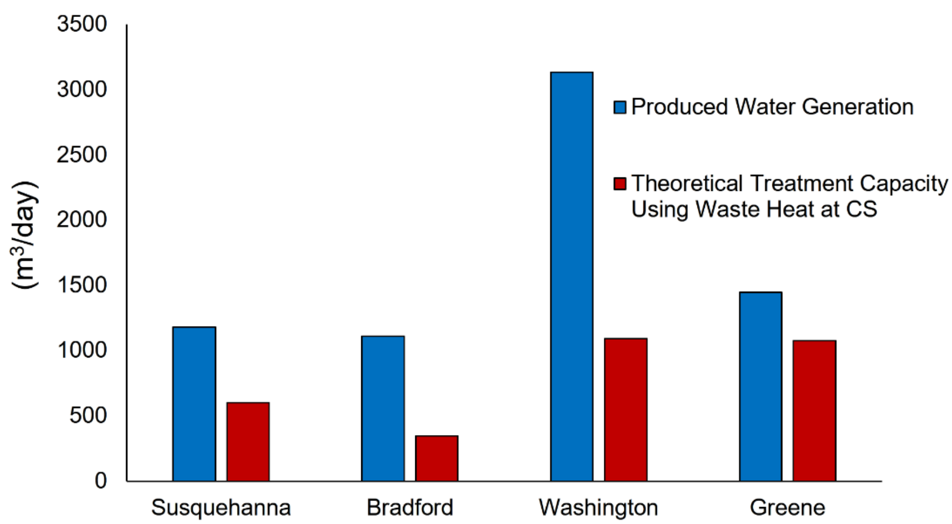

Figure 20. produced water generation and theoretical treatment capacity at NG CS in four case studies

The results of optimization modeling are shown in Table 4. These results are presented for two TDS levels: 100 and 250 g/L. The optimal solution in all four counties comprises of two different management strategies: (1) onsite treatment at shale gas sites either at the same site where produced water is generated or another shale gas site where the produced water from multiple sites is gathered and being treated and (2) treatment at NG CS where available waste heat can be exploited to offset the thermal energy requirements of the MD treatment process. The breakdown of total cost into transportation, treatment, and injection is also shown in Table 4. Associated cost of produced water management for Greene, Washington, Susquehanna, and Bradford counties is 5.19, 12.7, 14.5, and $12.1 million/year for TDS level of 100 g/L and increases to 8.8, 17.2, 31.0, and $26.3 million/year for TDS level of 250 g/L, respectively. The results reveal that the total management cost is sensitive to the TDS level of produced water as the recovery factor for MD treatment decreases with an increase in TDS level, indicating that a greater portion of produced water must be disposed at SWD wells.

Moreover, for each case study two additional scenarios are examined: (1) a scenario in which all the produced water is managed using BAU strategy which is direct disposal into SWD wells without any treatment processes and (2) a scenario in which available waste heat at NG CS is not utilized. In the latter scenario, the optimal solution includes onsite treatment of wastewater. The total cost of optimal management strategy is then compared to associated cost of these two scenarios in order to provide insights regarding the benefits of optimal management strategy. The results of this comparison are shown in Figure 21-Figure 24. Optimal management strategy can provide 31% benefit over the BAU strategy in Washington county, 47% in Greene county, and above 60% in Susquehanna and Bradford counties as these counties in Southwest PA are in close proximity to disposal wells in Ohio as compared to the counties in Northeast PA. These findings are compelling as they suggest that treatment of high salinity produced water using MD could result in significant reduction in produced water management cost. It is important to note that

MD is an advanced desalination technology with higher associated cost compared to conventional desalination technologies when it is not integrated with a source of waste heat, nonetheless, treating produced water using MD is accompanied with major economic benefit over BAU management strategy primarily due to significant reduction in cost of transportation of wastewater.

Table 4. Optimal solution for four case studies

County		TDS (g/L)	Treatment Cost	Injection Cost	Transportation Cost	Total Cost
			million USD/year			
Greene	Optimal Solution	100	1.08	1.10	3.02	5.19
		250	0.76	2.77	5.28	8.80
	Onsite Treatment	100	3.06	1.10	2.18	6.33
		250	2.77	0.93	5.23	8.93
	Direct disposal	100	0.00	3.32	6.65	9.97
		250	0.00	3.32	6.65	9.97
Washington	Optimal Solution	100	6.49	2.37	3.82	12.68
		250	2.02	5.99	9.22	17.23
	Onsite Treatment	100	6.63	2.37	3.71	12.72
		250	2.02	5.99	9.22	17.23
	Direct disposal	100	0.00	7.19	11.27	18.46
		250	0.00	7.19	11.27	18.46
Susquehanna	Optimal Solution	100	2.18	0.90	11.44	14.52
		250	0.76	2.26	27.95	30.97
	Onsite Treatment	100	2.50	0.90	11.21	14.61
		250	0.76	2.26	27.95	30.97
	Direct disposal	100	0.00	2.71	33.92	36.63
		250	0.00	2.71	33.92	36.63
Bradford	Optimal Solution	100	1.71	0.84	9.56	12.11
		250	0.66	2.12	23.53	26.32
	Onsite Treatment	100	2.35	0.84	9.34	12.53
		250	0.72	2.12	23.50	26.34
	Direct disposal	100	0.00	2.55	28.32	30.87
		250	0.00	2.55	28.32	30.87

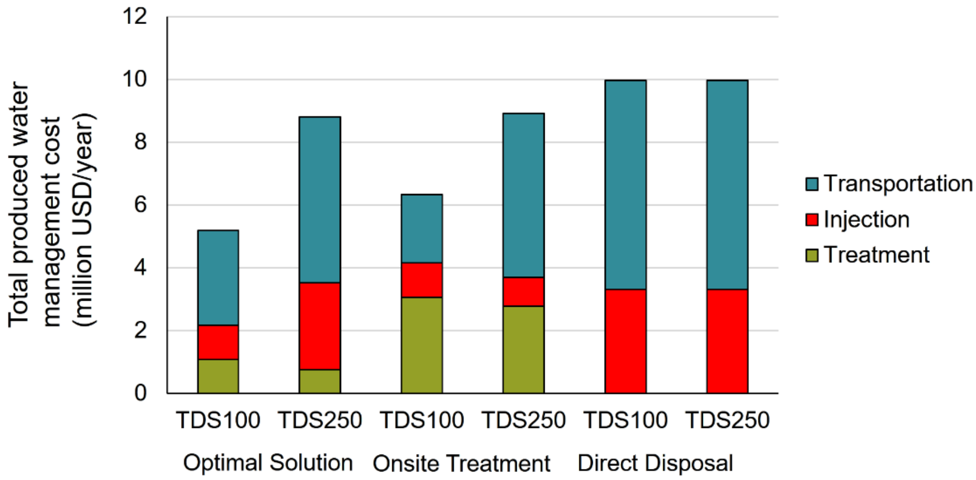

Figure 21. Optimal solution versus direct disposal and onsite treatment for Greene county

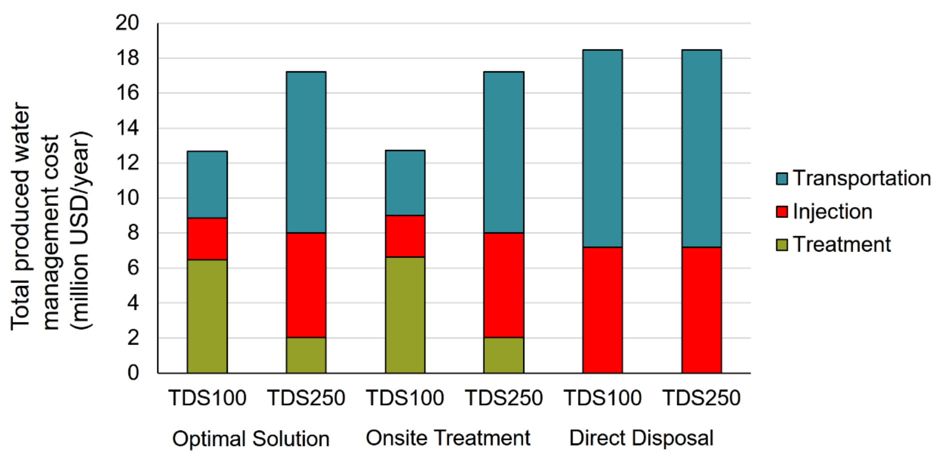

Figure 22. Optimal solution versus direct disposal and onsite treatment for Washington county

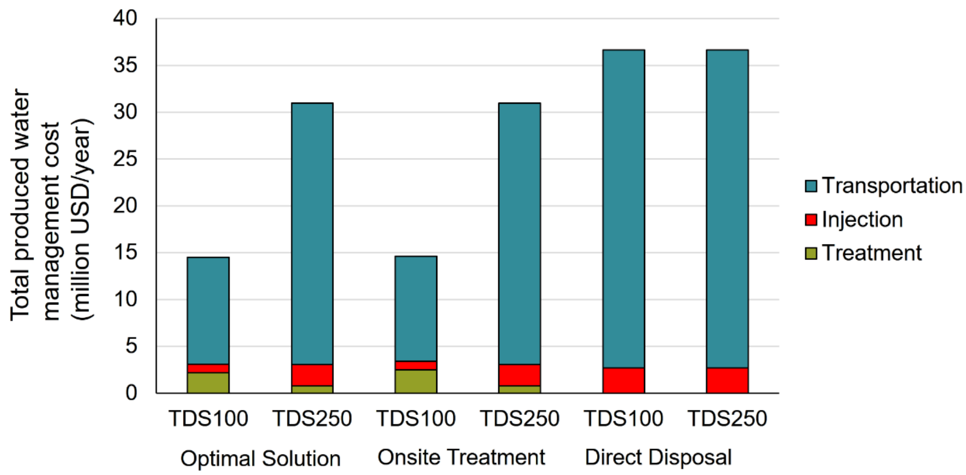

Figure 23. optimal solution versus direct disposal and onsite treatment for Susquehanna county

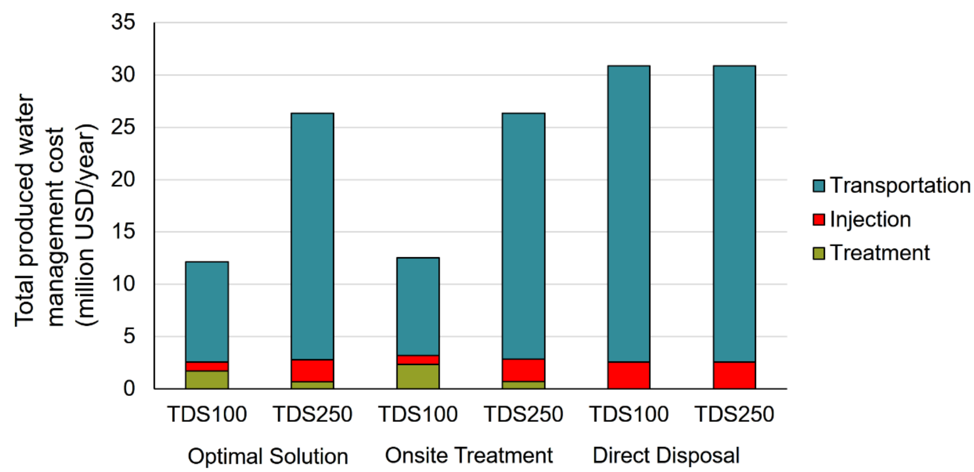

Figure 24. Optimal solution versus direct disposal and onsite treatment for Bradford county

Sensitivity analysis is performed to understand how variations in cost of different strategies affect the choice of optimum produced water management strategy. The results of sensitivity analysis are shown for produced water with TDS level of 100 g/L in the Greene county. This analysis revealed that the result of optimization model is most sensitive to changes in transportation cost (Figure 25). The results in Figure 25 show that a 20% increase in the transportation cost (i.e., from \$0.25/m^3/mile to \$0.3/m^3/mile) resulted in 12% increase in total management cost indicating the high sensitivity of produced water management to transportation cost. Moreover, we investigated at which point direct disposal into SWD wells will be included in the optimal solution. As shown from Figure 25, direct disposal is not included in optimum management strategy unless the transportation cost could be as low as \$0.07/m^3/mile which is not currently a realistic transportation cost. However, it is important to note that direct disposal is chosen as part of optimal solution along with onsite treatment at shale gas sites and treatment at NG CS when transportation cost is \$0.07/m^3/mile. It is interesting to note that changes in treatment cost have a comparatively minimal impact on the total cost of produced water treatment (Figure 26).

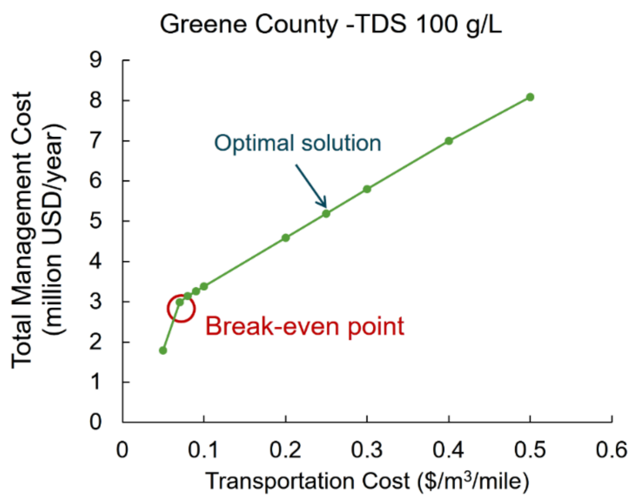

Figure 25. Sensitivity analysis of transportation cost on total produced water management cost for Greene County

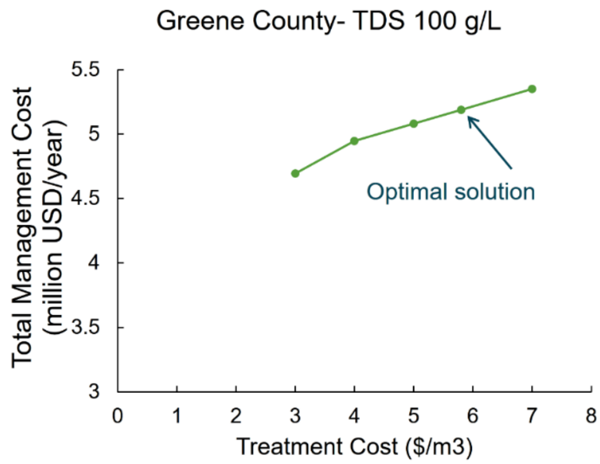

Figure 26. Sensitivity analysis of treatment cost using MD on total cost of produced water management cost

4.4 DISCUSSION

This work is proof of concept that shale gas produced water treatment using MD technology is a promising strategy which could be significantly more economical than BAU management strategy in addition to potential benefits it can provide in terms of environmental sustainability. The results of this work have shown that treating produced water at shale gas sites or NG CS using available waste heat has the highest economic performance for the examined case studies in PA, and suggest that volume reduction close to source of generation can achieve enormous cost savings, with more than 60% reduction in total management cost relative to the BAU in the best case. Furthermore, the results of this work have shown that transportation cost dominates every other cost element in the entire management process, constituting about 80% of total wastewater management cost in Northeast PA.

It is important to note that this study does not consider any economic benefit for the permeate generated from the treatment process which is a conservative assumption for the present study primarily because PA is a water rich state. This could be of interest in water scarce shale regions such as Texas or Oklahoma. Specifically, when MD is used as the treatment technology, the permeate has pure water quality [174, 260-262] and hence is above the standard limits for re-injection purposes which makes it applicable for agriculture uses or surface water release. Inclusion of potential beneficiary uses of the permeate and subsequent economic benefits merits further investigation.

In addition to feed TDS level, the temperature of feed water could play an important role in associated cost of onsite treatment of produced water as it will significantly impact the energy requirements of MD process. In the results presented here, it is assumed that produced water is at ambient temperature and it must be heated up to reach the desired temperature for MD operation which is a conservative assumption, nonetheless, onsite treatment is chosen as the optimum management strategy in the optimization model. However, the temperature of produced water could be as high as 100^{o}C [38] which could result in major cost savings for onsite treatment of produced water.

While MD technology proposed in this study has been demonstrated at the laboratory scale with over 99.9% of TDS removal capability [39], and the performance of this technique has been simulated at the plant scale [216], additional pilot-scale testing and techno-economic analysis is necessary as MD is plagued with technological uncertainty and is yet to be effectively demonstrated at a commercial scale to ensure that the process is practically and economically feasible at larger scales. Further, membrane distillation crystallization (MDC) systems should be considered for their potential for enhanced volume reduction and improving the economics of shale gas wastewater management as it results in minimization of transportation costs [174, 231] and simultaneously generating salt as a useful byproduct [263, 264]. Waste heat integrated MDC systems with promising thermal energy requirements and waste minimization show merit for the coproduction of permeate and salt and should be considered in future shale gas wastewater management studies.

While the results of this study suggest that transportation of produced water should be minimized from an economic point of view, it is important to note that transportation is also associated with high GHG emissions which may result in more favorable results for treatment of shale gas high salinity wastewater. Worldwide transportation-related energy demand is projected to increase by 25% between 20 and 2040, as such, reducing emissions from the transportation sector could play a critical role in global GHG emissions reduction [265]. Inclusion of carbon footprint of different management strategies merits further investigation as single-objective optimization fails to capture the environmental impacts that may compromise the long-term sustainability of these strategies. Accordingly, additional criteria such as infrastructure (roads) damage and traffic-related environmental impacts of hydraulic fracturing must be considered so that shale gas production does not inadvertently shift environment impacts [266]. In addition, it is important to recognize that available waste heat at NG CS will displace the heat that would otherwise have to be derived by combustion of NG, as such, avoided GHG emissions should be credited to the treatment of produced water using waste heat management strategy.

The optimization model developed here has been applied to four case studies differing in terms of their proximity to disposal wells in Ohio as well as the amount and spatial distribution of available waste heat sources, however, direct disposal into SWD wells is not part of the optimal management strategy for any of the examined case studies. However, cost of transportation and transportation distance to disposal wells could significantly alter the results of optimization. Transportation cost varies across the states and counties primarily due to changes in average speed limit and road conditions. As such, the results could be different across shale plays in the U.S. and merits further investigation.

Shale gas wells are integrated into wellpads based on longitude-latitude information published by PA DEP [252]. While it is technically feasible to drill 12 wells or more per wellpad, the majority of wellpads contain 1, 2, or 3 wells as development of singular wells could help companies to secure the long-term rights to the mineral acreage [24, 267]. As shale gas sites mature, the number of wells per wellpad will have a more even distribution which is likely to marginally alter the results of this work and merits further investigation, however, the broad-based conclusions of this study remain unchanged. In addition, it is important to recognize that two types of NG are trapped in Marcellus shale play: dry NG which mainly comprised of methane and is more prevalent in central and northeast PA and wet NG that constitutes other hydrocarbons such as ethane and butane, collectively known as natural gas liquids (NGL) in addition to methane. Due to increased interest in NGL, future studies should take into account the profit gained from natural gas and NGL production and its consequent impact on the economics of shale gas wastewater management.

Notation

Sets:

I = set of shale gas sites (wellpads) indexed by i

J = set of natural gas compressor stations sites indexed by j

A= set of capacity ranges for compressor stations (a_1, a_2, a_3)

O = set of on-site treatment sites indexed by o

L= set of capacity ranges for on-site treatment units (l_1, l_2, l_3)

M = set of centralized MD plants indexed by m

K= set of capacity ranges for centralized MD plants (k_1, k_2, k_3)

D = set of disposal wells indexed by d

T = set of time periods indexed by t

Parameters:

$PW_{i,t}$ = total produced water at shale gas site i at time period t

TJ_j = maximum treatment capacity at compressor station j

TM_m = maximum treatment capacity at centralized MD plant m

TO_o = maximum treatment capacity at on-site treatment facility o

$DJ_{i,j}$ = Transportation distance from shale gas site i to compressor station j

$DM_{i,m}$ = Transportation distance from shale gas site i to centralized treatment plant m

$DO_{i,o}$ = Transportation distance from shale gas site i to onsite treatment o

$DD_{i,d}$ = Transportation distance from shale gas site i to disposal well d

$SJ_{j,d}$ = Transportation distance from compressor station j to disposal well d (sludge disposal)

$SM_{m,d}$ = Transportation distance from centralized treatment plant m to disposal well d

$SO_{o,d}$ = Transportation distance from on-site treatment o to disposal well d

VTC = variable transportation costs by trucking ($/m^3.mile)

$CJ_{j,c,a}$ = unit treatment cost at compressor station j with size a

$CM_{m,c,k}$ = unit treatment cost at centralized MD plant m with size k

$CO_{o,c,l}$ = unit treatment cost at onsite treatment unit o with size l

CD = unit cost of injecting produced water at disposal wells ($/m^3)

CR = correlation coefficient for recovery factor (1-CR = concentrated brine production)

Continuous variables

$wj_{i,j,t}$ = amount of produced water transported from shale gas site i to compressor station j at time period t

$wm_{i,m,c,t}$ = amount of TDS concentration level c produced water from shale gas site i transported to centralized MD treatment plant m at time period t

$wd_{i,d,c,t}$ = amount of TDS concentration level c produced water from shale gas site i transported to disposal well d at time period t

$wo_{i,o,c,t}$ = amount of TDS concentration level c produced water from shale gas site i treated at onsite treatment o at time period t

$sj_{j,d,t}$ = amount of sludge from compressor station j transported to disposal well d at time period t

$sm_{m,d,t}$ = amount of sludge from centralized MD plant m transported to disposal well d at time period t

$so_{o,d,t}$ = amount of sludge from onsite treatment unit o transported to disposal well d at time period t

Binary variables

U_1-U_6 =0-1 variable used to decide the size of treatment facilities at NG CS, centralized treatment plants, and onsite treatment units.

5.0 CONCLUSIONS AND FUTURE WORK

Shale gas is touted as a revolutionary source of clean energy with lower GHG emissions relative to other fossil fuels. However, its large-scale commercialization without proper consideration of the potential widespread consequences for the environment could be problematic. Multiple studies have shown that the extraction and production of unconventional natural gas has resulted in detrimental impacts on the ecosystem and environment including increased greenhouse gas (GHG) emissions at shale gas extraction sites [5-7], high water footprint [12], and high salinity wastewater management [13, 14]. As energy systems are inherently interconnected and complex, it is crucial to understand the potential widespread impact of shale gas production on economics, environment, and human welfare prior to their widespread adoption and commercialization. To date, the scientific consensus is inconclusive on several pivotal questions within the shale gas sustainability discourse, including: (I) the quality and quantity of wastewater generated from hydraulic fracturing, (II) the cost of shale gas wastewater treatment using advanced treatment technologies such as emerging membrane distillation (MD), (III) how the cost of shale gas wastewater treatment can be improved by exploring regional industrial ecology opportunities e.g., offsetting the energy requirements of the treatment process by utilizing available industrial waste hear sources, (IV) how much waste heat is available at NG CS that could potentially be integrated into shale gas wastewater treatment process, and (V) the optimum management strategy for shale gas wastewater management which can provide the greatest potential economic benefits, and (VI) how treatment of shale gas high salinity wastewaters compares with BAU strategy. This work sought to answer these questions piecewise using a case-study approach.

Chapter 2 investigated the waste heat recovery opportunities from NG CS on a state level in the contiguous United States (RQ #1). Thermodynamic analysis based on energy and exergy provided a scientifically rigorous approach for quantifying the amount of waste heat in the exhaust stream of compressor engines, while concurrently addressing several existing uncertainties in waste heat estimation due to lack of specific information on configuration and operation of individual compressor stations by applying statistical approaches. The results indicate that a large amount of high quality waste heat is available at NG CS. Although the waste heat recovery is plagued with technological uncertainty it has potential for improving energy efficiency via synergies with industrial process. In addition, the results of waste heat estimation revealed that states with major shale gas development such as Pennsylvania, Texas, and Oklahoma have also the greatest share of available waste heat recovery opportunities, thus making it suitable for developing industrial symbiotic opportunities for shale gas wastewater treatment using available waste heat.

The critical parameters in waste heat estimation were determined to be installed capacity of compressor stations, the type of compressor engines, and the operating hours of compressor stations. Due to lack of information on compressor engine type and operating hours of individual compressor stations, a combination of k-nearest neighbor algorithm for pattern recognition and Monte-Carlo simulation for modeling the load factor of compressor stations were employed to capture the uncertainty in waste heat estimation. Key research opportunities and challenges in waste heat recovery from NG CS are discusses in this work, however, for actual implementation of waste heat recovery facilities in a compressor station and its integration with shale gas wastewater treatment, detailed information on compressor engine type and operating hours of specific compressor stations are required and merits further investigation in order to determine their technical feasibility and commercial applicability. Future work should focus on understanding the technological and economic feasibility of implementing commercial scale waste heat recovery facilities at NG CS in addition to waste heat integrated MD technology. Moreover, a comprehensive evaluation of end-uses for available waste heat at NG CS is encouraged in the future work particularly in states with no shale gas activities where waste heat cannot be integrated with shale gas wastewater treatment process as the available waste heat at NG CS is of high quality, thus making the recovery of waste heat thermodynamically feasible for a wide range of uses.

Chapter 3 developed a techno-economic assessment (TEA) model to quantify the cost of shale gas produced water treatment using membrane distillation (MD) as well as evaluating the total cost of treatment when available waste heat at NG CS could be utilized to provide the energy requirements of desalination process (RQ #2). This work revealed that the cost of treating shale gas high salinity wastewater is highly dependent on thermal energy price reflected in the decreased treatment cost when MD is coupled with a source of waste heat. Waste heat integrated MD treatment is more cost-efficient compared to conventional desalination technologies such as reverse osmosis (RO) and forward osmosis (FO) which are not energetically viable for treatment of high salinity wastewaters in addition to being more energy intensive in terms of electricity requirements for their operation. Additionally, total cost of water treatment using MD technology is found to be highly dependent on the salinity level of feed water and the uncertainty in total cost is captured by sensitivity analysis in this work. Given that wastewater characteristics, including the presence of organics, is highly dependent on the shale formation location, further investigation for other shale plays as the results of this study are presented for Marcellus shale play in Pennsylvania.

In addition, this work has shown that produced water treatment could result in substantial economic benefits as compared to BAU management strategy which is direct disposal into SWD wells primarily due to high transportation cost associated with disposal of produced water. This work highlighted the fallacies of traditional TEA for desalination of produced water, and showed that inclusion of cost of produced water intake and disposal can provide valuable insights into the economic sustainability of shale gas wastewater treatment. However, technological maturation and optimization as well as commercial scale adaptation of membrane distillation technology in addition to coupling treatment process with waste heat sources have the potential for enhancing the economics of produced water treatment while concurrently increasing the sustainability of shale gas production. Future work should focus on understanding the technological and economic feasibility of implementing commercial scale MD plants in addition to waste heat integrated MD systems.

Chapter 4 proposes a novel optimization framework for long-term planning of shale gas wastewater management to guarantee the sustainable development of unconventional natural gas industry. A systems-level optimization model is developed to identify the optimum shale gas wastewater management strategy for multiple shale gas development regions in Pennsylvania accounting for associated cost of transportation, treatment, and injection of shale gas wastewater with each management strategy (RQ #3). This work revealed that optimum shale gas wastewater management which includes: (1) onsite treatment of produced water using MD at shale gas extraction sites and (2) treatment of produced water at NG CS sites where available waste heat could be utilized to offset the energy requirements of treatment process has economic advantage over the most common management strategy in the U.S. which is disposal into SWD wells. Optimum management strategies were found to have promising economic savings, with up to 60% reduction in total wastewater management cost relative to direct disposal in northeast PA. Transportation cost was found to constitute up to ~80% of total wastewater management in the worst-case and 30% in the best-case which calls for further wastewater volume reduction and show merit for evaluation of membrane distillation crystallization technologies, and thus should be considered in future studies.

This dissertation has shown that shale gas wastewater treatment has the capacity for cost abatement relative to BAU management strategy. However, MD technology proposed in this study is highly energy intensive and requires substantial thermal energy for the distillation process. In addition, technologies for treatment of shale gas high salinity wastewater are emerging fields, which in part explains why treatment cost using MD in the base-case is higher than that of conventional desalination technologies. This indicates that broad advances in commercialization of this technology is required if advanced treatment of produced water is to be competitive with established wastewater management strategies in shale plays in the U.S. However, the differential in cost between treatment and direct disposal is substantial and is expected to further increase over time. It is important to recognize that the economic benefits of reducing transportation cost occurs by concentrating the produced water using MD, and that the thermal energy required for the distillation process could be provided by synergistic integration of MD process with available waste heat sources in the industrial sector including NG CS.

Future work should investigate the carbon footprint of different shale gas wastewater management strategies in order develop a multi-objective optimization framework accounting for economic and environmental impacts criteria that can guarantee the long-term sustainability of these strategies. Moreover, each management strategy is accompanied by a range of harmful impacts such as infrastructure (roads) damage and traffic-related environmental impacts that should also be considered in future work. In addition, variations in wastewater management strategy according to location i.e., state or shale play would further improve the conclusions drawn from this study. In particular, availability of SWD wells in states such as Texas and differences in transportation cost are likely to alter the results of the optimization model presented here and merits further investigation.

APPENDIX A

SUPPLEMENTAL MATERIAL FOR CHAPTER 2

A.1 COMPRESSOR STATIONS MECHANICAL DRIVE TYPE

Table 5. Probability distribution for having an internal combustion engine within different installed capacity ranges stated as horsepower (HP)

Lower capacity range (HP)	Upper capacity range (HP)	Probability of being Internal Combustion
42	800	1.00
800	1558	0.91
1558	2316	0.98
2316	3075	1.00
3075	3833	0.83
3833	4591	0.75
4591	5349	0.62
5349	6107	0.71
6107	6865	0.63
6865	7624	0.40
7624	8382	0.67
8382	9140	0.13
9140	9898	0.00
9898	10656	0.29
10656	11414	0.25
11414	12173	0.33
12173	12931	0.00
12931	13689	0.00
13689	14447	0.00

Table 5 (continued).

14447	15205	0.00
15205	15963	0.00
15963	16722	0.00
16722	17480	0.00
17480	18238	0.00
18238	18996	0.00
18996	19754	0.00
19754	20512	0.00
20512	21270	0.00
21270	22029	0.00
22029	22787	0.00
22787	23545	0.00
23545	24303	0.00
24303	25061	0.00
25061	25819	0.00
25819	26578	0.00
26578	27336	0.00
27336	28094	0.00
28094	28852	0.00
28852	29610	0.00
29610	30368	0.00
30368	31127	0.00
31127	31885	0.00
31885	32643	0.00
32643	33401	0.00
33401	34159	0.00
34159	34917	0.00
34917	35676	0.00
35676	36434	0.00
36434	37192	0.00
37192	37950	0.00

A.2 THERMODYNAMIC ANALYSIS FOR WASTE HEAT ESTIMATION

A.2.1. Gas turbine CS

Figure 27 shows a process schematic of a typical gas turbine NG CS.

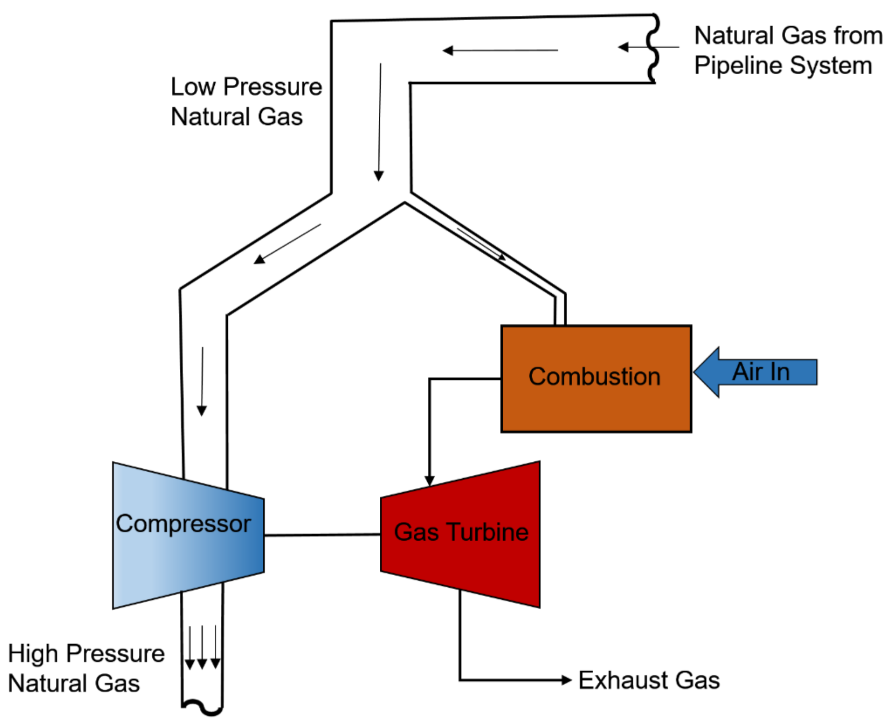

Figure 27. Simplified flow diagram of compressing NG and generating waste heat at gas turbine NG CS [135]

Adiabatic flame temperature calculation

In order to calculate the adiabatic flame temperature,[268] we define the initial condition of 1 atm pressure, *298°K* initial temperature and a 3.76 molar ratio for nitrogen to oxygen in the air. We also need to calculate fuel-air equivalence ratio (∅) which is defined as the ratio of actual fuel-to-air ratio ($(\frac{Fuel}{air})_{ac}$) to stoichiometry fuel-to-air ratio ($(\frac{Fuel}{air})_{st}$) for a given mixture.[269, 270] The actual combustion reaction with 100% excess air is written as equation 62 and the stoichiometric reaction is shown as equation 63. The equivalence ratio is then calculated as shown in equation 64.

$$CH_4 + 2 * 2(O_2 + 3.67\ N_2) \rightarrow CO_2 + 2H_2O + \ 2O_2 + 14.68N_2 \tag{62}$$

$$CH_4 + 2(O_2 + 3.67\ N_2) \rightarrow CO_2 + 2H_2O + 7.34\ N_2 \tag{63}$$

$$\emptyset = \frac{(\frac{Fuel}{air})_{ac}}{(\frac{Fuel}{air})_{st}} = \frac{(\frac{12+4}{2*2*32})}{(\frac{12+4}{2*32})} = 0.5 \tag{64}$$

We use *Cantera* online software toolkit[271] to calculate the adiabatic flame temperature and the resulting temperature is *1478°K* for combustion of methane with 100% excess air.

Flue gas composition and enthalpy calculations

The fuel composition for natural gas is shown in Table 6. We assume complete combustion with 10% excess air where air is composed of 21% oxygen and 79% Nitrogen.

Table 6. Assumed fuel composition (volumetric percentage)

Natural Gas	
Methane (CH_4)	93.27%
Ethane (C_2H_6)	3.79%
Propane (C_3H_8)	0.57%
Butane (C_4H_{10})	0.29%
Nitrogen	1.19%
Water	0.00%
Carbon Dioxide	0.79%

Methane is the primary constituent of the NG and the stoichiometric equation for combustion of methane with 10% excess air is shown equation 65.

$$CH_4 + 1.1 * 2(O_2 + 3.67\ N_2) \rightarrow CO_2 + 2H_2O + 0.2\ O_2 + 8.272N_2 \tag{65}$$

The combustion equation is written for each species in the fuel and the mole fraction of combustion products in the exhaust gas is determined as shown in Table 7. These values are used to calculate the enthalpy for each constituent of exhaust gas.

Table 7. Exhaust gas composition [93]

Flue Gas Species	Natural Gas
CO_2	9.7%
H_2O	18.7%
N_2	71.6%

Enthalpy values for each species in gas turbine inlet and outlet stream are calculated based on the temperature as following [137].

$$@\, T_{in} = 1400°K:$$

$$h_{Co_2} = 65271 \;\; kJ/kmol$$

$$h_{H_2O} = 55351 \;\; kJ/kmol$$

$$h_{N_2} = 43605 \;\; kJ/kmol$$

$$@\, T_{in} = 921°K:$$

$$h_{Co_2} = 38467 \;\; kJ/kmol$$

$$h_{H_2O} = \; 32629 \; kJ/kmol$$

$$h_{N_2} = 27532 \;\; kJ/kmol$$

The mass flow rate of exhaust gas is calculated as shown in equation 66. These calculations are carried out as an example for a compressor station with the capacity of *12000 HP* (*32214236.6 kJ/hr*) which is the average capacity of a compressor station in the U.S.

$$32214236.6 = \dot{m}\big(0.097(65217 - 38467) + 0.187(55351 - 32629) + 0.716(43606 - 27532)\big) \tag{66}$$

$$\dot{m} = 1755.35\ kmol/hr$$

In order to estimate the heat contained in the exhaust stream, we assume that the exhaust stream will be cooled down to *60°C (333°K)* [93, 147]. Available waste heat at this compressor station is calculated as shown in equation 67.

$@\ T_{in} = 921°K$:

$h_{Co_2} = 38467\ \ kJ/kmol$

$h_{H_2O} = \ 32629\ kJ/kmol$

$h_{N_2} = 27532\ \ kJ/kmol$

$@\ T_{in} = 333°K$:

$h_{Co_2} = 10570\ \ kJ/kmol$

$$h_{H_2O} = 10976 \ kJ/kmol$$

$$h_{N_2} = 9597 \ kJ/kmol$$

$$q = \dot{m}(h_{in} - h_{out}) = 1755.35 \frac{kmol}{hr} * (29545.834 - 9949.254) \frac{kJ}{kmol} = 34398853.74 \frac{kJ}{hr} \quad (67)$$

Table 8. List of all mathematical symbols and definition

Symbol	Definition
$\dot{W}_{comp}$	Power of compressor station
$\dot{W}_{turb}$	Power of gas turbine
$\dot{m}$	Mass flow rate
h_{in}	Inlet enthalpy
h_{out}	Outlet enthalpy
T_{in}	Inlet temperature
T_{out}	Outlet temperature
P_{in}	Inlet Pressure
P_{out}	Outlet Pressure
η	Gas turbine isentropic efficiency
k	Ratio of specific heat
h_{Co_2}	Enthalpy of Carbon Dioxide
h_{H_2O}	Enthalpy of Steam
h_{N_2}	Enthalpy of Nitrogen Gas

A.2.2. Reciprocating internal combustion (IC) engine CS

Figure 28 shows the schematic of four principal states of a cycle in an IC engine. Each cycle consists of two processes (processes 1-2 and 3-4) in which there is work but no heat transfer and two processes (processes 2-3 and 4-1) in which there is heat transfer but no work [137].

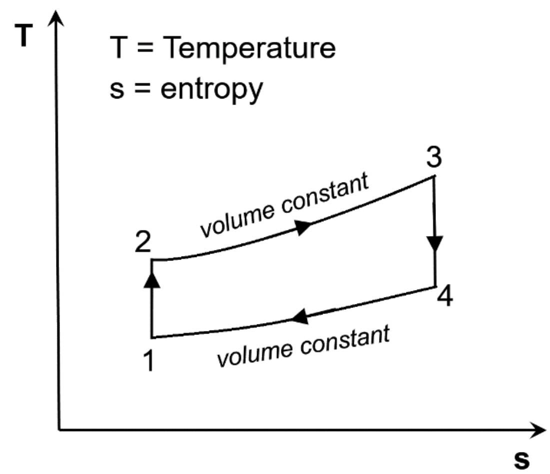

Figure 28. T-s diagram of four principal states of a cycle in an IC engine [137]

A.3 STATE SPECIFIC ELECTRICITY MIX

Table 9. Electricity generation mix by state [272]

Alaska (AK)	%	**Montana (MT)**	%
Coal	9.61	Coal	53.74
Hydroelectric Conventional	22.10	Hydroelectric Conventional	34.81
Natural Gas	52.66	Natural Gas	2.22
Other Biomass	0.80	Other	1.20
Petroleum	12.60	Other Gases	0.00
Wind	2.24	Petroleum	1.67

Table 9 (continued).

Alabama (AL)	
Coal	31.25
Hydroelectric Conventional	8.57
Natural Gas	30.94
Nuclear	27.11
Other Biomass	0.01
Other Gases	0.18
Petroleum	0.05
Wood and Wood Derived Fuels	1.90
Arkansas (AR)	
Coal	52.89
Hydroelectric Conventional	4.40
Natural Gas	20.13
Nuclear	19.81
Other	0.03
Other Biomass	0.17
Petroleum	0.07
Wood and Wood Derived Fuels	2.48
Arizona (AZ)	
Coal	38.39
Hydroelectric Conventional	5.22
Natural Gas	26.20
Nuclear	27.74
Other Biomass	0.06
Petroleum	0.04
Solar Thermal and Photovoltaic	1.86
Wind	0.40
Wood and Wood Derived Fuels	0.09
California (CA)	
Coal	0.44
Hydroelectric Conventional	12.66
Natural Gas	63.72
Nuclear	9.55
Other	0.44
Other Biomass	1.52
Other Gases	0.75
Petroleum	0.04
Solar Thermal and Photovoltaic	2.03
Wind	6.84
Wood and Wood Derived Fuels	2.02
Colorado (CO)	
Coal	63.33
Hydroelectric Conventional	2.28
Natural Gas	20.12
Other	0.09
Other Biomass	0.15
Petroleum	0.02
Solar Thermal and Photovoltaic	0.47
Wind	13.54
Wind	6.34
Wood and Wood Derived Fuels	0.02
North Carolina (NC)	
Coal	37.38
Hydroelectric Conventional	5.48
Natural Gas	22.22
Nuclear	31.95
Other	0.45
Other Biomass	0.33
Petroleum	0.17
Solar Thermal and Photovoltaic	0.27
Wood and Wood Derived Fuels	1.75
North Dakota (ND)	
Coal	78.46
Hydroelectric Conventional	5.29
Natural Gas	0.15
Other	0.11
Other Biomass	0.02
Other Gases	0.12
Petroleum	0.09
Wind	15.76
Nebraska (NE)	
Coal	72.14
Hydroelectric Conventional	3.03
Natural Gas	1.18
Nuclear	18.50
Other Biomass	0.18
Petroleum	0.11
Wind	4.86
New Hampshire (NH)	
Coal	7.40
Hydroelectric Conventional	7.22
Natural Gas	20.73
Nuclear	55.25
Other	0.31
Other Biomass	0.69
Petroleum	0.53
Wind	1.97
Wood and Wood Derived Fuels	5.91
New Jersey (NJ)	
Coal	3.11
Hydroelectric Conventional	0.03
Natural Gas	41.69
Nuclear	51.39
Other	0.96
Other Biomass	1.54
Other Gases	0.34
Petroleum	0.25
Solar Thermal and Photovoltaic	0.67

Table 9 (continued).

Wood and Wood Derived Fuels	0.01	Wind	0.02
Connecticut (CT)		**New Mexico (NM)**	
Coal	1.91	Coal	67.31
Hydroelectric Conventional	1.13	Hydroelectric Conventional	0.26
Natural Gas	44.31	Natural Gas	25.02
Nuclear	47.96	Other Biomass	0.05
Other	2.00	Petroleum	0.16
Other Biomass	1.82	Solar Thermal and Photovoltaic	1.08
Petroleum	0.86	Wind	6.11
Wood and Wood Derived Fuels	0.01	**Nevada (NV)**	
Delaware (DE)		Coal	15.56
Coal	19.90	Hydroelectric Conventional	7.94
Natural Gas	76.43	Natural Gas	73.33
Other Biomass	0.74	Other	0.08
Other Gases	2.00	Other Biomass	0.07
Petroleum	0.30	Other Gases	0.02
Solar Thermal and Photovoltaic	0.58	Petroleum	0.06
Wind	0.06	Solar Thermal and Photovoltaic	2.21
Florida (FL)		Wind	0.74
Coal	20.84	**New York (NY)**	
Hydroelectric Conventional	0.11	Coal	3.44
Natural Gas	62.49	Hydroelectric Conventional	18.29
Nuclear	11.93	Natural Gas	39.80
Other	1.39	Nuclear	32.77
Other Biomass	1.04	Other	0.65
Petroleum	1.15	Other Biomass	1.23
Solar Thermal and Photovoltaic	0.09	Petroleum	0.74
Wood and Wood Derived Fuels	0.96	Solar Thermal and Photovoltaic	0.05
Georgia (GA)		Wind	2.59
Coal	33.15	Wood and Wood Derived Fuels	0.44
Hydroelectric Conventional	3.06	**Ohio (OH)**	
Natural Gas	33.23	Coal	68.88
Nuclear	27.11	Hydroelectric Conventional	0.40
Other	0.07	Natural Gas	15.80
Other Biomass	0.34	Nuclear	11.74
Petroleum	0.23	Other	0.01
Solar Thermal and Photovoltaic	0.01	Other Biomass	0.35
Wood and Wood Derived Fuels	2.81	Other Gases	0.69
Hawaii (HI)		Petroleum	1.01
Coal	14.05	Solar Thermal and Photovoltaic	0.03
Hydroelectric Conventional	0.78	Wind	0.83
Other	3.94	Wood and Wood Derived Fuels	0.25
Other Biomass	3.30	**Oklahoma (OK)**	
Other Gases	0.41	Coal	40.68
Petroleum	72.28	Hydroelectric Conventional	2.95
Solar Thermal and Photovoltaic	0.19	Natural Gas	40.75
Wind	5.04	Other Biomass	0.17
Iowa (IA)		Petroleum	0.01
Coal	58.76	Wind	15.14

Table 9 (continued).

Hydroelectric Conventional	1.32
Natural Gas	2.52
Nuclear	9.39
Other Biomass	0.28
Petroleum	0.25
Wind	27.47
Idaho (ID)	
Coal	0.60
Hydroelectric Conventional	55.94
Natural Gas	22.39
Other	0.51
Other Biomass	1.31
Wind	16.24
Wood and Wood Derived Fuels	3.00
Illinois (IL)	
Coal	43.31
Hydroelectric Conventional	0.06
Natural Gas	3.36
Nuclear	47.85
Other	0.14
Other Biomass	0.30
Other Gases	0.18
Petroleum	0.04
Solar Thermal and Photovoltaic	0.03
Wind	4.74
Indiana (IN)	
Coal	83.94
Hydroelectric Conventional	0.35
Natural Gas	8.18
Other	0.40
Other Biomass	0.34
Other Gases	2.18
Petroleum	1.42
Solar Thermal and Photovoltaic	0.03
Wind	3.15
Kansas (KS)	
Coal	61.41
Hydroelectric Conventional	0.03
Natural Gas	4.09
Nuclear	14.79
Other Biomass	0.12
Petroleum	0.11
Wind	19.46
Kentucky (KY)	
Coal	92.83
Hydroelectric Conventional	3.65
Natural Gas	1.58
Other	0.01
Other Biomass	0.11
Wood and Wood Derived Fuels	0.30
Oregon (OR)	
Coal	6.29
Hydroelectric Conventional	55.41
Natural Gas	24.05
Other	0.06
Other Biomass	0.49
Petroleum	0.01
Solar Thermal and Photovoltaic	0.03
Wind	12.48
Wood and Wood Derived Fuels	1.17
Pennsylvania (PA)	
Coal	38.91
Hydroelectric Conventional	1.11
Natural Gas	21.97
Nuclear	34.63
Other	0.37
Other Biomass	0.81
Other Gases	0.29
Petroleum	0.20
Solar Thermal and Photovoltaic	0.03
Wind	1.47
Wood and Wood Derived Fuels	0.22
Rhode Island (RI)	
Hydroelectric Conventional	0.07
Natural Gas	98.28
Other Biomass	0.77
Petroleum	0.81
Solar Thermal and Photovoltaic	0.03
Wind	0.04
South Carolina (SC)	
Coal	25.41
Hydroelectric Conventional	3.29
Natural Gas	12.32
Nuclear	56.49
Other	0.06
Other Biomass	0.22
Petroleum	0.11
Solar Thermal and Photovoltaic	0.00
Wood and Wood Derived Fuels	2.10
South Dakota (SD)	
Coal	28.19
Hydroelectric Conventional	40.19
Natural Gas	4.97
Petroleum	0.07
Wind	26.59
Tennessee (TN)	
Coal	40.76
Hydroelectric Conventional	15.61

Table 9 (continued).

Petroleum	1.57
Wood and Wood Derived Fuels	0.25
Louisiana (LA)	
Coal	20.43
Hydroelectric Conventional	1.02
Natural Gas	51.48
Nuclear	16.62
Other	0.67
Other Biomass	0.08
Other Gases	2.20
Petroleum	4.85
Wood and Wood Derived Fuels	2.65
Massachusetts (MA)	
Coal	11.91
Hydroelectric Conventional	2.98
Natural Gas	63.92
Nuclear	13.02
Other	2.63
Other Biomass	3.19
Petroleum	1.17
Solar Thermal and Photovoltaic	0.32
Wind	0.62
Wood and Wood Derived Fuels	0.23
Maryland (MD)	
Coal	43.34
Hydroelectric Conventional	4.82
Natural Gas	8.05
Nuclear	39.79
Other	0.84
Other Biomass	1.15
Petroleum	0.53
Solar Thermal and Photovoltaic	0.18
Wind	0.90
Wood and Wood Derived Fuels	0.40
Maine (ME)	
Coal	0.45
Hydroelectric Conventional	25.38
Natural Gas	34.74
Other	2.86
Other Biomass	1.57
Petroleum	1.70
Wind	7.47
Wood and Wood Derived Fuels	25.84
Michigan (MI)	
Coal	52.96
Hydroelectric Conventional	1.34
Natural Gas	11.61
Nuclear	27.21
Other	0.29
Natural Gas	6.29
Nuclear	35.75
Other Biomass	0.11
Other Gases	0.02
Petroleum	0.16
Solar Thermal and Photovoltaic	0.03
Wind	0.06
Wood and Wood Derived Fuels	1.20
Texas (TX)	
Coal	34.47
Hydroelectric Conventional	0.11
Natural Gas	47.03
Nuclear	8.84
Other	0.06
Other Biomass	0.17
Other Gases	0.55
Petroleum	0.22
Solar Thermal and Photovoltaic	0.04
Wind	8.28
Wood and Wood Derived Fuels	0.23
Utah (UT)	
Coal	81.25
Hydroelectric Conventional	1.20
Natural Gas	15.66
Other	0.38
Other Biomass	0.17
Petroleum	0.06
Solar Thermal and Photovoltaic	0.00
Wind	1.28
Virginia (VA)	
Coal	27.10
Hydroelectric Conventional	1.61
Natural Gas	29.01
Nuclear	37.56
Other	0.61
Other Biomass	1.23
Petroleum	0.40
Wood and Wood Derived Fuels	2.49
Vermont (VT)	
Hydroelectric Conventional	18.68
Natural Gas	0.04
Nuclear	70.39
Other Biomass	0.37
Petroleum	0.07
Solar Thermal and Photovoltaic	0.25
Wind	3.43
Wood and Wood Derived Fuels	6.76
Washington (WA)	
Coal	5.90

Table 9 (continued).

Other Biomass	0.93
Other Gases	0.90
Petroleum	0.50
Wind	2.63
Wood and Wood Derived Fuels	1.62
Minnesota (MN)	
Coal	45.85
Hydroelectric Conventional	1.00
Natural Gas	12.28
Nuclear	20.87
Other	0.70
Other Biomass	1.12
Petroleum	0.05
Solar Thermal and Photovoltaic	0.01
Wind	16.10
Wood and Wood Derived Fuels	2.02
Missouri (MO)	
Coal	83.33
Hydroelectric Conventional	1.24
Natural Gas	4.82
Nuclear	9.16
Other	0.02
Other Biomass	0.07
Petroleum	0.07
Wind	1.28
Wood and Wood Derived Fuels	0.01
Mississippi (MS)	
Coal	16.48
Natural Gas	60.17
Nuclear	20.57
Other	0.01
Other Biomass	0.03
Petroleum	0.03
Wood and Wood Derived Fuels	2.71
Hydroelectric Conventional	68.46
Natural Gas	10.01
Nuclear	7.41
Other	0.11
Other Biomass	0.25
Other Gases	0.36
Petroleum	0.02
Solar Thermal and Photovoltaic	0.00
Wind	6.14
Wood and Wood Derived Fuels	1.34
Wisconsin (WI)	
Coal	61.62
Hydroelectric Conventional	3.00
Natural Gas	12.28
Nuclear	17.70
Other	0.10
Other Biomass	0.73
Petroleum	0.46
Wind	2.36
Wood and Wood Derived Fuels	1.74
West Virginia (WV)	
Coal	95.28
Hydroelectric Conventional	2.29
Natural Gas	0.36
Other Biomass	0.01
Other Gases	0.04
Petroleum	0.20
Wind	1.83
Wyoming (WY)	
Coal	88.48
Hydroelectric Conventional	1.35
Natural Gas	0.98
Other	0.13
Other Gases	0.54
Petroleum	0.07
Wind	8.45

A.4 LIFE CYCLE GHG EMISSIONS INTENSITY FOR DIFFERENT ELECTRICITY GENERATION TECHNOLOGIES

Table 10. Life cycle GHG emissions intensity for different electricity generation technologies

Fuel Source	Database	GHG emission factor for producing 1 MJ electricity
Coal	USLCI[153]	0.301
Hydroelectric Conventional	ELCD[273]	0.00678
Natural gas	USLCI[153]	0.203
Nuclear	USLCI[153]	0.00322
Other	Ecoinvent[149]	0.0407
Other Biomass	USLCI[153]	0.0126
Other Gases	Ecoinvent[149]	0.524
Petroleum	USLCI[153]	0.315
Solar Thermal and Photovoltaic	Ecoinvent[149]	0.0132
Wind	ELCD[273]	0.00184
Wood and Wood Derived Fuels	USLCI[153]	0.0144

A.5 ENERGY CONTENT OF AVAILABLE WASTE HEAT

The waste heat estimation procedure described in the methodology section of main paper only takes into account the first law of thermodynamics and quantifies the thermal energy content of waste heat streams available at existing NG CS. The first law of thermodynamics has the limitation of assuming substitutability between energy resources and failing to distinguish between the quality of energy (e.g. heat vs work). For example, as per the first law of thermodynamics, 1 Joule of heat available at 400^0K is substitutable with 1 Joule of heat at 500^0K. We address this limitation by quantifying the exergy content of available waste heat at existing NG CS. Exergy represents the maximum amount of work that can be extracted from a system when it is brought in thermodynamic equilibrium with the surroundings (also defined as the reference state). Exergy is particularly appealing since it considers both the first and second law of thermodynamics and provides a better representation of the ability of different energy streams to do work.[274-276] Specifically, we quantify the thermal aspect of exergy,[277] E, which is induced by the temperature difference between exhaust stream and the surrounding environment using eq 7[278] where Q and T are the energy and temperature of exhaust stream, and T_0 is the ambient temperature. The results for exergy content of available waste heat from NG CS are provided Figure 29.

$$E = Q.\left|1 - \frac{T_0}{T-T_0} ln \frac{T}{T_0}\right| \tag{7}$$

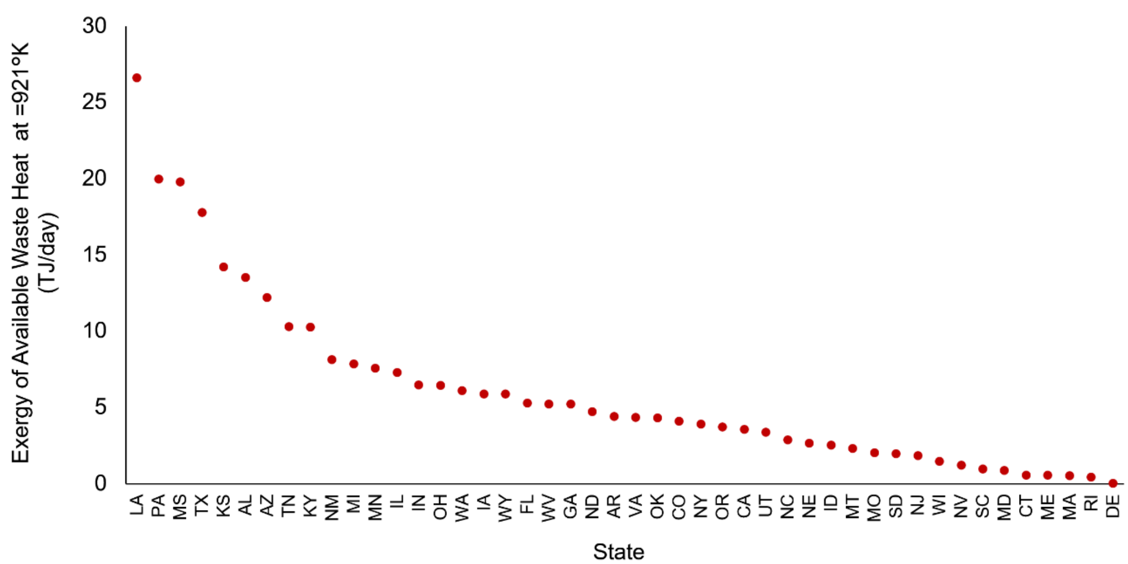

Figure 29. Exergy content of available waste heat at NG CS by state

APPENDIX B

SUPPLEMENTAL MATERIAL FOR CHAPTER 3

Table 11. Summary of data and assumptions used in the TEA model

Plant life time	30 years
Plant capacity	500,000 gallon/day
Plant availability	90% [41, 194, 196, 221]
Interest rate	5% [41, 208, 220]
Amortization factor	0.065
Electricity cost	\$0.069/kWh [223]
Steam price	\$0.008/kg [41]
Membrane cost	\$60/m^2 [217]
Membrane replacement	20%/year
Feed water storage tank	0.5(\$/gal) [218, 219]
Permeate storage tank	0.4(\$/gal) [218, 219]
Site development	\$26.42/m^3/day [211]
Controls, pressure vessels, and electrical subsystems	\$140/(m^3/day) [197]
Shipping and installation	\$44.9(m^3/day) [197]
Equipment related engineering	\$44.9(m^3/day) [197]
Filter	\$0.0132/m^3 [197]
Pretreatment	\$80/m^3/day [197]
Utilities	\$42.27/m^3/day [197, 211]
Spares cost	\$0.033/m^3 [197, 211]
Labor cost	\$0.03/m^3 [41, 196, 197]
Chemicals cost	\$0.018/m^3 [197, 202, 211]

Table 11 (continued).

Produced water transportation cost	\$0.25/mile/m^3[20, 68]
Brine injection cost	\$6.29/m^3 [69, 225]
Transportation distance from shale gas sites to hypothetical DCMD plant	100 miles
Transportation distance from hypothetical DCMD plant to disposal wells	400 miles
Transportation distance from shale gas sites to disposal wells	500 miles [20, 68]

The detailed calculation process for capital and O&M costs for a 0.5 MGD DCMD plant is shown in Table 12.

Table 12. Water desalination cost calculations for a 0.5 MGD MD plant

Capital cost	
Direct capital cost	
Site development 1893(m^3/day)×0.667×26.42(\$/m^3/day)×1.245=\$41,545	*Controls, pressure vessels, electrical subsystem* 1,893(m^3/day)×0.667×140(\$/m^3/day)×1.245=\$220,149
Heat exchanger Required heat exchanger area based on ASPEN simulation: HX-1=2430m^2, HX-2=719m^2, HX-3=208m^2, HX-4=975m^2 Total cost of heat exchangers: 2) MD base case: (\$298,940+\$88,473+\$34,000)×2.08[a]×(598.45/382.8)[b]= \$1,370,336 2) MD with waste heat integration: (\$298,940+\$88,473+\$34,000+\$119,958)×2.08[a]×(598.45/382.8)[b]= \$1,760,410	*Feed pumps* Required pump capacity based on plant flowsheet: Feed pump flowrate: 900(m^3/hr) Recycle pump flowrate: 714(m^3/hr) Permeate pump flowrate: 814(m^3/hr) Condensate pump flowrate: 53(m^3/hr) Total cost of pumps= ((19811+17000) ×3.33[c]+(17911+4400)×1.8[d])×(956.2/648.5)[e]=\$239,964 *Shipping and installation* 1,893(m^3/day)×0.667×44.9(\$/m^3/day)×1.245=\$70,605
Pretreatment 1893(m^3/day)×0.667×79.25(\$/m^3/day)×1.245=\$124,620	*Equipment related engineering* 1,893(m^3/day)×0.667×44.9(\$/m^3/day)×1.245=\$70,605
Membrane Required membrane area=52914(kg/hr)/26.5(kg/m^2.hr)=1997 m^2 Cost of membrane=1997m^2×60\$/m^2=\$119,805	Total direct capital cost \$4,408,724
Membrane module 1,893(m^3/day)×0.667×103(\$/m^3/day)×1.245=\$161,967	Indirect capital cost 4,408,724×0.1=\$440,872

Table 12 (continued).

Permeate storage tank

1893(m^3/day)×0.667×264.17(gal/m^3)×0.4($/gal)×5 days=$666,667

Feed water storage tank

1893(m^3/day)×264.17(gal/m^3)×0.5($/gal)×5 days=$1,250,000

Utilities

1893(m^3/day)×0.667×42.27($/m^3/day)×1.245=$66,469

Total capital cost

4,408,724+440,872=$4,849,506

Annual capital cost

$4,849,506\times\left(\frac{0.05(1+0.05)^{30}}{(1+0.05)^{30}-1}\right)$=$315,473/year

Normalized annual capital cost

1) 315,473/(1893×0.9×365)=$0.51/m$^3_{feed}$

Operating and maintenance

Thermal energy

Required amount of steam based on ASPEN simulation: 49272 kg/hr

Cost of thermal energy=49272(kg/hr)×0.008($/kg)×24(hr/day) ×0.9×365(day/year)=$3,107,653/year

Electricity

Electricity requirement for each pump is calculated as follows:

$$E_{Feed\ pump}=\frac{20\ psi\times6.9\times10^3\left({}^{Pa}/_{psi}\right)\times0.25\ \left({}^{m^3}/_{s}\right)}{0.8}=43.1\ kW$$

$$E_{Recycle\ pump}=\frac{10\ psi\times6.9\times10^3\left({}^{Pa}/_{psi}\right)\times0.20\ \left({}^{m^3}/_{s}\right)}{0.8}=17.1\ kW$$

$$E_{Permeate\ pump}=\frac{10\ psi\times6.9\times10^3\left({}^{Pa}/_{psi}\right)\times0.23\ \left({}^{m^3}/_{s}\right)}{0.8}=19.5\ kW$$

$$E_{condensate\ pump}=\frac{150\ psi\times6.9\times10^3\left({}^{Pa}/_{psi}\right)\times0.015\ \left({}^{m^3}/_{s}\right)}{0.8}=19.1kW$$

Cost of electricity =(43.1+17.1+19.5+19.1)(kW)×0.069($/kWh)×24hr/day×0.9×365days/year= $53,738/year

Filter

1,893(m^3/day)×0.667×0.9×365×0.0132($/m^3)=$5,478/year

Chemicals

1893(m^3/day)×0.667×0.9×365×0.018($/m^3)=$7,465/year

Spares

1893(m^3/day)×0.667×0.9×365×0.033($/m^3)=$13,685/year

Labor

1893(m^3/day)×0.667×0.9×365×0.03($/m^3)=$12,441/year

Membrane replacement

0.2×119805=$23,961/year

Total annual O&M cost

$3,225,620/year

Annual normalized O&M charges

3,225,620/(1893×0.9×365)=$5.19/m$^3_{feed}$

Total water cost

MD base case: 0.51+5.19=$5.70/m$^3_{feed}$

MD with waste heat integration: 0.55+0.19=$0.74/m$^3_{feed}$

[a] Correction coefficient for material use. NETL cost curves are provided for carbon steel heat exchangers and we used the correction coefficient to adjust all cost for Monel.

[b] Correction coefficient used to account for inflation. Cost curves published by NETL dates back to the base year 1998 and we used the most recent CEPCI for heat exchangers to convert all costs to year 2015.

[c] Correction coefficient for material use. NETL cost curves are provided for carbon steel pumps and we used the correction coefficient to adjust all cost for Monel (produced water feed pump and produced water circulation pump).

[d] Correction coefficient for material use. NETL cost curves are provided for carbon steel pumps and we used the correction coefficient to adjust all cost for stainless steel 316 (permeate circulation pump and steam condensate).

[e] Correction coefficient used to account for inflation. Cost curves published by NETL dates back to the base year 1998 and we used the most recent CEPCI for pumps to convert all costs to year 2015.

BIBLIOGRAPHY

1. Kerr, R.A., *Natural gas from shale bursts onto the scene*. 2010, American Association for the Advancement of Science.

2. EIA, U.S. *Technically Recoverable Shale Oil and Shale Gas Resources: An Assessment of 137 Shale Formations in 41 Countries Outside the United States*. June 2013.

3. EIA, U.S. *Annual Energy Outlook 2015*. April 2015; Available from: http://www.eia.gov/forecasts/AEO/pdf/0383(2015).pdf.

4. USEIA, *US Energy Information Administration*, https://www.eia.gov/todayinenergy/detail.php?id=32412 *(accessed October 4, 2017).* 2017.

5. Laurenzi, I.J. and G.R. Jersey, *Life cycle greenhouse gas emissions and freshwater consumption of Marcellus shale gas.* Environmental science & technology, 2013. **47**(9): p. 4896-4903.

6. Allen, D.T., et al., *Measurements of methane emissions at natural gas production sites in the United States.* Proceedings of the National Academy of Sciences, 2013. **110**(44): p. 17768-17773.

7. Dale, A.T., et al., *Process based life-cycle assessment of natural gas from the Marcellus Shale.* Environmental science & technology, 2013. **47**(10): p. 5459-5466.

8. Steinzor, N., W. Subra, and L. Sumi, *Investigating links between shale gas development and health impacts through a community survey project in Pennsylvania.* NEW SOLUTIONS: A Journal of Environmental and Occupational Health Policy, 2013. **23**(1): p. 55-83.

9. Schmidt, C.W., *Blind rush? Shale gas boom proceeds amid human health questions.* Environmental Health Perspectives, 2011. **119**(8): p. a348.

10. Jackson, R.B., et al., *Increased stray gas abundance in a subset of drinking water wells near Marcellus shale gas extraction.* Proceedings of the National Academy of Sciences, 2013. **110**(28): p. 11250-11255.

11. Llewellyn, G.T., et al., *Evaluating a groundwater supply contamination incident attributed to Marcellus Shale gas development.* Proceedings of the National Academy of Sciences, 2015. **112**(20): p. 6325-6330.

12. Laurenzi, I.J., J.A. Bergerson, and K. Motazedi, *Life cycle greenhouse gas emissions and freshwater consumption associated with Bakken tight oil.* Proceedings of the National Academy of Sciences, 2016. **113**(48): p. E7672-E7680.

13. Ferrar, K.J., et al., *Assessment of effluent contaminants from three facilities discharging Marcellus Shale wastewater to surface waters in Pennsylvania.* Environmental science & technology, 2013. **47**(7): p. 3472-3481.

14. Vidic, R.D., et al., *Impact of shale gas development on regional water quality.* Science, 2013. **340**(6134): p. 1235009.

15. Gregory, K.B., R.D. Vidic, and D.A. Dzombak, *Water management challenges associated with the production of shale gas by hydraulic fracturing.* Elements, 2011. **7**(3): p. 181-186.

16. Vidic, R., et al., *Impact of shale gas development on regional water quality.* Science, 2013. **340**(6134): p. 1235009.

17. Entrekin, S., et al., *Rapid expansion of natural gas development poses a threat to surface waters.* Frontiers in Ecology and the Environment, 2011. **9**(9): p. 503-511.

18. Barbot, E., et al., *Spatial and temporal correlation of water quality parameters of produced waters from Devonian-age shale following hydraulic fracturing.* Environmental science & technology, 2013. **47**(6): p. 2562-2569.

19. King, G.E., *Hydraulic fracturing 101: what every representative, environmentalist, regulator, reporter, investor, university researcher, neighbor, and engineer should know about hydraulic fracturing risk.* Journal of Petroleum Technology, 2012. **64**(04): p. 34-42.

20. Slutz, J.A., et al. *Key shale gas water management strategies: an economic assessment*. in *International Conference on Health, Safety and Environment in Oil and Gas Exploration and Production*. 2012. Society of Petroleum Engineers.

21. Abualfaraj, N., P.L. Gurian, and M.S. Olson, *Characterization of Marcellus shale flowback water.* Environmental Engineering Science, 2014. **31**(9): p. 514-524.

22. Yang, L., I.E. Grossmann, and J. Manno, *Optimization models for shale gas water management.* AIChE Journal, 2014. **60**(10): p. 3490-3501.

23. Mason, C.F., L.A. Muehlenbachs, and S.M. Olmstead, *The economics of shale gas development.* Annu. Rev. Resour. Econ., 2015. **7**(1): p. 269-289.

24. Manda, A.K., et al., *Evolution of multi-well pad development and influence of well pads on environmental violations and wastewater volumes in the Marcellus shale (USA).* Journal of environmental management, 2014. **142**: p. 36-45.

25. Rodriguez, R.S. and D.J. Soeder, *Evolving water management practices in shale oil & gas development.* Journal of Unconventional Oil and Gas Resources, 2015. **10**: p. 18-24.

26. Yang, L., et al., *Investment optimization model for freshwater acquisition and wastewater handling in shale gas production.* AIChE Journal, 2015. **61**(6): p. 1770-1782.

27. Clark, C. and J. Veil, *Produced water volumes and management practices in the United States*. 2009, Argonne National Laboratory (ANL).

28. Lutz, B.D., A.N. Lewis, and M.W. Doyle, *Generation, transport, and disposal of wastewater associated with Marcellus Shale gas development.* Water Resources Research, 2013. **49**(2): p. 647-656.

29. McCurdy, R. *Underground injection wells for produced water disposal*. in *Proceedings of the Technical Workshops for the Hydraulic Fracturing Study: Water Resources Management. EPA*. 2011.

30. *SAFER PA, The Shale Alliance for Energy Research, Pennsylvania, Life cycle management of future waste challengers for shale development in Pennsylvania,* http://www.saferpa.org/Pages/Life-Cycle-Management-of-Future-Waste-Challenges-4-Shale-Development-in-PA.aspx *(accessed July 18, 2017).* 2015.

31. Council, N.R., *Induced seismicity potential in energy technologies*. 2013: National Academies Press.

32. Hammer, R., J. VanBriesen, and L. Levine, *In fracking's wake: new rules are needed to protect our health and environment from contaminated wastewater.* Natural Resources Defense Council, 2012. **11**.

33. Reins, L., *The shale gas extraction process and its impacts on Water Resources.* Review of European, Comparative & International Environmental Law, 2011. **20**(3): p. 300-312.

34. Hickenbottom, K.L., et al., *Forward osmosis treatment of drilling mud and fracturing wastewater from oil and gas operations.* Desalination, 2013. **312**: p. 60-66.

35. Cline, J., et al. *Advances in Water Treatment Technology and Potential Affect on Application of USDW*. in *GWPC: 2009 Underground Injection Control Conference, Antonio, TX*. 2009.

36. McGinnis, R.L., et al., *Pilot demonstration of the NH 3/CO 2 forward osmosis desalination process on high salinity brines.* Desalination, 2013. **312**: p. 67-74.

37. Thiel, G.P., et al., *Energy consumption in desalinating produced water from shale oil and gas extraction.* Desalination, 2015. **366**: p. 94-112.

38. Shaffer, D.L., et al., *Desalination and reuse of high-salinity shale gas produced water: drivers, technologies, and future directions.* Environmental science & technology, 2013. **47**(17): p. 9569-9583.

39. Lokare, O.R., et al., *Fouling in direct contact membrane distillation of produced water from unconventional gas extraction.* Journal of Membrane Science, 2017. **524**: p. 493-501.

40. Lokare, O.R., et al., *Importance of feed recirculation for the overall energy consumption in membrane distillation systems.* Desalination, 2018. **428**: p. 250-254.

41. Kesieme, U.K., et al., *Economic analysis of desalination technologies in the context of carbon pricing, and opportunities for membrane distillation.* Desalination, 2013. **323**: p. 66-74.

42. Ghaffour, N., T.M. Missimer, and G.L. Amy, *Technical review and evaluation of the economics of water desalination: current and future challenges for better water supply sustainability.* Desalination, 2013. **309**: p. 197-207.

43. Mezher, T., et al., *Techno-economic assessment and environmental impacts of desalination technologies.* Desalination, 2011. **266**(1): p. 263-273.

44. Thiel, G.P., et al., *Energy consumption in desalinating produced water from shale oil and gas extraction.* Desalination, 2015. **366**: p. 94-112.

45. Subramani, A. and J.G. Jacangelo, *Emerging desalination technologies for water treatment: A critical review.* Water research, 2015. **75**: p. 164-187.

46. Li, B. and K.K. Sirkar, *Novel membrane and device for direct contact membrane distillation-based desalination process.* Industrial & engineering chemistry research, 2004. **43**(17): p. 5300-5309.

47. Cath, T.Y., V.D. Adams, and A.E. Childress, *Experimental study of desalination using direct contact membrane distillation: a new approach to flux enhancement.* Journal of Membrane Science, 2004. **228**(1): p. 5-16.

48. Shirazi, M., *Desalination of saline water using direct contact membrane distillation.* J. Appl. Chem. Res, 2011. **17**: p. 28-36.

49. Chen, W., et al., *High-flux water desalination with interfacial salt sieving effect in nanoporous carbon composite membranes.* arXiv preprint arXiv:1604.07567, 2016.

50. Kesieme, U.K., et al., *Recovery of water and acid from leach solutions using direct contact membrane distillation.* Water Science and Technology, 2014. **69**(4): p. 868-875.

51. Xie, M., et al., *A forward osmosis–membrane distillation hybrid process for direct sewer mining: system performance and limitations.* Environmental science & technology, 2013. **47**(23): p. 13486-13493.

52. Gryta, M., K. Karakulski, and A. Morawski, *Purification of oily wastewater by hybrid UF/MD.* Water research, 2001. **35**(15): p. 3665-3669.

53. Tun, C.M., et al., *Membrane distillation crystallization of concentrated salts—flux and crystal formation.* Journal of Membrane Science, 2005. **257**(1-2): p. 144-155.

54. Ji, X., et al., *Membrane distillation-crystallization of seawater reverse osmosis brines.* Separation and Purification Technology, 2010. **71**(1): p. 76-82.

55. Li, B. and K.K. Sirkar, *Novel membrane and device for vacuum membrane distillation-based desalination process.* Journal of Membrane Science, 2005. **257**(1): p. 60-75.

56. Meindersma, G., C. Guijt, and A. De Haan, *Desalination and water recycling by air gap membrane distillation.* Desalination, 2006. **187**(1): p. 291-301.

57. Martinez, L., *Comparison of membrane distillation performance using different feeds.* Desalination, 2004. **168**: p. 359-365.

58. Zolotarev, P., et al., *Treatment of waste water for removing heavy metals by membrane distillation.* Journal of hazardous materials, 1994. **37**(1): p. 77-82.

59. Zakrzewska-Trznadel, G., M. Harasimowicz, and A.G. Chmielewski, *Concentration of radioactive components in liquid low-level radioactive waste by membrane distillation.* Journal of Membrane Science, 1999. **163**(2): p. 257-264.

60. Hsu, S., K. Cheng, and J.-S. Chiou, *Seawater desalination by direct contact membrane distillation.* Desalination, 2002. **143**(3): p. 279-287.

61. Calabro, V., B.L. Jiao, and E. Drioli, *Theoretical and experimental study on membrane distillation in the concentration of orange juice.* Industrial & engineering chemistry research, 1994. **33**(7): p. 1803-1808.

62. Gunko, S., et al., *Concentration of apple juice using direct contact membrane distillation.* Desalination, 2006. **190**(1): p. 117-124.

63. Alves, V. and I. Coelhoso, *Orange juice concentration by osmotic evaporation and membrane distillation: a comparative study*. Journal of Food Engineering, 2006. **74**(1): p. 125-133.

64. Tomaszewska, M., M. Gryta, and A. Morawski, *Study on the concentration of acids by membrane distillation.* Journal of Membrane Science, 1995. **102**: p. 113-122.

65. *Marcellus Region production continues growth*. 2014; Available from: http://www.eia.gov/todayinenergy/detail.cfm?id=17411.

66. Pathak, M., et al. *Suppression in the Bubble Points of Oils in Shales Combined Effect of Presence of Organic Matter and Confinement*. in *SPE Unconventional Resources Conference*. 2017. Society of Petroleum Engineers.

67. Veil, J.A., et al., *A white paper describing produced water from production of crude oil, natural gas, and coal bed methane.* Argonne National Laboratory, Technical Report, 2004.

68. Gao, J. and F. You, *Optimal design and operations of supply chain networks for water management in shale gas production: MILFP model and algorithms for the water-energy nexus.* AIChE Journal, 2015. **61**(4): p. 1184-1208.

69. McCurdy, R. *Underground injection wells for produced water disposal*. in *USEPA Technical Workshops for the Hydraulic Fracturing Study: Water Resource Management. United States Environmental Protection Agency, Office of Research and Development*. 2011.

70. Slutz, J.A., et al., *Key Shale Gas Water Management Strategies: An Economic Assessment*. Society of Petroleum Engineers.

71. Hayes, T. and T. Smith, *Techno-economic Assessment of Water Management Solutions.* Marcellus Shale Gas Water Management Initiative, Canonsburg, PA, 2011.

72. Kargbo, D.M., R.G. Wilhelm, and D.J. Campbell, *Natural gas plays in the Marcellus shale: Challenges and potential opportunities.* Environmental science & technology, 2010. **44**(15): p. 5679-5684.

73. Ellsworth, W.L., *Injection-induced earthquakes.* Science, 2013. **341**(6142): p. 1225942.

74. Zoback, M., S. Kitasei, and B. Copithorne, *Addressing the environmental risks from shale gas development*. Vol. 21. 2010: Worldwatch Institute.

75. Keranen, K.M., et al., *Sharp increase in central Oklahoma seismicity since 2008 induced by massive wastewater injection.* Science, 2014. **345**(6195): p. 448-451.

76. McGarr, A., et al., *Coping with earthquakes induced by fluid injection.* Science, 2015. **347**(6224): p. 830-831.

77. USEIA, *US Energy Information Administration,* https://www.eia.gov/maps/pdf/marcellus-upd.pdf *(accessed July 17, 2018).* 2014.

78. USEIA, *US Energy Information Administration.* 2016.

79. Elsayed, N.A., M.A. Barrufet, and M.M. El-Halwagi, *An integrated approach for incorporating thermal membrane distillation in treating water in heavy oil recovery using SAGD.* Journal of Unconventional Oil and Gas Resources, 2015. **12**: p. 6-14.

80. Singh, D. and K.K. Sirkar, *Desalination of brine and produced water by direct contact membrane distillation at high temperatures and pressures.* Journal of Membrane Science, 2012. **389**: p. 380-388.

81. Singh, D., P. Prakash, and K.K. Sirkar, *Deoiled produced water treatment using direct-contact membrane distillation.* Industrial & Engineering Chemistry Research, 2013. **52**(37): p. 13439-13448.

82. Macedonio, F., et al., *Direct contact membrane distillation for treatment of oilfield produced water.* Separation and Purification Technology, 2014. **126**: p. 69-81.

83. Duong, H.C., et al., *Scaling control during membrane distillation of coal seam gas reverse osmosis brine.* Journal of Membrane Science, 2015. **493**: p. 673-682.

84. Duong, H.C., et al., *Treatment of RO brine from CSG produced water by spiral-wound air gap membrane distillation—A pilot study.* Desalination, 2015. **366**: p. 121-129.

85. Zhang, X., et al., *Exploration and optimization of two-stage vacuum membrane distillation process for the treatment of saline wastewater produced by natural gas exploitation.* Desalination, 2016. **385**: p. 117-125.

86. Gálvez, J.B., L. García-Rodríguez, and I. Martín-Mateos, *Seawater desalination by an innovative solar-powered membrane distillation system: the MEDESOL project.* Desalination, 2009. **246**(1): p. 567-576.

87. Xu, Y., B.-K. Zhu, and Y.-y. Xu, *Pilot test of vacuum membrane distillation for seawater desalination on a ship.* Desalination, 2006. **189**(1): p. 165-169.

88. Hanemaaijer, J.H., et al., *Memstill membrane distillation – a future desalination technology.* Desalination, 2006. **199**(1): p. 175-176.

89. Tavakkoli, S., et al., *A Systems-level Analysis of Waste Heat Recovery Opportunities from Natural Gas Compressor Stations in the US.* ACS Sustainable Chemistry & Engineering, 2016.

90. Sims, R., *Renewables for Heating and Cooling. An Untapped Potential*. 2007, Joint report for the Renewable Energy Technology Deployment Implementing Agreement and the Renewable Energy Working Party published by the International Energy Agency, Paris, France.

91. Fox, D.B., D. Sutter, and J.W. Tester, *The thermal spectrum of low-temperature energy use in the United States.* Energy & Environmental Science, 2011. **4**(10): p. 3731-3740.

92. *US DOE (Department of Energy).* The Water-Energy Nexus: Challenges and Opportunities, 2014.

93. Johnson, I., et al., *Waste heat recovery: technology and opportunities in US industry.* US Department of Energy, Office of Energy Efficiency and Renewable Energy, Industrial Technologies Program, 2008.

94. Fang, H., et al., *Industrial waste heat utilization for low temperature district heating.* Energy Policy, 2013. **62**: p. 236-246.

95. Conti, J. *Annual Energy Outlook 2007*. in *Energy Information Administration (EIA) Energy Outlook, Modeling, and Data Conference, Washington, DC*. 2007.

96. Ross, C., G. Tincher, and G. Tincher, *Glass melting technology: A technical and economic assessment.* GMIC, October, 2004.

97. van Oss, H., *G., Cement, 2005 US Minerals Yearbook, US Department of the Interior.* US Geological Survey, 2007: p. 16.1-16.9.

98. Martin, N., E. Worrell, and L. Price, *Energy efficiency and carbon dioxide emissions reduction opportunities in the US cement industry.* Lawrence Berkeley National Laboratory, 1999.

99. Margolis, N. and L. Sousa, *Energy and environmental profile of the US iron and steel industry*, in *1997 ACEEE summer study on energy efficiency in industry: Proceedings, refereed papers, and summary monographs*. 1997.

100. Prevention, I.P., *Control (IPPC): Best Available Techniques Reference Document on the Production of Iron and Steel.* European Commission, 2001.

101. Pattanapunt, P., et al., *Waste Heat Recovery From Boiler Of Large-Scale Textile Industry.* American Journal of Environmental Sciences, 2013. **9**(3): p. 231.

102. Li, T., et al., *Performance of secondary aluminum melting: Thermodynamic analysis and plant-site experiments.* Energy, 2006. **31**(12): p. 1769-1779.

103. Schifo, J. and J. Radia, *Theoretical/best practice energy use in metalcasting operations.* US Department of Energy Industrial Technologies Program, Report, 2004.

104. Eppich, R., *Energy use in selected metalcasting facilities-2003.* Energy, 2004.

105. Hendricks, T. and W.T. Choate, *Engineering scoping study of thermoelectric generator systems for industrial waste heat recovery.* US Department of Energy, 2006. **20**(0): p. 6.

106. Goswami, D.Y. and F. Kreith, *Handbook of energy efficiency and renewable energy*. 2007: Crc Press.

107. Butcher, C. and B. Reddy, *Second law analysis of a waste heat recovery based power generation system.* International Journal of Heat and Mass Transfer, 2007. **50**(11): p. 2355-2363.

108. Morrow, C.W., et al., *Water Recovery Using Waste Heat from Coal Fired Power Plants.* Sandia national laboratories, New York, NY, 2011.

109. Ozalp, N., *Utilization of heat, power, and recovered waste heat for industrial processes in the US chemical industry.* Journal of Energy Resources Technology, 2009. **131**(2): p. 022401.

110. Gingerich, D.B. and M.S. Mauter, *Quantity, quality, and availability of waste heat from United States thermal power generation.* Environmental science & technology, 2015. **49**(14): p. 8297-8306.

111. *Annual Energy Outlook, Energy Information Administration.* Department of Energy, 2010.

112. PHMSA, *Pipeline and Hazardous Materials Safety Administration,* http://www.phmsa.dot.gov/pipeline/library/data-stats/annual-report-mileage-for-natural-gas-transmission-and-gathering-systems, *(accessed March 30, 2016).* 2016.

113. USEPA, *Inventory of U.S. Greenhouse Gas Emissions and Sinks: 1990-2012, EPA 430-R-14-003, Washington, DC.* 2014.

114. Zimmerle, D.J., et al., *Methane emissions from the natural gas transmission and storage system in the United States.* Environmental science & technology, 2015. **49**(15): p. 9374-9383.

115. EIA, *U.S. Energy Information Administration* https://www.eia.gov/dnav/ng/ng_cons_sum_dcu_nus_m.htm *(accessed April 4, 2016).* 2016.

116. Mitchell, A.L., et al., *Measurements of methane emissions from natural gas gathering facilities and processing plants: Measurement results.* Environmental science & technology, 2015. **49**(5): p. 3219-3227.

117. INGAA, *Natural Gas Pipeline and Storage Infrastructure Pojections Trough 2030 Prepared for INGAA Foundation.* Inc. by: ICF International, 2009.

118. He, M., et al., *A combined thermodynamic cycle used for waste heat recovery of internal combustion engine.* Energy, 2011. **36**(12): p. 6821-6829.

119. Wong, P.J. and R.E. Larson, *Optimization of natural-gas pipeline systems via dynamic programming.* Automatic Control, IEEE Transactions on, 1968. **13**(5): p. 475-481.

120. Steinbach, M.C., *On PDE solution in transient optimization of gas networks.* Journal of computational and applied mathematics, 2007. **203**(2): p. 345-361.

121. Banda, M.K. and M. Herty, *Towards a space mapping approach to dynamic compressor optimization of gas networks.* Optimal control applications and methods, 2011. **32**(3): p. 253-269.

122. Martin, A., M. Möller, and S. Moritz, *Mixed integer models for the stationary case of gas network optimization.* Mathematical programming, 2006. **105**(2-3): p. 563-582.

123. Nguyen, H.H. and C.W. Chan, *Applications of artificial intelligence for optimization of compressor scheduling.* Engineering Applications of Artificial Intelligence, 2006. **19**(2): p. 113-126.

124. Ríos-Mercado, R.Z., et al., *A reduction technique for natural gas transmission network optimization problems.* Annals of Operations Research, 2002. **117**(1): p. 217-234.

125. Haddad, J. and R. Behbahani, *Optimization of a natural Gas transmission system.* International Journal of Computer Applications, 2013. **66**(11).

126. Wu, S., et al., *Model relaxations for the fuel cost minimization of steady-state gas pipeline networks.* Mathematical and Computer Modelling, 2000. **31**(2): p. 197-220.

127. Ohanian, S. and R. Kurz, *Series of parallel arrangement in a two-unit compressor station.* Journal of engineering for gas turbines and power, 2002. **124**(4): p. 936-941.

128. Hedman, B.A., *Waste energy recovery opportunities for interstate natural gas pipelines.* Interstate Natural Gas Association of America. Retrieved July, 2008. **25**: p. 2011.

129. Tu, T., *U.S. Energy Information Administration.* May 18, 2015.

130. USEPA, *Inventory of U.S. Greenhouse Gas Emissions and Sinks: 1990 – 2013.* 2015.

131. Todd Jerry H., *Capstone Turbine Corporation* June 8, 2015.

132. Hughes Tom, *FlexEnergy*. June 12, 2015.

133. Perless Robert, *Iroquois Gas Transmission System.* June 20, 2015.

134. Altman, N.S., *An introduction to kernel and nearest-neighbor nonparametric regression.* The American Statistician, 1992. **46**(3): p. 175-185.

135. *STI (Strive To Innovate) group.* http://setxind.com/midstream/compressor-stations-what-how-why/, 2015.

136. Calise, F., et al., *Simulation and exergy analysis of a hybrid solid oxide fuel cell (SOFC)–gas turbine system.* Energy, 2006. **31**(15): p. 3278-3299.

137. Moran, M.J., et al., *Fundamentals of engineering thermodynamics*. 2010: John Wiley & Sons.

138. Martínez, F.R., et al., *Evaluation of the Gas Turbine Inlet Temperature with Relation to the Excess Air.* Energy and Power Engineering, 2011. **3**(04): p. 517.

139. Lugo-Leyte, R., et al., *Methodology to determine the appropriate amount of excess air for the operation of a gas turbine in a wet environment.* Energy, 2010. **35**(2): p. 550-555.

140. Valero, A., et al., *CGAM problem: definition and conventional solution.* Energy, 1994(19): p. 279-286.

141. Petchers, N., *Combined heating, cooling & power handbook: Technologies & applications: An integrated approach to energy resource optimization*. 2003: The Fairmont Press, Inc.

142. Martinez, A.S., *Simulation of Dynamic Operation and Coke-Based Degradation for SOFC-GT-Powered Medium and Long Haul Locomotives*. 2011: University of California, Irvine.

143. Chan, S., H. Ho, and Y. Tian, *Modelling of simple hybrid solid oxide fuel cell and gas turbine power plant.* Journal of Power Sources, 2002. **109**(1): p. 111-120.

144. Ma, F., et al., *Experimental study on thermal efficiency and emission characteristics of a lean burn hydrogen enriched natural gas engine.* International Journal of Hydrogen Energy, 2007. **32**(18): p. 5067-5075.

145. Mohitpour, M., H. Golshan, and A. Murray, *Pipeline design and construction: A practical approach The American Society of Mechanical Engineers.* Three Park Av., New York, NY, 2007: p. 10016.

146. Capstone, *Capstone Turbine Corporation.* http://www.capstoneturbine.com/, 2015.

147. Braun, R., S. Klein, and D. Reindl, *Evaluation of system configurations for solid oxide fuel cell-based micro-combined heat and power generators in residential applications.* Journal of Power Sources, 2006. **158**(2): p. 1290-1305.

148. Subramanian, R., et al., *Methane emissions from natural gas compressor stations in the transmission and storage sector: Measurements and comparisons with the EPA greenhouse gas reporting program protocol.* Environmental science & technology, 2015. **49**(5): p. 3252-3261.

149. Weidema, B., et al., *The Ecoinvent Database: Overview and Methodology, Data Quality Guideline for the Ecoinvent Database Version 3*. 2013.

150. Rosen, M.A., *Energy-and exergy-based comparison of coal-fired and nuclear steam power plants.* Exergy, An International Journal, 2001. **1**(3): p. 180-192.

151. Rosen, M.A. and I. Dincer, *Exergoeconomic analysis of power plants operating on various fuels.* Applied Thermal Engineering, 2003. **23**(6): p. 643-658.

152. EIA, *U.S. Energy Information Administration* http://www.eia.gov/electricity/data/state/ *(accessed October 1, 2015).* 2015.

153. USLCI, *U.S. Life Cycle Inventory Database.* National Renewable Energy Laboratory, 2012.

154. EIA, *U.S. Energy Information Administration* https://www.eia.gov/todayinenergy/detail.cfm?id=22252 *(accessed December 7, 2015).* 2015.

155. Rattner, A.S. and S. Garimella, *Energy harvesting, reuse and upgrade to reduce primary energy usage in the USA.* Energy, 2011. **36**(10): p. 6172-6183.

156. Zevenhoven, R. and A. Beyene, *The relative contribution of waste heat from power plants to global warming.* Energy, 2011. **36**(6): p. 3754-3762.

157. Hasegawa, T., S. Mochida, and A. Gupta, *Development of advanced industrial furnace using highly preheated combustion air.* Journal of propulsion and power, 2002. **18**(2): p. 233-239.

158. Choi, G.-M. and M. Katsuki, *Advanced low NOx combustion using highly preheated air.* Energy conversion and Management, 2001. **42**(5): p. 639-652.

159. Air, P.C., *Energy Tips–Process Heating.* Process Heating, 2007.

160. Turner, W.C. and S. Doty, *Energy management handbook*. 2007: The Fairmont Press, Inc.

161. Bell, L.E., *Cooling, heating, generating power, and recovering waste heat with thermoelectric systems.* Science, 2008. **321**(5895): p. 1457-1461.

162. Gou, X., H. Xiao, and S. Yang, *Modeling, experimental study and optimization on low-temperature waste heat thermoelectric generator system.* Applied energy, 2010. **87**(10): p. 3131-3136.

163. Yodovard, P., J. Khedari, and J. Hirunlabh, *The potential of waste heat thermoelectric power generation from diesel cycle and gas turbine cogeneration plants.* Energy sources, 2001. **23**(3): p. 213-224.

164. Mirolli, M.D. *The Kalina cycle for cement kiln waste heat recovery power plants*. in *Cement Industry Technical Conference, 2005. Conference Record*. 2005. IEEE.

165. Duffy, D., *Better cogeneration through chemistry: the organic Rankine cycle.* Distributed Energy, 2005.

166. Zhou, X., D.B. Gingerich, and M.S. Mauter, *Water Treatment Capacity of Forward Osmosis Systems Utilizing Power Plant Waste Heat.* Industrial & Engineering Chemistry Research, 2015.

167. McGinnis, R.L. and M. Elimelech, *Energy requirements of ammonia–carbon dioxide forward osmosis desalination.* Desalination, 2007. **207**(1): p. 370-382.

168. McCutcheon, J.R., R.L. McGinnis, and M. Elimelech, *A novel ammonia—carbon dioxide forward (direct) osmosis desalination process.* Desalination, 2005. **174**(1): p. 1-11.

169. Li, C., et al., *A new combined power and desalination system driven by low grade heat for concentrated brine.* Energy, 2012. **46**(1): p. 582-595.

170. Jansen, A., et al., *Development and pilot testing of full-scale membrane distillation modules for deployment of waste heat.* Desalination, 2013. **323**: p. 55-65.

171. Walton, J., et al., *Solar and Waste Heat Desalination by Membrane Distillation.* Desalination Research and Development Program, Bureau of Reclamation, Denver, USA, 2000.

172. Tobin, J., *Natural gas compressor stations on the interstate pipeline network: developments since 1996.* Energy Information Administration, Office of Oil and Gas, 2007: p. 1-12.

173. Kapil, A., et al., *Process integration of low grade heat in process industry with district heating networks.* Energy, 2012. **44**(1): p. 11-19.

174. Curcio, E. and E. Drioli, *Membrane distillation and related operations—a review.* Separation and Purification Reviews, 2005. **34**(1): p. 35-86.

175. Mielke, E., L.D. Anadon, and V. Narayanamurti, *Water consumption of energy resource extraction, processing, and conversion.* Belfer Center for Science and International Affairs, 2010.

176. Fakhru'l-Razi, A., et al., *Review of technologies for oil and gas produced water treatment.* Journal of Hazardous Materials, 2009. **170**(2): p. 530-551.

177. Ezechi, E.H., M.H. Isa, and S.R.B.M. Kutty, *Boron in produced water: challenges and improvements: a comprehensive review.* Journal of Applied Sciences, 2012. **12**(5): p. 402.

178. Brown, V.J., *Radionuclides in fracking wastewater: managing a toxic blend*, in *Wastewater and Shale Formation Development: Risks, Mitigation, and Regulation*. 2015, Apple Academic Press. p. 115-126.

179. Warner, N.R., et al., *Impacts of shale gas wastewater disposal on water quality in western Pennsylvania.* Environmental science & technology, 2013. **47**(20): p. 11849-11857.

180. Olmstead, S.M., et al., *Shale gas development impacts on surface water quality in Pennsylvania.* Proceedings of the National Academy of Sciences, 2013. **110**(13): p. 4962-4967.

181. *Shaping Proposed Changes to Pennsylvania's TOTAL DISSOLVED SOLIDS STANDARD A Guide to the Proposal and the Commenting Process,* http://extension.psu.edu/water/conservation/consumption-and-usage/TDShighres-updateDec09.pdf/view *(accessed October 25, 2016).* 2010.

182. Campos, J.C., et al., *Oilfield wastewater treatment by combined microfiltration and biological processes.* Water Research, 2002. **36**(1): p. 95-104.

183. Alkhudhiri, A., N. Darwish, and N. Hilal, *Produced water treatment: Application of air gap membrane distillation.* Desalination, 2013. **309**: p. 46-51.

184. Camacho, L.M., et al., *Advances in membrane distillation for water desalination and purification applications.* Water, 2013. **5**(1): p. 94-196.

185. Banat, F., R. Jumah, and M. Garaibeh, *Exploitation of solar energy collected by solar stills for desalination by membrane distillation.* Renewable Energy, 2002. **25**(2): p. 293-305.

186. Ding, Z., et al., *Analysis of a solar-powered membrane distillation system.* Desalination, 2005. **172**(1): p. 27-40.

187. Koschikowski, J., M. Wieghaus, and M. Rommel, *Solar thermal driven desalination plants based on membrane distillation.* Water Science and Technology: Water Supply, 2003. **3**(5-6): p. 49-55.

188. Olwig, R., et al., *Techno-economic analysis of combined concentrating solar power and desalination plant configurations in Israel and Jordan.* Desalination and Water Treatment, 2012. **41**(1-3): p. 9-25.

189. Kullab, A. and A. Martin, *Membrane distillation and applications for water purification in thermal cogeneration plants.* Separation and Purification Technology, 2011. **76**(3): p. 231-237.

190. Kuipers, N., et al., *Techno-economic assessment of boiler feed water production by membrane distillation with reuse of thermal waste energy from cooling water.* Desalination and Water Treatment, 2015. **55**(13): p. 3506-3518.

191. Karagiannis, I.C. and P.G. Soldatos, *Water desalination cost literature: review and assessment.* Desalination, 2008. **223**(1): p. 448-456.

192. Blank, J., G. Tusel, and S. Nisanc, *The real cost of desalted water and how to reduce it further.* Desalination, 2007. **205**(1): p. 298-311.

193. Van der Bruggen, B., *Desalination by distillation and by reverse osmosis—trends towards the future.* Membrane Technology, 2003. **2003**(2): p. 6-9.

194. Wade, N.M., *Distillation plant development and cost update.* Desalination, 2001. **136**(1): p. 3-12.

195. Fritzmann, C., et al., *State-of-the-art of reverse osmosis desalination.* Desalination, 2007. **216**(1): p. 1-76.

196. Al-Obaidani, S., et al., *Potential of membrane distillation in seawater desalination: thermal efficiency, sensitivity study and cost estimation.* Journal of Membrane Science, 2008. **323**(1): p. 85-98.

197. Sirkar, K.K. and L. Song, *Pilot-scale studies for direct contact membrane distillation-based desalination process*. 2009: US Department of the Interior, Bureau of Reclamation.

198. Guillén-Burrieza, E., et al., *Techno-economic assessment of a pilot-scale plant for solar desalination based on existing plate and frame MD technology.* Desalination, 2015. **374**: p. 70-80.

199. Kim, J., et al., *Membrane distillation (MD) integrated with crystallization (MDC) for shale gas produced water (SGPW) treatment.* Desalination, 2016.

200. Burnett, D.B., *Potential for Beneficial Use of Oil and Gas Produced Water.* available at online http://www. circleofblue. org/waternews/wp-content/uploads/2010/08/beneficialuses-producedwater. pdf, 2004.

201. Xu, P., J.E. Drewes, and D. Heil, *Beneficial use of co-produced water through membrane treatment: technical-economic assessment.* Desalination, 2008. **225**(1): p. 139-155.

202. Helal, A., et al., *Optimal design of hybrid RO/MSF desalination plants Part I: Modeling and algorithms.* Desalination, 2003. **154**(1): p. 43-66.

203. Sorour, M.H., et al., *Preliminary techno-economics assessment of developed desalination/salt recovery facility based on membrane and thermal techniques.* Desalination and Water Treatment, 2015. **55**(9): p. 2416-2422.

204. Macedonio, F., E. Curcio, and E. Drioli, *Integrated membrane systems for seawater desalination: energetic and exergetic analysis, economic evaluation, experimental study.* Desalination, 2007. **203**(1): p. 260-276.

205. Horton, S., *Disposal of hydrofracking waste fluid by injection into subsurface aquifers triggers earthquake swarm in central Arkansas with potential for damaging earthquake.* Seismological Research Letters, 2012. **83**(2): p. 250-260.

206. Keranen, K.M., et al., *Potentially induced earthquakes in Oklahoma, USA: Links between wastewater injection and the 2011 Mw 5.7 earthquake sequence.* Geology, 2013. **41**(6): p. 699-702.

207. Tavakkoli, S., et al., *Systems-level analysis of waste heat recovery opportunities from natural gas compressor stations in the United States.* ACS Sustainable Chemistry & Engineering, 2016. **4**(7): p. 3618-3626.

208. Ettouney, H.M., et al., *Evaluating the economics of desalination.* Chemical Engineering Progress, 2002. **98**(12): p. 32-40.

209. Peters, M.S., et al., *Plant design and economics for chemical engineers*. Vol. 4. 1968: McGraw-Hill New York.

210. Younos, T., *The economics of desalination.* Journal of Contemporary Water Research & Education, 2005. **132**(1): p. 39-45.

211. Ho, W.W. and K.K. Sirkar, *Membrane handbook*. 1992: Springer Science & Business Media.

212. Loh, H., J. Lyons, and C.W. White, *Process equipment cost estimation.* National Energy Technology Center, Report No. DOE/NETL-2002/1169, 2002.

213. Vatavuk, W.M., *Updating the CE plant cost index.* Chemical Engineering, 2002. **109**(1): p. 62.

214. CEPCI, *Chemical Engineering Plant Cost Index,* http://www.chemengonline.com/pci *(accessed May 29, 2016).* 2016.

215. Perry, R.H. and D.W. Green, *Perry's chemical engineers' handbook.* 1999: McGraw-Hill Professional.

216. Lokare, O.R., et al., *Integrating membrane distillation with waste heat from natural gas compressor stations for produced water treatment in Pennsylvania.* Desalination, 2017. **413**: p. 144-153.

217. Wright, T., *Sterlitech Corporation.* Personal Communication, May 17, 2016.

218. Mullins, G., *Mid Atlantic Storage Systems Inc, Personal Communication, June 1, 2016.*

219. Montroy, M., *Superior Tank Company Inc, Personal Communication, May 25, 2016.*

220. Ettouney, H., *Visual basic computer package for thermal and membrane desalination processes.* Desalination, 2004. **165**: p. 393-408.

221. Kavvadias, K. and I. Khamis, *The IAEA DEEP desalination economic model: a critical review.* Desalination, 2010. **257**(1): p. 150-157.

222. Ulrich, G.D. and P.T. Vasudevan, *How to estimate utility costs.* Chemical Engineering, 2006. **113**(4): p. 66.

223. USEIA, *US Energy Information Administration,* https://www.eia.gov/forecasts/steo/report/electricity.cfm *(accessed June 23, 2016).* 2016.

224. WaterReuseAssociation, *Seawater desalination costs,* https://www.watereuse.org/wp-content/uploads/2015/10/WateReuse_Desal_Cost_White_Paper.pdf *(accessed June 24, 2016).* 2012.

225. Boschee, P., *Handling produced water from hydraulic fracturing.* Oil and Gas Facilities, 2012. **1**(01): p. 22-26.

226. Duraisamy, R.T., A.H. Beni, and A. Henni, *State of the art treatment of produced water*. 2013: INTECH Open Access Publisher.

227. Lokare, O.R., et al., *Integrating membrane distillation with waste heat from natural gas compressor stations for produced water treatment in Pennsylvania.* Desalination, 2017. **413**: p. 144-153.

228. Glazer, Y.R., et al., *Potential for using energy from flared gas for on-site hydraulic fracturing wastewater treatment in Texas.* Environmental Science & Technology Letters, 2014. **1**(7): p. 300-304.

229. Plappally, A., *Energy requirements for water production, treatment, end use, reclamation, and disposal.* Renewable and Sustainable Energy Reviews, 2012. **16**(7): p. 4818-4848.

230. Maguire-Boyle, S.J. and A.R. Barron, *Organic compounds in produced waters from shale gas wells.* Environmental Science: Processes & Impacts, 2014. **16**(10): p. 2237-2248.

231. Guan, G., et al., *Analysis of membrane distillation crystallization system for high salinity brine treatment with zero discharge using Aspen flowsheet simulation.* Industrial & engineering chemistry research, 2012. **51**(41): p. 13405-13413.

232. Geertman, R., *SODIUM CHLORIDE: CRYSTALLIZATION*. 2000.

233. Sedivy, V., *Purification of salt for chemical and human consumption.* Industrial Minerals, 1996(343): p. 73-83.

234. Keister, T., J. Sleigh, and M. Briody, *Sequential Precipitation-Fractional crystallization treatment of Marcellus shale flowback and production wastewaters,* http://www.prochemtech.com/Literature/Technical/IWC_12-72_Paper.pdf *(accessed July 2, 2016).* International Water Conference 2012.

235. Tinto, J. and R. Solomon, *Water recovery via thermal evaporative processes for high saline frac water flowback,* https://www.gewater.com/kcpguest/salesedge/documents/Technical%20Papers_Cust/Am

ericas/English/TPte_IWC_10-66_mobile_evaporator.pdf *(accessed July 2, 2016).* International Water Conference, 2010.

236. Tavakkoli, S., et al., *A techno-economic assessment of membrane distillation for treatment of Marcellus shale produced water.* Desalination, 2017. **416**: p. 24-34.

237. Clark, C.E., R.M. Horner, and C.B. Harto, *Life cycle water consumption for shale gas and conventional natural gas.* Environmental science & technology, 2013. **47**(20): p. 11829-11836.

238. Jiang, M., et al., *Life cycle greenhouse gas emissions of Marcellus shale gas.* Environmental Research Letters, 2011. **6**(3): p. 034014.

239. Stephenson, T., J.E. Valle, and X. Riera-Palou, *Modeling the relative GHG emissions of conventional and shale gas production.* Environmental science & technology, 2011. **45**(24): p. 10757-10764.

240. Weber, C.L. and C. Clavin, *Life cycle carbon footprint of shale gas: Review of evidence and implications.* Environmental science & technology, 2012. **46**(11): p. 5688-5695.

241. Cafaro, D.C. and I.E. Grossmann, *Strategic planning, design, and development of the shale gas supply chain network.* AIChE Journal, 2014. **60**(6): p. 2122-2142.

242. Yang, L., et al., *Investment optimization model for freshwater acquisition and wastewater handling in shale gas production.* AIChE Journal, 2015.

243. Rahman, M., M. Rahman, and S. Rahman, *An integrated model for multiobjective design optimization of hydraulic fracturing.* Journal of Petroleum Science and Engineering, 2001. **31**(1): p. 41-62.

244. Guerra, O.J., et al., *An Optimization Framework for the Integration of Water Management and Shale Gas Supply Chain Design.* Computers & Chemical Engineering, 2016.

245. Lira-Barragán, L.F., et al., *Optimal water management under uncertainty for shale gas production.* Industrial & Engineering Chemistry Research, 2016. **55**(5): p. 1322-1335.

246. Zhang, X., A.Y. Sun, and I.J. Duncan, *Shale gas wastewater management under uncertainty.* Journal of environmental management, 2016. **165**: p. 188-198.

247. Gao, J. and F. You, *Deciphering and handling uncertainty in shale gas supply chain design and optimization: Novel modeling framework and computationally efficient solution algorithm.* AIChE Journal, 2015. **61**(11): p. 3739-3755.

248. Gao, J. and F. You, *Shale gas supply chain design and operations toward better economic and life cycle environmental performance: MINLP model and global optimization algorithm.* ACS Sustainable Chemistry & Engineering, 2015. **3**(7): p. 1282-1291.

249. McDonough, W. and M. Braungart, *The next industrial revolution.* The Atlantic Monthly, 1998. **282**(4): p. 82-92.

250. Ehrenfeld, J., *Industrial ecology: a new field or only a metaphor?* Journal of cleaner production, 2004. **12**(8): p. 825-831.

251. Hayes, T. *Characterization of Marcellus and Barnett Shale flowback waters and technology development for water reuse*. in *Hydraulic fracturing technical workshop*. 2011.

252. PADEP, *Pennsylvania Department of Environmental Protection,* http://www.depweb.state.pa.us *(accessed July 15, 2015).* 2015.

253. PADEP, *Pennsylvania Department of Environmental Protection,* http://www.depreportingservices.state.pa.us/ReportServer/Pages/ReportViewer.aspx?%2fOil_Gas%2fOil_Gas_Well_Historical_Production_Report *(accessed May 15, 2015).* 2015.

254. Yoxtheimer, D., *Appalachian shale energy produced fluids management and UIC well disposal trends,* http://www.saferpa.org/Documents/Resources/TechBrief-08-2015/Appalachian-Shale-Energy-Produced-Fluids-Management-UIC-Well-Disposal-Trends_SaferPA-08-20-2015.pdf *(accessed May 20, 2015).* 2015.

255. Slutz, J., *Personal Communication, Global Energy Strategies, April 27, 2017.*

256. Anderson, J., *Personal Communication, Leonard Rice Engineers, May 5, 2017.*

257. Robusto, C.C., *The cosine-haversine formula.* The American Mathematical Monthly, 1957. **64**(1): p. 38-40.

258. Gao, J. and F. You. *Stochastic programming approach to optimal design and operations of shale gas supply chain under uncertainty*. in *2015 54th IEEE Conference on Decision and Control (CDC)*. 2015. IEEE.

259. Miralinaghi, M., et al., *Capacitated refueling station location problem with traffic deviations over multiple time periods.* Networks and Spatial Economics, 2017. **17**(1): p. 129-151.

260. Souhaimi, M.K. and T. Matsuura, *Membrane distillation: principles and applications*. 2011: Elsevier.

261. Alkhudhiri, A., N. Darwish, and N. Hilal, *Membrane distillation: a comprehensive review.* Desalination, 2012. **287**: p. 2-18.

262. Lawson, K.W. and D.R. Lloyd, *Membrane distillation. II. Direct contact MD.* Journal of Membrane Science, 1996. **120**(1): p. 123-133.

263. Sedivy, V., *Purification of salt for chemical and human consumption.* Industrial Minerals, 1996. **343**: p. 73-83.

264. TINTO, J. and R. SOLOMON, *Water Recovery via Thermal Evaporative Processes for High Saline Frac Water Flowback.* IWC, 2012. **10**: p. 66.

265. ExxonMobil, *2017 Outlook for energy: A view to 2040*, http://cdn.exxonmobil.com/~/media/global/files/outlook-for-energy/2017/2017-outlook-for-energy.pdf, *(accessed November 29, 2017).* 2017 Outlook for energy: A view to 2040.

266. Goodman, P.S., et al., *Investigating the traffic-related environmental impacts of hydraulic-fracturing (fracking) operations.* Environment international, 2016. **89**: p. 248-260.

267. Ladlee, J. and J. Jacquet, *The implications of multi-well pads in the Marcellus Shale.* Research & Policy Briefs Series, 2011. **43**.

268. Poinsot, T. and D. Veynante, *Theoretical and Numerical Combustion, 2011.* URL http://elearning. cerfacs. fr/combustion/onlinePoinsotBook/onlinethirdedition/index. php, 2014.

269. Kuo, K.K., *Principles of combustion.* 1986.

270. Williams, G., *Combustion theory.* 1985.

271. Goodwin, D., et al., *Cantera: An object-oriented software toolkit for chemical kinetics, thermodynamics, and transport processes.* Caltech, Pasadena, CA, 2009.

272. EIA, *Energy Information Administration*, http://www.eia.gov/electricity/data/state/. 2013.

273. ELCD, *European Commission, Joint Research Centre - Institute for Environment and Sustainability and DG Environment - Directorate G.* European Reference Life Cycle Database, version 2.0, 2008.

274. Szargut, J., D.R. Morris, and F.R. Steward, *Exergy analysis of thermal, chemical, and metallurgical processes.* 1987.

275. Szargut, J., *Exergy method: technical and ecological applications*. Vol. 18. 2005: WIT press.

276. Dewulf, J., et al., *Exergy: its potential and limitations in environmental science and technology*. Environmental Science & Technology, 2008. **42**(7): p. 2221-2232.

277. Palazzo, P., *Thermal and mechanical aspect of entropy-exergy relationship.* International Journal of Energy and Environmental Engineering, 2012. **3**(1): p. 1-10.

278. Wall, G., *Exergetics.* 2009.